MODELING THE IMPACT OF CLIMATE CHANGE ON TICK POPULATION DYNAMICS AND TICK-BORNE DISEASE SPREAD

XIAOTIAN WU

A DISSERTATION SUBMITTED TO THE FACULTY OF GRADUATE STUDIES
IN PARTIAL FULFILMENT OF THE REQUIREMENTS
FOR THE DEGREE OF

DOCTOR OF PHILOSOPHY

GRADUATE PROGRAM IN MATHEMATICS AND STATISTICS
YORK UNIVERSITY
TORONTO, ONTARIO
JANUARY 2013

MODELING THE IMPACT OF CLIMATE CHANGE ON TICK POPULATION DYNAMICS AND TICK-BORNE DISEASE SPREAD

by **Xiaotian Wu**

a dissertation submitted to the Faculty of Graduate Studies of York University in partial fulfilment of the requirements for the degree of

DOCTOR OF PHILOSOPHY

© 2013

Permission has been granted to: a) YORK UNIVERSITY LIBRARIES to lend or sell copies of this dissertation in paper, microform or electronic formats, and b) LIBRARY AND ARCHIVES CANADA to reproduce, lend, distribute, or sell copies of this dissertation anywhere in the world in microform, paper or electronic formats *and* to authorise or procure the reproduction, loan, distribution or sale of copies of this dissertation anywhere in the world in microform, paper or electronic formats.

The author reserves other publication rights, and neither the dissertation nor extensive extracts for it may be printed or otherwise reproduced without the author's written permission.

MODELING THE IMPACT OF CLIMATE CHANGE ON TICK POPULATION DYNAMICS AND TICK-BORNE DISEASE SPREAD

by **Xiaotian Wu**

By virtue of submitting this document electronically, the author certifies that this is a true electronic equivalent of the copy of the dissertation approved by York University for the award of the degree. No alteration of the content has occurred and if there are any minor variations in formatting, they are as a result of the coversion to Adobe Acrobat format (or similar software application).

Examination Committee Members:

1. Jane Heffernan
2. Huaiping Zhu
3. Jianhong Wu (supervisor)

Abstract

There is increasing evidence that Lyme disease is an emerging threat for public health in Canada. In this dissertation, we study the impact of climate change on establishment/extinction of the Lyme disease tick vector *Ixodes scapularis* and Lyme pathogen *Borrelia burgdorferi* in the Canadian landscape by utilizing mathematical techniques and computer simulations. We develop principal mathematical frameworks using ordinary differential equations with periodic coefficients, partial differential equations with seasonality and a periodic system of delay differential equations with periodic delay. We develop analysis and tools to predict the long-term status of Lyme disease transmission dynamics in the vector population. We determine factors, which are of interest to public health policy makers, for Lyme disease prevention and control in Canada in varying environmental conditions. We provide the theoretical foundation of a risk map of Lyme disease in Canada.

Acknowledgements

I wish to express my sincere appreciation to my dissertation supervisor Professor Jianhong Wu for his valuable instruction and advice during the process of the completion of this dissertation. During my four years of study (one year for maternity leave), he has also provided me with huge chances to attend conferences, summer schools and workshops to broaden my outlook, to communicate with others, and to extend my knowledge. Thanks are due to the members of my supervisory committee: Professor Huaiping Zhu and Professor Jane Heffernan, for their helpful comments and suggestions, and their precious advice and assistance during my study at York University.

I would like to Drs. Yijun Lou and Venkata R.S.K Duvvuri for their valuable instruction and collaboration in some parts of this work.

I would like to thank Dr. Nicholas Ogden at Public Health Agency of Canada for giving me real data and insightful discussions and collaboration.

I would like to thank the excellent faculty and staff at the Department of Mathe-

matics and Statistics of York University and Mprime Centre for Disease Modelling for their support. I would also like to thank the Canada Research Chairs program (CRC), the Natural Sciences and Engineering Research Council of Canada (NSERC), the Mathematics for Information Technology and Complex Systems (MITACS), the GEOmatics for Informed Decision (GEOIDE) and the Public Health Agency of Canada (PHAC) for supporting projects of which this dissertation is a part.

Finally, I would like to thank my husband, Ye Zhang, and my two daughters, for their understanding and support during my study in York.

Table of Contents

List of Tables

List of Figures

Abbreviations

Abbreviation	Full description
$\mathcal{R}^{v,c}$	Basic reproduction ratio for tick population with constant coefficients in Chapter 2
$\mathcal{R}^{v,p}$	Basic reproduction ratio for tick population with periodic coefficients in Chapter 3
$\mathcal{R}^{s_1v,p}$	Basic reproduction ratio for simplified tick population with periodic coefficients in Chapter 4
$\mathcal{R}^{sv,p}$	Basic reproduction ratio for simplified tick population with periodic coefficients in Chapter 5
$\mathcal{R}^{d,p}$	Basic reproduction ratio for pathogen population with periodic coefficients in Chapter 5
$\mathcal{R}^{v,pd}$	Basic reproduction ratio for tick population with periodic delay in Chapter 6

1 Introduction

Lyme disease (LD) was first time described in 1977 following the investigation of a cluster of arthritis cases among children living near Lyme, Connecticut [95]. LD is universally acknowledged as the most common vector-borne infectious disease for most of the world, especially in Europe and North America, caused by a bacterium called *Borrelia burgdorferi.* The disease can affect both humans and animals with more than 30,000 human cases reported in United States alone in 2010 [17]. Usually mice, squirrels and shrews, and other small vertebrates can carry the bacterium that causes Lyme disease [88].

The black-legged tick, *Ixodes scapularis*, is the primary vector of *Borrelia burgdorferi* in north-eastern regions of North America [25, 45]. The immature ticks (i.e., larvae and nymphs) can become infected when they feed on normally small-size rodents carrying the bacteria, and then the infected immature ticks are able to transmit the pathogen to the next host in the subsequent blood meals. The life cycle of tick, *I. scapularis*, is very complex and takes place nearly two years to

reach the adult stage from an egg. After hatching from eggs, they have to pass through three developmental stages: larva, nymph, adult. Each of the three stages exhibits their activity in different seasons. Eggs are laid by an adult female tick in the spring and larvae hatch during the late summer. In all three stages, larvae, nymph and adult ticks, seek to attach a host to draw a blood meal, and then drop off to digest the meal. The fed larvae in the spring or summer moult and overwinter as nymphs; the very few larvae fed after September overwinter as engorged larvae and are ready to moult in the next spring. Unfed larvae survive less than one year hence no overlap can be seen with the successive cohorts. Most nymphs fed in spring or early summer will moult to adult ticks in the same year. Unfed nymphs able to survive throughout the spring or summer to the next year overlap with new generation of nymph cohorts. Adult ticks feed during fall and spring. The gravid females lay their eggs in early spring and die shortly. Unfed adults of fall overwinter and resume host-seeking in the spring and die, unless they feed during their first season, of questing [20, 106, 54, 79, 71].

Lyme disease has been recognized as an emerging disease in Canada. The risk of Lyme disease in Canada is changing rapidly due to the geographic range expansion of *I. scapularis* [46, 73]. A decade ago *I. scapularis* populations were geographically restricted to specific locations on the north shores of Lake Erie and Lake Ontario, one location in southeast Manitoba and one location in Nova Scotia [68]. How-

ever, more recently *I. scapularis* tick populations have been identified in multiple locations in southern Manitoba, New Brunswick and Nova Scotia and is spreading widely in some areas of southern Ontario and Quebec [46]. In addition, "adventitious" ticks, if infected with *B. burgdorferi*, can be found over a wide geographic range of Canada [74]. These ticks could transmit the bacterium to humans or animals residing in areas outside of LD endemic area. Thus, it is possible for people or animals to acquire LD in non-endemic areas across Canada. These "adventitious" ticks are dispersed from reproducing tick populations by hosts (particularly migratory birds [44, 62, 72]). Where climate conditions, host densities and habitats are suitable for establishment these adventitious ticks may seed new, reproducing and self-sustaining tick populations [72]. Field observations indicate that many woodland habitats in Canada are suitable for survival of ticks off-host, and in such habitats mortality rates of ticks over winter and summer are comparable [52, 74], most likely because the duff layer insulates ticks from deep freezing in winter and desiccation in the summer. The studies [74, 75] also suggest that the range of *I. scapularis* will continue to expand northward in the coming decades, and may be accelerated by global warming.

The geographic distribution of *I. scapularis* can be affected by many factors such as habitat suitability, host abundance, climate suitability and tick dispersal. Climate suitability, in particular, temperature variation, is regarded as the principal

restricting factor in the establishment of *I. scapularis*. Climate affects the survival of tick populations in a number of ways. First, climate indirectly affects tick survival in being a determinant of the occurrence of suitable communities of vertebrate animal hosts of the ticks, and of vegetation that allows development of a duff layer that provides refuge for off-host ticks from desiccation, drowning and extremes of temperature that can directly kill ticks. Second, host-seeking activity is affected by ambient temperature and humidity. Third, rates of development of ticks from one life stage to the next depend in most cases on temperature, being faster at higher temperature and zero at 0°C.

These factors are reviewed by [68] in which they were incorporated into a detailed process-based dynamical simulation model to explain and simulate "realistic, seasonal effects of temperature" on development and activity of *I. scapularis*. This model aimed to investigate the hypothesis that temperature conditions controlling the duration of the tick life cycle (via effects on interstadial development rates and activities) determine the northern geographic limits for this tick. Model simulations identified minimal seasonal-variable temperature conditions (best captured by the annual cumulative degree days > 0°C : $DD > 0$°C) to support the persistence of the vector population. However this structure is mathematically intractable and the calculation of the effects of climate change-induced increasing temperatures (or of other environmental changes) on basic reproductive ratio for the tick population

is not directly possible.

The development of mathematically tractable models capable of estimating basic reproductive ratios for both *I.* scapularis and its pathogen in the Canadian landscape under varying environmental conditions remains a major challenge. In this thesis, we will study the impact of climate change-induced increasing temperature on the establishment of Lyme disease tick vector *I.* scapularis, range expansion of the tick population and disease spread in the Canadian landscape based on the framework of Ogden et al (2005) [68].

Lyme disease spread involves complex interaction of a spirochete, multiple vertebrate hosts, and a vector with a two-year life cycle strongly influenced by the season rhythm. Mathematical models with different levels of complexity and different methodological approaches have been developed to investigate the ecological behavior of tick populations and disease transmission. Some examples include the differential equation (continuous) models the difference (discrete) models [4, 15, 64, 84]; or a periodic process in time [84, 81, 64, 31, 68]. Spatial spread dynamics has also been studied using a reaction-diffusion (partial differential) equation model by [16], and a metapopulation model by [39]. More specifically, for example, Sandberg et al. [84] first used a matrix model with month-dependent transition rates to investigate the seasonally varying population densities of questing ticks. Caraco

et al. [16] presented a reaction-diffusion model to identify factors influencing the rate at which the disease spreads spatially, and the study emphasized that the vector's stage-structured dynamics would govern the spatial expansion of infection. Norman et al. [66] studied two simple deterministic models to examine the effect of interactions of shared hosts on the persistence and dynamics of the tick-borne pathogens. Awerbuch-Friedlander et al. [4] formulated two delay difference systems to study the effect of seasonality on the behavior of the tick population by comparing the seasonal model with a non-seasonal one, and showed that seasonality can increase the stability of the system. Rosà et al. [83, 82] studied how the persistence of ticks and pathogens is affected by the dynamics of tick populations and by their host densities, and different transmission routes. However, how to derive a general framework of multi-host tick/pathegon dynamics through the integration of host movement behaviors and tick's seasonality in time-continuous process have not been studied yet, to our best knowledge.

In Chapter 2, we propose an ordinary differential equation model with constant coefficients based on the process-based dynamic population model [68], which comprises of 12 mutually exclusive states and investigate the influence of temperature change (time-independent) on the establishment of tick population in a large scale. The development rates from one state to next are temperature-dependent, here temperature means mean annual temperature in a given area. In this chapter, we

derive the basic reproductive ratio ($\mathcal{R}_0^{v,c}$) for *I. scapularis* and yield a threshold, summarizing the reproduction rate of the vector population during the two year life cycle, determining how the survival or extinction of tick vector population depends on the temperature as well as the host densities in a spatially homogeneous habitat.

In Chapter 3, we develop a periodic system of ordinary differential equations with periodic coefficients describing the influence of climate change on the establishment of Lyme disease tick vector *I. scapularis* in a fine scale. Firstly we parameterize and validate the system using existing surveillance data from Public Health Agency of Canada. We derive the key threshold, the basic reproductive ratio ($\mathcal{R}_0^{v,p}$) for *I. scapularis* in a periodic environment, by utilizing some recent developments [8, 99] about the qualitative theory for epidemic models with periodic coefficients. Our goal is to generate a risk map of Lyme disease tick vector *I. scapularis* by calculating the basic reproductive ratio $\mathcal{R}_0^{v,p}$ from a number of locations in southeastern Canada, which is a key step in our evolving ability to develop tools for assessment of Lyme disease risk emergence and for development of public health policies on surveillance, prevention and control. Finally, we carry out sensitive analysis on the basic reproductive ratio to explore how variation in temperature, host community composition and other key parameters in the model alter the rate of spread of *I. scapularis*.

Motivated by the recent range expansion of *I. scapularis* and its ecological ac-

tivities highly regulated by seasonality, in Chapter 4, we develop a periodic system of reaction-diffusion equations capturing some key features and stage developments of the tick population as well as the spatial random movements of involved hosts in an isolated landscape of Canada. Such a system may generate an order-preserving periodic process, but only some iteration of the periodic map can be strongly order-preserving due to the seasonal on-or-off biological activities. Hence how to derive qualitative properties of the periodic map from those of its iterations is of practical implication. By applying some recent results of strongly order-preserving periodic processes with strictly subhomogeneous nonlinearities [48, 49, 50] to a certain iteration of the associated periodic map, we establish the existence of periodic traveling waves and calculate the range expansion speed.

To better understand the effects of the seasonal temperature variation and host community composition on the pathogen transmission, in Chapter 5, we develop a detailed stage-structured periodic deterministic model integrating seasonal tick development and activity, multiple host species and complex transmission routes between ticks and hosts. We derive two basic reproductive ratios, one for ticks $\mathcal{R}_0^{sv,p}$, another for disease pathogen $\mathcal{R}_0^{d,p}$, analyzing how the two thresholds play important roles in determining the tick invasion and disease persistence. We carry out numerical simulations to describe the effect of climate warming and host diversity on population dynamics of the tick and pathogen. A sensitivity analysis is

also performed to determine the relative importance of the key factors to spirochete population.

Finally, motivated by the physiology of the tick population, namely the fact that the length of time from one life stage to the next varies periodically with time, we derive a system of delay differential equations with periodic delays. The time-periodic delayed system simultaneously contain two different types of effects in time: time-periodic coefficients and delays. There have been some studies of these two effects in the past, but most of these studies have concentrated on only one of the two effects separately. We have some very limited studies regarding on the examining two effects in a single mode. Moreover, none to date has studied the basic reproductive ratio for this type of delay differential equations to our best knowledge. Following the works of [96, 42, 8, 5, 99], we derive the basic reproductive ratio of the linearized system at the trivial solution, which is defined as the spectral radius of a linear integral operator, and a numerical algorithm to compute the basic reproductive ratio is presented in this chapter. The thesis ends with a final chapter that summarizes the results and describes a few topics which should be considered in the future.

2 Temperature change-driven tick population dynamics with non-seasonal development

2.1 Introduction

As described in Chapter 1, climate change, in particular increasing temperature, has been shown to facilitate the rapid geographical expansion of vector *I. scapularis* and such an expansion might establish Lyme disease in non-endemic areas of Canada. The risk of Lyme disease is tied to the abundance and distribution of the tick population. The environmental factor plays a vital role in the development of *I. scapularis* because 98% of the 2-year life cycle occurs off the host. Climate should act as an essential determinant of distribution of the tick population.

In this chapter we assume that there is a spatially homogeneous habitat with constant environmental conditions. Our first goal of the thesis is to predict the impact of temperature change on the complex tick population life cycle as well as on their establishment conditions in the presence of primary and secondary hosts in

a large scale, a preliminary step to understand the disease risk in terms of studying the population dynamics of its vector.

We convert the model of [68] into an ordinary differential system involving 12 mutually exclusive tick stages, investigating the influence of temperature change on the persistence/extinction of tick population. The model is a considerable simplification compared to the model of [68]. A key simplification here is that rather than taking account of development delay by accumulating daily proportions of development from one stage to next, we consider the mean proportion of development in a whole year (being the reciprocal of temperature-dependent or temperature-independent duration of development) as a development rate from this stage to the next. Another simplification is about the host community composition and we assume the community of hosts of *I. scapularis*, consists of white-footed mice serving as a host of immature tick and white-tailed deer as a primary source of nourishment for adult tick. This is not biologically accurate but adequate for our study purposes in this stage to identify the crucial temperature condition.

We consider the qualitative behaviors of the high-dimensional ordinary differential equations in section 2.2. We establish the positiveness and boundedness of the system and show the existence, uniqueness of an endemic equilibrium, and stability of the endemic equilibrium under the assumption of weak density dependent reduction in fecundity of egg-laying females. We find the threshold condition, in

terms of the basic reproductive ratio (denoted by $\mathcal{R}_0^{v,c}$), for tick persistence. We also conduct some numerical simulations to illustrate the analytical results. Our analysis indicates that lower or higher mean annual temperature will bring about threshold $\mathcal{R}_0^{v,c} < 1$, thereby forces the tick population to extinction in the habitat. Therefore temperature can be used as a decisive factor to predict the distribution, establishment of tick populations.

2.2 Model formulation and analysis

The life cycle of the tick has three developmental stages: larva, nymph and adult. Each stage subdivides in turn according to the phase of activity: 'questing', in which the unfed tick seeks a host; 'feeding', in which the attached tick feeds; and 'engorged' after feeding and then drop off their hosts. In the model, ticks are classified into 12 different states: eggs (x_2), hardening larvae (x_3), questing larvae (x_4), nymphs (x_7) and adults (x_{10}), feeding larvae (x_5), nymphs (x_8) and adult females (x_{11}), engorged larvae (x_6), nymphs (x_9) and adult females (x_{12}) and egg-laying adult females (x_1). Each state represents a specific point in the life of the ticks (Figure 2.1).

We assume that the development rates of pre-oviposition period (POP), pre-eclosion period (PEP), larva-to-nymph and nymph-to-adult are influenced by temperature, and questing activity is assumed to vary with temperature as well, where

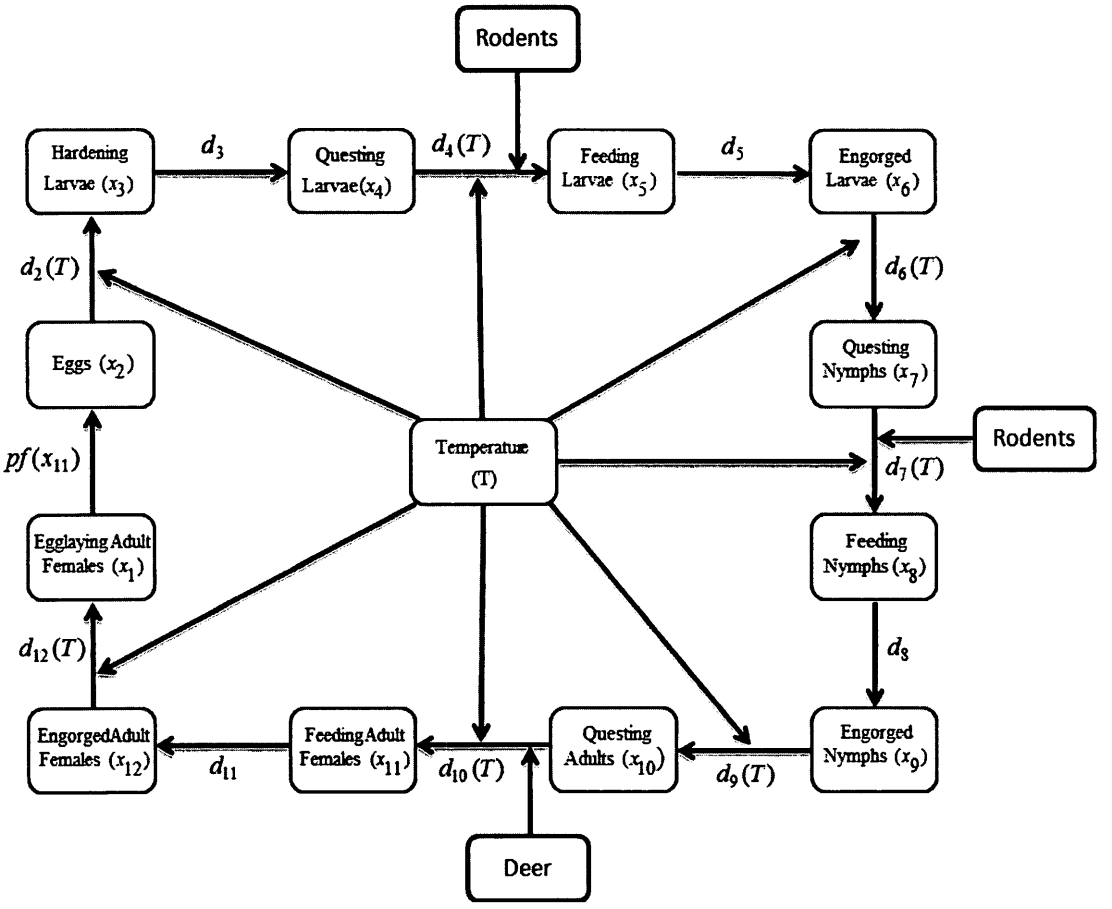

Figure 2.1: A diagram of tick population model adapted from Ogden et al., *Int. J. Parasitol.*, 35 (2005) 375-389.

temperature means mean annual temperature through this chapter.

With these assumptions, the model equations that describe tick population dynamics are as following:

$$\begin{aligned}
x_1'(t) &= d_{12}(T)x_{12} - \mu_1 x_1, \\
x_2'(t) &= pf(x_{11})x_1 - (d_2(T) + \mu_2)x_2, \\
x_3'(t) &= d_2(T)x_2 - (d_3 + \mu_3)x_3, \\
x_4'(t) &= d_3 x_3 - (d_4(T) + \mu_4)x_4, \\
x_5'(t) &= d_4(T)x_4 - (d_5 + \mu_5(x_5))x_5, \\
x_6'(t) &= d_5 x_5 - (d_6(T) + \mu_6)x_6, \\
x_7'(t) &= d_6(T)x_6 - (d_7(T) + \mu_7)x_7, \\
x_8'(t) &= d_7(T)x_7 - (d_8 + \mu_8(x_8))x_8, \\
x_9'(t) &= d_8 x_8 - (d_9(T) + \mu_9)x_9, \\
x_{10}'(t) &= d_9(T)x_9 - (d_{10}(T) + \mu_{10})x_{10}, \\
x_{11}'(t) &= \tfrac{1}{2}d_{10}(T)x_{10} - (d_{11} + \mu_{11}(x_{11}))x_{11}, \\
x_{12}'(t) &= d_{11}x_{11} - (d_{12}(T) + \mu_{12})x_{12},
\end{aligned} \tag{2.2.1}$$

with initial condition

$$x^0 = (x_1(0), x_2(0), \cdots, x_{12}(0))^T \in \mathbb{R}^{12}_+. \tag{2.2.2}$$

Where, $x_i'(t) = \frac{d}{dt}x_i(t)$ is the derivative of $x_i(t)$ with respect to the time variable t, and T is the mean annual temperature in Celsius (°C). Note here that we consider autonomous system in this chapter, and we use the mean annual temperature to

be considered in the progression rates. Note also that we use equal sex ratio (1/2), and we will discuss this issue in the last chapter. Here, $d_i/d_i(T)$ is the progression rate from the i-th stage to the next stage, $\mu_i/\mu_i(x_i)$ is the death rate for stage i, and p is the per-capita egg reproduction rate by egg-laying females. Note that in this model, we have three density-dependent death rates $\mu_5(x_5)$, $\mu_8(x_8)$, $\mu_{11}(x_{11})$ and we assume that each $\mu_j(x_j)$ is a monotonically increasing function of x_j with $\lim_{x_i \to +\infty} \mu_j(x_j) = +\infty$ for $j = 5, 8, 11$. To account for the density dependent reduction in fecundity of egg laying females, we suppose that $f(x_{11})$ is a decreasing function of x_{11} between 0 and 1. According to the form of $f(x_{11})$ (see Table 2.1), we assume that once $f(x_{11})$ attains zero at some point $\bar{x}_{11}$, then $f(x_{11})$ is zero when x_{11} is bigger than $\bar{x}_{11}$. The host population is fixed at 200 rodents and 20 deer as in [68] in our simulations.

Daily host-finding probabilities vary with host abundance according to the recommendations of [64] and as calibrated in [68] as follows:

λ_{ql}, the host-finding probability for questing larvae ($0.0013\mathrm{R}^{0.515}$);

λ_{qn}, the host-finding probability for questing nymphs ($0.0013\mathrm{R}^{0.515}$); and

λ_{qa}, the host-finding probability for questing adults ($0.086\mathrm{D}^{0.515}$),

where R is the number of rodents and D is the number of deer. The temperature-dependent factors for questing activities of immature ticks θ^i and adult ticks θ^a are

supplied by Public Health Agency of Canada. All parameter values for the tick model (2.2.1) are summarized in Table 2.1 .

2.2.1 Positivity and boundedness of solutions

We first show our mathematical model is biologically well-posed. Namely we prove that the model (2.2.1) with initial condition (2.2.2) has a unique globally defined, differentiable solution which remains nonnegative and bounded.

Lemma 2.2.1. *Each component of the solution of the system (2.2.1) for $t > 0$, subject to initial condition (2.2.2), remains nonnegative for all $t > 0$. Furthermore, each component of the above solution is also bounded for all $t > 0$.*

Proof. The nonnegativity of each $x_i(t)$ follows immediately from [92, Theorem 5.2.1]. Hence $\mathbb{R}^{12}_+$ is positively invariant for the system (2.2.1). It is easy to know every function of the right hand in system (2.2.1) is continuous, differentiable and locally Lipschitzian in $x = (x_1, x_2, \cdots, x_{12})^T$ on each compact subset of $\mathbb{R}^{12}_+$. Hence, there is a unique solution $x(t, x^0)$ for system (2.2.1) through the initial value $x^0 \in \mathbb{R}^{12}_+$ in its maximal interval of the existence. According to the properties of functions $\mu_5(x_5), \mu_8(x_8), \mu_{11}(x_{11})$, monotonically increasing functions with respect to their arguments x_5, x_8, and x_{11}, and the decreasing function $f(x_{11})$,

Table 2.1: Model parameter definitions and values adapted from [68] (all rates are per day).

Parameter	Description	Value
μ_1	Per capita mortality rate of egg-laying adult females	1
μ_2	Per capita mortality rate of eggs	0.002
μ_3	Per capita mortality rate of hardening larvae	0.006
μ_4	Per capita mortality rate of questing larvae	0.006
$\mu_5(x_5)$	Per capita mortality rate of feeding larvae on rodents	$(0.65 + [0.049ln(\{1.01 + x_5\}/R)])$
μ_6	Per capita mortality rate of engorged larvae	0.003
μ_7	Per capita mortality rate of questing nymphs	0.006
$\mu_8(x_8)$	Per capita mortality rate of feeding nymphs on rodents	$(0.55 + [0.049ln(\{1.01 + x_8\}/R)])$
μ_9	Per capita mortality rate of engorged nymphs	0.002
μ_{10}	Per capita mortality rate of questing adults	0.006
$\mu_{11}(x_{11})$	Per capita mortality rate of feeding adults on deer	$(0.5 + [0.049ln(\{1.01 + x_{11}\}/D)])$
μ_{12}	Per capita mortality rate of engorged adult females	0.0001
p	Per capita egg production by egg-laying adult females	3000
$f(x_{11})$	Reduction in fecundity of egg-laying adult females	$1 - [0.01 + 0.04ln\{1.01 + x_{11}/D\}]$
$d_2(T)$	Development rate from eggs to hardening larvae	$1/(34,234 \times T^{-2.27})$
d_3	Development rate from hardening larvae to questing larvae	1/21
$d_4(T)$	Host attaching rate for questing larvae	$\lambda_{ql} \times \theta^i$
d_5	Development rate from feeding larvae to engorged larvae	1/3
$d_6(T)$	Development rate from engorged larvae to questing nymphs	$1/(101,181 \times T^{-2.55})$
$d_7(T)$	Host attaching rate for questing nymphs	$\lambda_{qn} \times \theta^i$
d_8	Development rate from feeding nymphs to engorged nymphs	1/5
$d_9(T)$	Development rate from engorged nymphs to questing adults	$1/(1596 \times T^{-1.42})$
$d_{10}(T)$	Host attaching rate for questing adults	$\lambda_{qa} \times \theta^a$
d_{11}	Development rate from feeding adults females to engorged females	1/10
$d_{12}(T)$	Development rate from engorged females to egg-laying females	$1/(1300 \times T^{-1.42})$
R	Number of rodents	200
D	Number of deer	20

system (2.2.1) can be controlled by the following linear system

$$
\begin{aligned}
x_1'(t) &= d_{12}(T)x_{12} - \mu_1 x_1,\\
x_2'(t) &= pf(0)x_1 - (d_2(T) + \mu_2)x_2,\\
x_3'(t) &= d_2(T)x_2 - (d_3 + \mu_3)x_3,\\
x_4'(t) &= d_3 x_3 - (d_4(T) + \mu_4)x_4,\\
x_5'(t) &= d_4(T)x_4 - (d_5 + \mu_5(0))x_5,\\
x_6'(t) &= d_5 x_5 - (d_6(T) + \mu_6)x_6,\\
x_7'(t) &= d_6(T)x_6 - (d_7(T) + \mu_7)x_7,\\
x_8'(t) &= d_7(T)x_7 - (d_8 + \mu_8(0))x_8,\\
x_9'(t) &= d_8 x_8 - (d_9(T) + \mu_9)x_9,\\
x_{10}'(t) &= d_9(T)x_9 - (d_{10}(T) + \mu_{10})x_{10},\\
x_{11}'(t) &= \tfrac{1}{2}d_{10}(T)x_{10} - (d_{11} + \mu_{11}(0))x_{11},\\
x_{12}'(t) &= d_{11}x_{11} - (d_{12}(T) + \mu_{12})x_{12}.
\end{aligned}
\tag{2.2.3}
$$

Solutions of linear system (2.2.3) exist on $[0, \infty)$. By the comparison theorem [92, Theorem 5.1.1], every solution $x(t)$ of system (2.2.1) exists globally.

Next we establish the boundedness of solutions. The system (2.2.1) can be

controlled by the following cooperative and irreducible ordinary differential system:

$$
\begin{aligned}
x_1'(t) &= d_{12}(T)x_{12} - \mu_1 x_1,\\
x_2'(t) &= pf(0)x_1 - (d_2(T) + \mu_2)x_2,\\
x_3'(t) &= d_2(T)x_2 - (d_3 + \mu_3)x_3,\\
x_4'(t) &= d_3 x_3 - (d_4(T) + \mu_4)x_4,\\
x_5'(t) &= d_4(T)x_4 - (d_5 + \mu_5(0))x_5,\\
x_6'(t) &= d_5 x_5 - (d_6(T) + \mu_6)x_6,\\
x_7'(t) &= d_6(T)x_6 - (d_7(T) + \mu_7)x_7,\\
x_8'(t) &= d_7(T)x_7 - (d_8 + \mu_8(0))x_8,\\
x_9'(t) &= d_8 x_8 - (d_9(T) + \mu_9)x_9,\\
x_{10}'(t) &= d_9(T)x_9 - (d_{10}(T) + \mu_{10})x_{10},\\
x_{11}'(t) &= \tfrac{1}{2}d_{10}(T)x_{10} - (d_{11} + \mu_{11}(x_{11}))x_{11},\\
x_{12}'(t) &= d_{11}x_{11} - (d_{12}(T) + \mu_{12})x_{12}.
\end{aligned}
\tag{2.2.4}
$$

For the above system (2.2.4), there exists a threshold $\mathcal{R}^* > 0$ (in fact, $\mathcal{R}^* = \mathcal{R}_0^{v,c}$) such that there is a unique tick-free equilibrium when $\mathcal{R}^* \leq 1$, which is globally asymptotically stable according to [109, Corollary 3.2]. If $\mathcal{R}^* > 1$, system (2.2.4) admits a unique positive equilibrium (see next section for the uniqueness and existence of the positive equilibrium in a general form), which is also globally asymptotically stable for all nonzero solutions by [109, Corollary 3.2]. Hence, the comparison principle implies that every solution $x(t)$ of system (2.2.1) with

nonnegative initial value is bounded for all $t \in [0, \infty)$. □

2.2.2 Equilibria and reproductive ratio $\mathcal{R}_0^{v,c}$

System (2.2.1) has a tick-free equilibrium denoted by $E_0 := (x_1, x_2, \cdots, x_{12})^T = (0, 0, \cdots, 0)^T$. The following analysis of the local stability of E_0 yields the threshold condition under which the number of tick in all different stages will increase or decrease exponentially. This threshold condition is characterized by the reproductive ratio, denoted by $\mathcal{R}_0^{v,c}$ [21].

The Jacobian matrix of (2.2.1) at E_0 has the form $J_1 = F - V$, where F and V are given respectively by

$$F = \begin{pmatrix}
0 & 0 & 0 & 0 & 0 & 0 & 0 & 0 & 0 & 0 & 0 & d_{12}(T) \\
pf(0) & 0 & 0 & 0 & 0 & 0 & 0 & 0 & 0 & 0 & 0 & 0 \\
0 & d_2(T) & 0 & 0 & 0 & 0 & 0 & 0 & 0 & 0 & 0 & 0 \\
0 & 0 & d_3 & 0 & 0 & 0 & 0 & 0 & 0 & 0 & 0 & 0 \\
0 & 0 & 0 & d_4(T) & 0 & 0 & 0 & 0 & 0 & 0 & 0 & 0 \\
0 & 0 & 0 & 0 & d_5 & 0 & 0 & 0 & 0 & 0 & 0 & 0 \\
0 & 0 & 0 & 0 & 0 & d_6(T) & 0 & 0 & 0 & 0 & 0 & 0 \\
0 & 0 & 0 & 0 & 0 & 0 & d_7(T) & 0 & 0 & 0 & 0 & 0 \\
0 & 0 & 0 & 0 & 0 & 0 & 0 & d_8 & 0 & 0 & 0 & 0 \\
0 & 0 & 0 & 0 & 0 & 0 & 0 & 0 & d_9(T) & 0 & 0 & 0 \\
0 & 0 & 0 & 0 & 0 & 0 & 0 & 0 & 0 & \frac{1}{2}d_{10}(T) & 0 & 0 \\
0 & 0 & 0 & 0 & 0 & 0 & 0 & 0 & 0 & 0 & d_{11} & 0
\end{pmatrix}$$

and

$$\begin{aligned} V &= diag(\mu_1; d_2(T) + \mu_2; d_3 + \mu_3; d_4(T) + \mu_4; d_5 + \mu_5(0); d_6(T) + \mu_6; d_7(T) + \mu_7; \\ &\quad d_8 + \mu_8(0); d_9(T) + \mu_9; d_{10}(T) + \mu_{10}; d_{11} + \mu_{11}(0); d_{12}(T) + \mu_{12}). \end{aligned}$$

All real parts of the eigenvalues of J_1 are less than zeros if and only if the dominant eigenvalue of the positive matrix FV^{-1} is less than 1 according to [21, Theorem 6.13]. Furthermore, the characteristic equation of matrix FV^{-1} is $\lambda^{12} - \mathcal{R}_0^{v,c} = 0$, where

$$\mathcal{R}_0^{v,c} = \frac{d_2(T)}{d_2(T)+\mu_2}\frac{d_3}{d_3+\mu_3}\frac{d_4(T)}{d_4(T)+\mu_4}\frac{d_5}{d_5+\mu_5(0)}\frac{d_6(T)}{d_6(T)+\mu_6}\frac{d_7(T)}{d_7(T)+\mu_7}$$
$$\frac{d_8}{d_8+\mu_8(0)}\frac{d_9(T)}{d_9(T)+\mu_9}\frac{\frac{1}{2}d_{10}(T)}{d_{10}(T)+\mu_{10}}\frac{d_{11}}{d_{11}+\mu_{11}(0)}\frac{d_{12}(T)}{d_{12}(T)+\mu_{12}}\frac{pf(0)}{\mu_1}.$$

Note that each factor in the above multiplication except $\frac{f(0)}{\mu_1}$ represents the survival rate, where $\frac{f(0)}{\mu_1}$ is the net reproduction rate during the mean duration of egg-laying females ($\frac{1}{\mu_1}$).

This dominant eigenvalue is smaller than one if and only if $\mathcal{R}_0^{v,c} < 1$. The definition, given in [21], yields the reproductive ratio of such a system (though not really an epidemic model) as $\sqrt[12]{\mathcal{R}_0^{v,c}}$. Here, we tentatively consider this reproductive ratio as a threshold parameter. In Chapter 3, we will have more discussions about the basic reproductive ratio. Regardless, we conclude that E_0 is locally asymptotically stable if and only if $\mathcal{R}_0^{v,c} < 1$, and is also globally asymptotically stable according to lemma 2.2.1 and the comparison theorem [92, Theorem 5.1.1]; and E_0 is unstable if and only if $\mathcal{R}_0^{v,c} > 1$. We assume in the remaining part of this section that $\mathcal{R}_0^{v,c} > 1$.

Setting the right-hand sides of (2.2.1) to zeros, we obtain the following relations:

$$\begin{aligned} H(x_{11}): &= f(x_{11}) \times k_1 - (d_5 + \mu_5(x_5))(d_8 + \mu_8(x_8))(d_{11} + \mu_{11}(x_{11}), \\ x_8 &= k_2(d_{11} + \mu_{11}(x_{11}))x_{11}, \\ x_5 &= k_3(d_8 + \mu_8(x_8))x_8, \end{aligned}$$

where

$$\begin{aligned} k_1 &= \frac{d_2(T)}{d_2(T)+\mu_2} \cdot \frac{d_3}{d_3+\mu_3} \cdot \frac{d_4(T)}{d_4(T)+\mu_4} \cdot \frac{d_6(T)}{d_6(T)+\mu_6} \cdot \frac{d_7(T)}{d_7(T)+\mu_7} \cdot \frac{d_9(T)}{d_9(T)+\mu_9} \cdot \\ &\quad \frac{\frac{1}{2}d_{10}(T)}{d_{10}(T)+\mu_{10}} \cdot \frac{d_{12}(T)}{d_{12}(T)+\mu_{12}} \cdot \frac{p}{\mu_1} d_5 d_8 d_{11} > 0, \\ k_2 &= \frac{d_9(T)+\mu_9}{d_8} \cdot \frac{d_{10}(T)+\mu_{10}}{d_9(T)} \cdot \frac{1}{\frac{1}{2}d_{10}(T)} > 0, \\ k_3 &= \frac{d_6(T)+\mu_6}{d_5} \cdot \frac{d_7(T)+\mu_7}{d_6(T)} \cdot \frac{1}{d_7(T)} > 0. \end{aligned}$$

A unique positive equilibrium of system (2.2.1) exists if and only if there exists some unique $x_{11}^* > 0$ such that $H(x_{11}^*) = 0$.

We note that all of the terms $\mu_5(x_5)$, $\mu_8(x_8)$, $\mu_{11}(x_{11})$, which are functions of x_{11}, are monotonically increasing functions to x_{11}. Moreover, $f(x_{11})$ is a decreasing function of x_{11}. We hence conclude that $H(x_{11})$ is a monotonically decreasing function with respect to x_{11}. Moreover,

$$\begin{aligned} H(0) &= f(0) \times k_1 - (d_5 + \mu_5(0))(d_8 + \mu_8(0))(d_{11} + \mu_{11}(0)) \\ &= (d_5 + \mu_5(0))(d_8 + \mu_8(0))(d_{11} + \mu_{11}(0)(\mathcal{R}_0^{v,c} - 1) > 0. \end{aligned}$$

On the other hand, there exists $\bar{x}_{11} > 0$ such that $f(\bar{x}_{11}) = 0$ owing to the form of $f(x_{11})$, then $H(\bar{x}_{11}) = f(\bar{x}_{11})k_1 - (d_5 + \mu_5(x_5(\bar{x}_{11})))(d_8 + \mu_8(x_8(\bar{x}_{11})))(d_{11} + \mu_{11}(\bar{x}_{11})) < 0$. Therefore it follows that there exists a unique positive $0 < x_{11}^* < \bar{x}_{11}$ such that $H(x_{11}^*) = 0$. Consequently, a unique endemic equilibrium of system (2.2.1) exists if and only if $\mathcal{R}_0^{v,c} > 1$.

To address the stability of this unique endemic equilibrium, denote by $X^* := (x_1^*, x_2^*, \cdots, x_{12}^*) \in \mathbb{R}_+^{12} \backslash \{0\}$. We note that the Jacobian matrix J_2 at the endemic equilibrium can be expressed as $J_2 := A - B$, where A and B are given respectively by

$$A = \begin{pmatrix}
0 & 0 & 0 & 0 & 0 & 0 & 0 & 0 & 0 & 0 & 0 & d_{12}(T) \\
pf(x_{11}^*) & 0 & 0 & 0 & 0 & 0 & 0 & 0 & 0 & 0 & x_1^* pf'(x_{11}^*) & 0 \\
0 & d_2(T) & 0 & 0 & 0 & 0 & 0 & 0 & 0 & 0 & 0 & 0 \\
0 & 0 & d_3 & 0 & 0 & 0 & 0 & 0 & 0 & 0 & 0 & 0 \\
0 & 0 & 0 & d_4(T) & 0 & 0 & 0 & 0 & 0 & 0 & 0 & 0 \\
0 & 0 & 0 & 0 & d_5 & 0 & 0 & 0 & 0 & 0 & 0 & 0 \\
0 & 0 & 0 & 0 & 0 & d_6(T) & 0 & 0 & 0 & 0 & 0 & 0 \\
0 & 0 & 0 & 0 & 0 & 0 & d_7(T) & 0 & 0 & 0 & 0 & 0 \\
0 & 0 & 0 & 0 & 0 & 0 & 0 & d_8 & 0 & 0 & 0 & 0 \\
0 & 0 & 0 & 0 & 0 & 0 & 0 & 0 & d_9(T) & 0 & 0 & 0 \\
0 & 0 & 0 & 0 & 0 & 0 & 0 & 0 & 0 & \frac{1}{2}d_{10}(T) & 0 & 0 \\
0 & 0 & 0 & 0 & 0 & 0 & 0 & 0 & 0 & 0 & d_{11} & 0
\end{pmatrix}$$

and

$$B = diag(\mu_1; d_2(T) + \mu_2; d_3 + \mu_3; d_4(T) + \mu_4; d_5 + \mu_5(x_5^*) + \mu_5'(x_5^*)x_5^*; d_6(T) + \mu_6; d_7(T) + \mu_7; d_8 + \mu_8(x_8^*) + \mu_8'(x_8^*)x_8^*; d_9(T) + \mu_9; d_{10}(T) + \mu_{10}; d_{11} + \mu_{11}(x_{11}^*) + \mu_{11}'(x_{11}^*)x_{11}^*; d_{12}(T) + \mu_{12}).$$

Therefore, J_2 can be written as

$$J_2 := \begin{pmatrix} -a_{1,1} & & & & & a_{1,12} \\ a_{2,1} & -a_{2,2} & & & -a_{2,11} & \\ & a_{3,2} & -a_{3,3} & & & \\ & & \ddots & \ddots & & \\ & & & a_{11,10} & -a_{11,11} & \\ & & & & a_{12,11} & -a_{12,12} \end{pmatrix},$$

where $a_{i,j} > 0$ and all other empty entries are zeros. Hence, the endemic equilibrium is locally stable if all eigenvalues of J_2 have negative real parts.

Let λ be an eigenvalue of J_2 and a corresponding eigenvector be $X := (x_1, x_2, \cdots, x_{12})^T$. Then we have

$$(\lambda + a_{1,1})x_1 = a_{1,12}x_{12}, \tag{2.2.5}$$

$$(\lambda + a_{2,2})x_2 = a_{2,1}x_1 - a_{2,11}x_{11}, \tag{2.2.6}$$

$$(\lambda + a_{i,i})x_i = a_{i,i-1}x_{i-1} \quad i = 3, \cdots, 12. \tag{2.2.7}$$

It follows from (2.2.7) that

$$x_i = \frac{a_{i,i-1}}{\lambda + a_{i,i}} x_{i-1}, \quad i = 3, \cdots, 12. \tag{2.2.8}$$

Therefore, we have

$$x_{12} = \prod_{i=3}^{12} \frac{a_{i,i-1}}{\lambda + a_{i,i}} x_2, \tag{2.2.9}$$

$$x_{11} = \prod_{i=3}^{11} \frac{a_{i,i-1}}{\lambda + a_{i,i}} x_2. \tag{2.2.10}$$

Substituting (2.2.9) and (2.2.10) into (2.2.5) and (2.2.6) yields

$$\begin{cases} (\lambda + a_{1,1})x_1 - a_{1,12}\prod_{i=3}^{12}\frac{a_{i,i-1}}{\lambda+a_{i,i}}x_2 = 0, \\ -a_{2,1}x_1 + \left[(\lambda + a_{2,2}) + a_{2,11}\prod_{i=3}^{11}\frac{a_{i,i-1}}{\lambda+a_{i,i}}\right]x_2 = 0. \end{cases} \tag{2.2.11}$$

Then we arrive at the simplified characteristic equation

$$\begin{aligned} F(\lambda) &= \prod_{i=1}^{12}(\lambda + a_{i,i}) + (\lambda + a_{1,1})(\lambda + a_{12,12})a_{2,11}\prod_{i=3}^{11}a_{i,i-1} - a_{1,12}\prod_{i=2}^{12}a_{i,i-1} \\ &= 0. \end{aligned} \tag{2.2.12}$$

Note that the system (2.2.1) admits the endemic equilibrium $X^* = (x_1^*, \cdots, x_{12}^*) \in \mathbb{R}_+^{12} \setminus \{0\}$ if $\mathcal{R}_0^{v,c} > 1$. Putting the right-hand side of system (2.2.1) to zero at the endemic equilibrium X^* and following the relations below

$$d_i + \mu_i(x_i^*) = a_{i,i} - \mu_i'(x_i^*), \quad i = 5,\ 8,\ 11,$$

with a tedious but straightforward calculation, we can verify that

$$\prod_{i=1}^{12}a_{i,i} > a_{1,12}\prod_{i=2}^{12}a_{i,i-1}. \tag{2.2.13}$$

Recall that $f(x_{11}) = r_0 - \epsilon\ln(1.01 + x_{11}/D)$ $(0 < r_0 < 1,\ \epsilon > 0)$ (see Table 2.1). We start with the case $\epsilon = 0$, then $a_{2,11} = 0$. This leads to the matrix J_2 to be irreducible and quasi-positive. According to [97, TheoremA.45], then $\lambda := s(J_2)$ is an eigenvalue of J_2 with strictly positive eigenvectors, where $s(J_2)$ is the largest real part of all eigenvalues of J_2. Assuming $\lambda \geq 0$ and substituting λ into (2.2.12), it follows that

$$F(\lambda) = \prod_{i=1}^{12}(\lambda + a_{i,i}) - a_{1,12}\prod_{i=2}^{12}a_{i,i-1} \geq \prod_{i=1}^{12}a_{i,i} - a_{1,12}\prod_{i=2}^{12}a_{i,i-1} > 0,$$

a contradiction. Therefore matrix J_2 with ϵ is zero has only eigenvalues with negative real parts. The continuous dependence of solutions on the parameter ϵ implies that all eigenvalues of J_2 have negative real parts if ϵ is small enough, namely, the endemic equilibrium is locally asymptotically stable when we have the weak density dependent reduction in fecundity of egg-laying females. In summary, we have

Theorem 2.2.2. *When $\mathcal{R}_0^{v,c} < 1$, the system (2.2.1) has a unique tick-free equilibrium, which is globally asymptotically stable. When $\mathcal{R}_0^{v,c} > 1$, then an endemic equilibrium exists, and it is unique and locally asymptotically stable if $\epsilon << 1$.*

Next we investigate the persistence of the tick population. Recall that $f(x_{11})$ is a decreasing function of x_{11}. Replacing $f(x_{11})$ by $f(0)$ in the system (2.2.1), we get a system of ordinary differential equations system:

$$\dot{\tilde{x}}_i(t) = \tilde{f}_i(\tilde{x}_i, \tilde{x}_{i-1}), \quad i = 1, 2, \cdots, 12 \tag{2.2.14}$$

with denoting $\tilde{x_0} = \tilde{x}_{12}$. We have the following

Theorem 2.2.3. *For system (2.2.14), there exists a unique endemic equilibrium which is globally asymptotically stable, when $\mathcal{R}_0^{v,c} > 1$.*

The proof of the existence of the endemic equilibrium is similar to the proof for equations (2.2.1), by considering the function

$$G(\tilde{x}_{11}) = (d_5 + \mu_5(\tilde{x_5}))(d_8 + \mu_8(\tilde{x_8}))(d_{11} + \mu_{11}(\tilde{x}_{11})) - f(0)k_1. \tag{2.2.15}$$

Since system (2.2.14) is a positive feedback cyclic system, then the system has a unique positive equilibrium in the positively invariant set $\mathbb{R}^{12}_+$ in case of $\mathcal{R}_0^{v,c} > 1$, the forward trajectory of every initial point of $\mathbb{R}^{12}_+\backslash\{0\}$ approaches the equilibrium $\tilde{X}^*$.

Now, let $X(t, X_0)$ be a solution of system (2.2.1) starting initial point $X_0 \in \mathbb{R}^{12}_+\backslash\{0\}$, let $\tilde{X}(t, X_0)$ be a solution of system (2.2.14) with the same initial data. By a standard comparison argument, we get $X(t, X_0) \leq \tilde{X}(t, X_0), \forall t \geq 0$. Taking limit both sides gives $\lim_{t\to\infty} X(t, X_0) \leq \lim_{t\to\infty} \tilde{X}(t, X_0) = \tilde{X}^*$. Choosing initial value $X_0 = X^* \in \mathbb{R}^{12}_+$ in the above inequality gives $X^* = \lim_{t\to\infty} X(t, X^*) \leq \lim_{t\to\infty} \tilde{X}(t, X^*) \leq \tilde{X}^*$. Moreover, $\limsup_{t\to\infty} X(t, X_0) \leq \tilde{X}^*$. This implies, when t is large enough, that $0 < X(t, X_0) \leq \tilde{X}^*$. In particular, $\forall\, \varepsilon \geq 0$, $\exists\, t_1 > 0$ so that for $t \geq t_1$ we have $x_{11}(t, X_0) \leq \tilde{x}^*_{11} + \varepsilon$. Thus since f is decreasing, $f(x_{11}(t, X_0)) \geq f(\tilde{x}^*_{11} + \varepsilon)$, when t large enough. Taking $\varepsilon \to 0$, we obtain $f(x_{11}(t, X_0)) \geq f(\tilde{x}^*_{11})$. Now, replacing $f(x_{11})$ by $f(\tilde{x}^*_{11})$ at second equation of system (2.2.1), this arrives at the third system

$$\dot{\hat{x}}_i = \hat{f}_i(\hat{x}_{i-1}, \hat{x}_i), \quad i = 1, \cdots, 12 \tag{2.2.16}$$

with $\hat{x}_0 = \hat{x}_{12}$.

Theorem 2.2.4. *when $\mathcal{R}_0^{v,c} > \frac{f(0)}{f(\tilde{x}^*_{11})} > 1$, then system (2.2.16) has a unique en-*

demic equilibrium $\hat{X}^* > 0$. *Moreover,*

$$\hat{X}^* \leq X^* \leq \tilde{X}^*, \textit{and} \;\; \hat{X}^* \leq X(t, X_0) \leq \tilde{X}^*, \textit{when } t \textit{ large enough.} \tag{2.2.17}$$

Proof. Using same arguments as above, we arrive at the following equation

$$L(\hat{x}_{11}) = (d_5 + \mu_5(\hat{x_5}))(d_8 + \mu_8(\hat{x_8}))(d_{11} + \mu_{11}(\hat{x}_{11})) - f(\tilde{x}^*_{11})k_1 = 0. \tag{2.2.18}$$

Similarly, the function $L(\hat{x}_{11})$ is also a strictly increasing function of $\hat{x}_{11}$. So, equation (2.2.18) has a unique positive solution $\hat{X}^*$ if and only if $L(0) < 0$, which is equivalent to $\frac{f(\tilde{x}^*_{11})}{f(0)}\mathcal{R}_0^{v,c} > 1$, i.e., $\mathcal{R}_0^{v,c} > \frac{f(0)}{f(\tilde{x}^*_{11})} > 1$.

A standard comparison argument gives

$$\hat{X}(t, X_0) \leq X(t, X_0), \forall \text{ initial value } X_0, \text{when } t \text{ large enough.} \tag{2.2.19}$$

Choosing $X_0 = X^*$. Then

$$\hat{X}(t, X^*) \leq X(t, X^*). \tag{2.2.20}$$

Since system (2.2.16) is also a positive feedback cyclic system, the forward trajectory of every nonzero initial point approaches the equilibrium $\hat{X}^*$. Taking limit for (2.2.20), we obtain

$$\hat{X}^* = \lim_{t\to\infty} \hat{X}(t, X^*) \leq \lim_{t\to\infty} X(t, X^*) = X^*. \tag{2.2.21}$$

From (2.2.19), it follows that

$$\hat{X}^* = \lim_{t\to\infty} \hat{X}(t, X_0) \leq \liminf_{t\to\infty} X(t, X_0). \tag{2.2.22}$$

Then there exists $\varepsilon \geq 0$ such that

$$\hat{X}^* - \varepsilon \leq X(t, X_0), \text{when t large enough.}$$

Taking limit, i.e., $\varepsilon \to 0$, we have

$$\hat{X}^* \leq X(t, X_0), \text{when t large enough.} \tag{2.2.23}$$

Therefore, $\hat{X}^* \leq X(t, X_0) \leq \tilde{X}^*$ when t large enough and $\hat{X}^* \leq X^* \leq \tilde{X}^*$, completing the proof. □

2.3 Simulations and discussions

To illustrate these theoretical results, we perform numerical simulations using MATLAB R2009a version for both case $\mathcal{R}_0^{v,c} < 1$ and $\mathcal{R}_0^{v,c} > 1$ using all parameters presented in Table 2.1.

Figure 2.2 (left graph) explains how the reproductive ratio $\mathcal{R}_0^{v,c}$ change is influenced by temperature (mean annual temperature in fact) when we fix other environmental conditions. For example, temperatures at 14.5 degree Celsius, $\mathcal{R}_0^{v,c} = 0.7018 < 1$ in this case, would not provide favorable environment for the development of vectors, thereby the spread of pathogen. Tick population can survive at temperature 15.5 degree Celsius which leads to $\mathcal{R}_0^{v,c} = 1.5770 > 1$. To depict the balance of host densities and temperature on reproductive ratio of the tick population, Figure 2.2 shows that low host densities could impede the growth of tick

developmental stages due to the scarcity of blood meal, further reduce the Lyme disease risk to the public owing to the low infection maintenance and spread.

Figures 2.3 and 2.4 confirm the theoretical results by capturing the trends of some key developmental stages: feeding larvae, feeding nymphs and feeding adults females over time period based on $\mathcal{R}_0^{v,c}$ value. These simulation results indicate all tick populations will die out under the temperature condition in case $\mathcal{R}_0^{v,c} < 1$ and tick population has the persistent development at certain temperature conditions when $\mathcal{R}_0^{v,c} > 1$.

In summary, we formulate and present a mathematical model based on the ecological history of the tick population, to analyse the effects of temperature change and hosts (rodents and deer) densities on the tick developmental stages and their establishment, in terms of the threshold value $\mathcal{R}_0^{v,c}$. Furthermore, this model helps to reveal the role of environment condition, mainly mean annual temperature, for *I. scapularis* population sustenance. As observed in the left graph of Figure 2.2, lower or higher temperature will not support the establishment of tick populations in an area by postponing or speeding up intersstadial development and limiting the time availability of tick activity. However high host densities can provide enough food and nourishment (right graph of Figure 2.2), thereby help in tick survival, development and even spread of *B. burgdorferi* infection. Our findings are in agreement with the earlier research on the Lyme disease ecology and with the earlier work

on tick population and Lyme disease models [79, 14, 4]. In general, our finding indicates temperature can be used as a crucial factor to predict the distribution, establishment of tick populations and thus the risk of Lyme disease in the new regions.

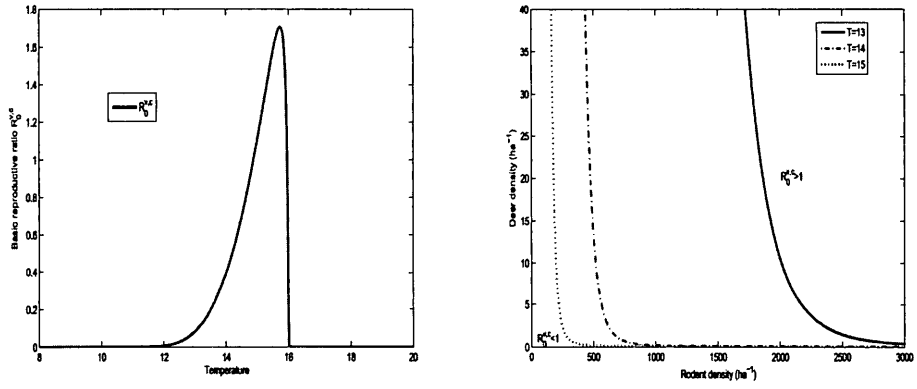

Figure 2.2: The relationship between $\mathcal{R}_0^{v,c}$ and mean annual temperature and number of hosts. Left graph represents the impact of mean annual temperature on reproductive ratio $\mathcal{R}_0^{v,c}$; right graph represents the effect of host densities and mean annual temperature on reproductive ratio $\mathcal{R}_0^{v,c}$.

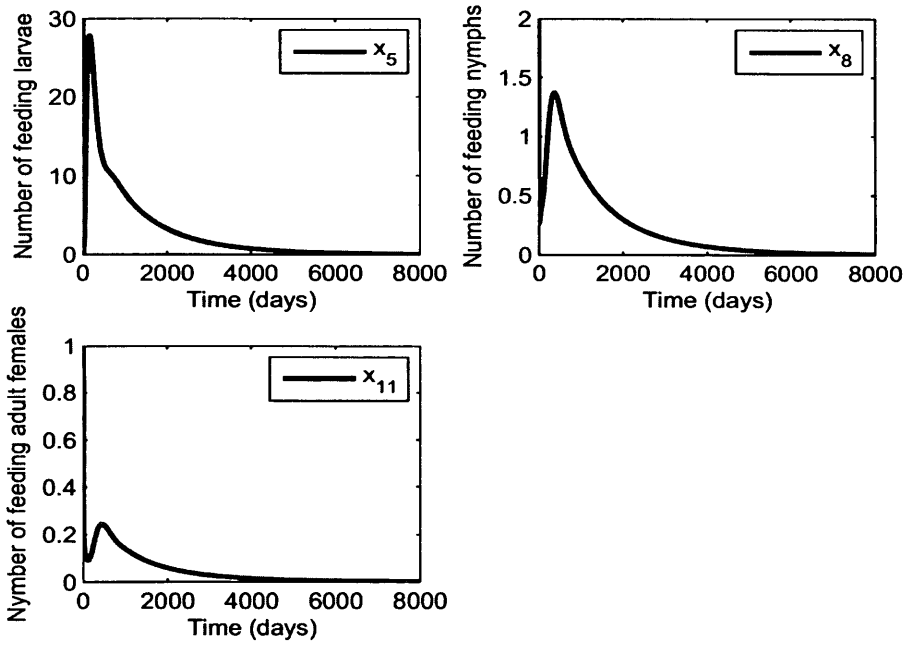

Figure 2.3: A graphic illustration of the result in Theorem 2.2.2 when $\mathcal{R}_0^{v,c} < 1$. Tick-free equilibrium is globally asymptotically stable in case $\mathcal{R}_0^{v,c} = 0.7018 < 1$, where the initial value is [0, 20, 30, 75, 30, 350, 100, 2, 10, 2, 1, 20], temperature sets as 14.5°C, and all other parameter values are the same as listed in Table 2.1.

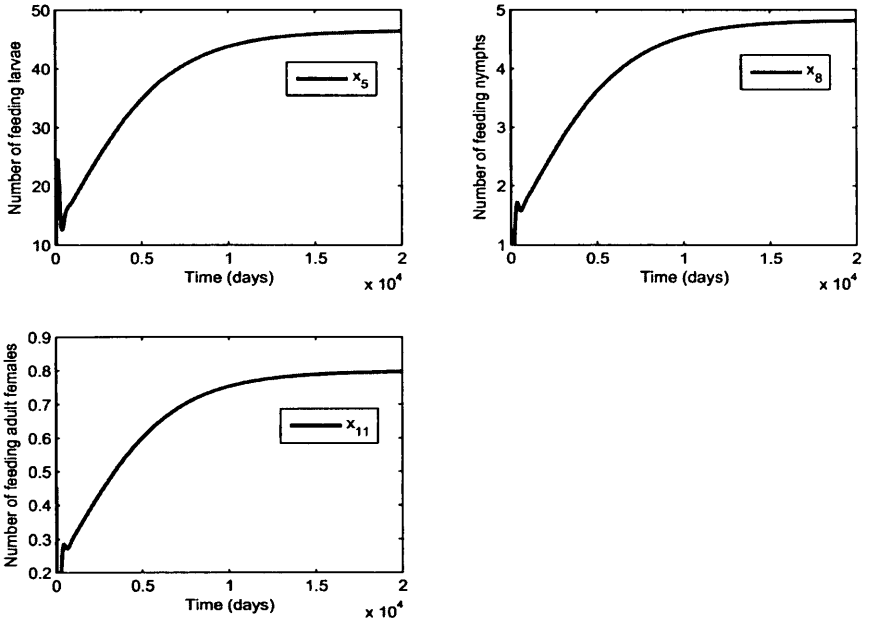

Figure 2.4: A graph of solution behavior when $\mathcal{R}_0^{v,c} > 1$. The tick-free equilibrium is unstable and the solution evolves to an endemic equilibrium which is global asymptotically stable in case $\mathcal{R}_0^{v,c} = 1.5770 > \frac{f(0)}{f(\tilde{x}_{11}^*)} = 1.0001 > 1$. Here the initial value is [0, 0, 0, 0, 0, 0, 0, 0, 0, 10, 0.4, 10], temperature sets as 15.5°C and all other parameter values are listed in Table 2.1.

3 Climate change-driven tick population dynamics with seasonal development

3.1 Introduction

In this chapter, we study the impact of climate change, in particular, mean monthly temperature change induced by seasonal force, on establishment of tick population in Canada. We develop a model for *I. scapularis* that is capable of providing values for basic reproductive ratio, denoted by $\mathcal{R}_0^{v,p}$. This is a key step in our evolving ability to develop tools for assessment of Lyme disease risk emergence and for development of public health policies on surveillance, prevention and control.

Ogden et al. (2005) used multiple simulations of their model [68], one for each of a number of locations in southeastern Canada, to obtain a threshold of monthly temperature conditions for *I. scapularis* population survival below which the duration of the lifecycle was too long to support long-term survival for particular field-observed rates of daily per capita mortality of the ticks. This allowed map-

ping of the geographic extent of limits for *I. scapularis* establishment, development of projected future limits for establishment according to predicted future climate change, as well as risk maps for tick establishment accounting for tick dispersion trajectories [68, 74, 75]. These practical and validated outcomes were possible because the simulation model precisely models the effects of temperature (and temperature-independent diapause) as delays in transition from one state to another (e.g. engorged larva to questing nymph) to produce a biologically realistic life-cycle length for the tick given the particular monthly temperature conditions for each location for which a simulation was run. The threshold of temperature condition for tick population survival (i.e. the number of ticks is eventually zero) was that at which the lifecycle of the tick is so long that the total number of ticks that die (the sum of daily mortalities) is greater than the number of eggs produced by mated females. This sort of model structure has been used in a number of studies of ticks [63, 79, 24] that aim to predict seasons of tick activity and variations in tick abundance in different locations.

Whether tick populations can persist or not under climate or other environmental conditions (e.g., temperature) may be summarized by the basic reproductive ratio $\mathcal{R}_0^{v,p}$, a key value in the field of infectious disease epidemiology for assessing environmental conditions under which micro-or macro-parasites can persist in nature. For microparasites it is defined as the average number of secondary cases

produced by one infectious primary case in a totally susceptible population and for macroparasites it is defined as the number of new female parasites produced by a female parasite when there are no density dependent constraints acting anywhere in the life cycle of the parasites [2]. The model structure [68] was developed to provide field-comparable values for numbers of ticks as an index of the effective reproductive number at model equilibrium. However, values for $\mathcal{R}_0^{v,p}$ cannot be obtained from this mechanistic model using existing mathematical techniques.

Our aim in this chapter is to derive an analytic formula to calculate $\mathcal{R}_0^{v,p}$ so we can evaluate the effects of climate and other environmental changes on $\mathcal{R}_0^{v,p}$. This is highly desirable because $\mathcal{R}_0^{v,p}$ is the universally accepted value to describe the propensity for a parasite or microparasite to survive and be propagated. To achieve this aim, we develop an appropriate, mathematically tractable model to which currently developed algorithms for calculating $\mathcal{R}_0^{v,p}$ can be applied directly.

We start, in section 3.2, to bring out a periodic system of ordinary differential equations, derive the basic reproductive ratio of *I. scapularis* as the spectral radius of an abstract integral operator, examine the condition under which the tick population can persist or not. We then use the derived $\mathcal{R}_0^{v,p}$ formula for validation of the outcomes of the model, sensitivity analysis and, for the first time, direct estimation of the effects of climate (in terms of ambient temperature) on $\mathcal{R}_0^{v,p}$ of *I. scapularis* to produce a map of $\mathcal{R}_0^{v,p}$ for this tick.

3.2 Model formulation and analysis

We refine the mechanistic model of [68] to examine the monthly temperature effect on each stage of the tick life cycle. Unlike those development rates of Chapter 2 (time-independent development rates), the rates of development and questing activity here vary according to mean monthly temperature at each day of each month of the year, which are time-dependent. This leads to a periodic system of ordinary differential equations. The system is essentially a mathematical simplification of a complex biological system, but by comparing output from the new model and the original mechanistic model [68] and field observation, we are able to show that the differential equation model developed here adequately describes the biological system for practical purposes and the objectives of our study. We adapt the same mathematical notations as those of Chapter 2 to denote a specific point of the tick's life cycle, that is egg-laying adult females (x_1), eggs (x_2), hardening larvae (x_3), questing larvae (x_4), feeding larvae (x_5), engorged larvae (x_6), questing nymphs (x_7), feeding nymphs (x_8), engorged nymphs (x_9), questing adults (x_{10}), feeding

adult females (x_{11}) and engorged adult females (x_{12}). The model is given by

$$
\begin{aligned}
x_1' &= d_{12}(t)x_{12} - \mu_1(t)x_1, \\
x_2' &= p(t)f(x_{11})x_1 - (d_2(t) + \mu_2(t))x_2, \\
x_3' &= d_2(t)x_2 - (d_3(t) + \mu_3(t))x_3, \\
x_4' &= d_3(t)x_3 - (d_4(t) + \mu_4(t))x_4, \\
x_5' &= d_4(t)x_4 - (d_5(t) + \mu_5(t, x_5))x_5, \\
x_6' &= d_5(t)x_5 - (d_6(t) + \mu_6(t))x_6, \\
x_7' &= d_6(t)x_6 - (d_7(t) + \mu_7(t))x_7, \\
x_8' &= d_7(t)x_7 - (d_8(t) + \mu_8(t, x_8))x_8, \\
x_9' &= d_8(t)x_8 - (d_9(t) + \mu_9(t))x_9, \\
x_{10}' &= d_9(t)x_9 - (d_{10}(t) + \mu_{10}(t))x_{10}, \\
x_{11}' &= \tfrac{1}{2}d_{10}(t)x_{10} - (d_{11}(t) + \mu_{11}(t, x_{11}))x_{11}, \\
x_{12}' &= d_{11}(t)x_{11} - (d_{12}(t) + \mu_{12}(t))x_{12}.
\end{aligned}
\tag{3.2.1}
$$

All the parameter definitions are the same as those in Table 2.1 of Chapter 2 except the values which vary in time. That is to say, $d_i(t)$ is the time-dependent progession rate from the i-th stage to the next, $\mu_i(t)/\mu_i(t, x_i)$ is the time-dependent or/and density-dependent death rate for stage i, and $p(t)$ is the time-dependent per-capita egg production rate by egg-laying adults females. We assume that each coefficient is a periodic function of time t with the same period of one year.

3.2.1 Mathematical analysis

For the stage-structured periodic tick model (3.2.1), we first rigorously show that it is biologically and mathematically well-posed, which ensures that the population size for each stage can not become negative (that is $x_i(t) \geq 0$ for each i), as established in the next lemma.

Lemma 3.2.1. *For any $x^0 \in \mathbb{R}^{12}_+$, system (3.2.1) has a unique nonnegative solution with $x(0) = x^0$, and each component of the solution is bounded for all $t > 0$.*

Proof. Re-writing the model system in the vector form

$$x'(t) = g(t, x),$$

we can see that $g(t, x)$ is continuous and Lipschitzian in x in each compact set in $\mathbb{R}^{12}_+$. Hence, there is a δ_x such that a unique non-continuable solution of system (3.2.1) exists on $[0, \delta_x)$ with $x(0) = x^0$. Note that $g_i(t, x) \geq 0$ whenever $x \in \mathbb{R}^{12}_+$ and $x_i = 0$. It then follows from [92, Theorem 5.2.1] that $\mathbb{R}^{12}_+$ is positively invariant.

Since $x_{11}(t) \geq 0$ and $f(x_{11})$ is a decreasing function of x_{11}, system (3.2.1) can

be controlled by the following linear system

$$
\begin{aligned}
x_1' &= d_{12}(t)x_{12} - \mu_1(t)x_1,\\
x_2' &= p(t)f(0)x_1 - (d_2(t) + \mu_2(t))x_2,\\
x_3' &= d_2(t)x_2 - (d_3(t) + \mu_3(t))x_3,\\
x_4' &= d_3(t)x_3 - (d_4(t) + \mu_4(t))x_4,\\
x_5' &= d_4(t)x_4 - d_5(t)x_5,\\
x_6' &= d_5(t)x_5 - (d_6(t) + \mu_6(t))x_6,\\
x_7' &= d_6(t)x_6 - (d_7(t) + \mu_7(t))x_7,\\
x_8' &= d_7(t)x_7 - d_8(t)x_8,\\
x_9' &= d_8(t)x_8 - (d_9(t) + \mu_9(t))x_9,\\
x_{10}' &= d_9(t)x_9 - (d_{10}(t) + \mu_{10}(t))x_{10},\\
x_{11}' &= \tfrac{1}{2}d_{10}(t)x_{10} - d_{11}(t)x_{11},\\
x_{12}' &= d_{11}(t)x_{11} - (d_{12}(t) + \mu_{12}(t))x_{12}.
\end{aligned}
\tag{3.2.2}
$$

Note that the solution for linear system (3.2.2) exists on $[0, \infty)$. By the comparison theorem (see, e.g., [92, Theorem 5.1.1]), each solution $x(t)$ of the nonlinear system (3.2.1) with initial value $x^0 \in \mathbb{R}^{12}_+$ exists globally.

Let $\hat{p} = \max_{t\in[0,\omega]} p(t)$, $\hat{d}_i = \max_{t\in[0,\omega]} d_i(t)$, $\tilde{d}_i = \min_{t\in[0,\omega]} d_i(t)$ for $i \in \{2, \cdots, 12\}$, $\tilde{\mu}_j = \min_{t\in[0,\omega]} \mu_j(t)$ for $j \in \{1, \cdots, 12\}\backslash\{5, 8, 11\}$, $\tilde{\mu}_j(0) = \min_{t\in[0,\omega]} \mu_j(t, 0)$ for $j = 5, 8$, $\tilde{\mu}_{11}(x_{11}) =$

$\min_{t\in[0,\omega]} \mu_{11}(t, x_{11})$. Then the original system (3.2.1) can be controlled by the following

$$
\begin{aligned}
x_1' &= \hat{d}_{12}x_{12} - \tilde{\mu}_1 x_1, \\
x_2' &= \hat{p}f(0)x_1 - (\tilde{d}_2 + \tilde{\mu}_2)x_2, \\
x_3' &= \hat{d}_2 x_2 - (\tilde{d}_3 + \tilde{\mu}_3)x_3, \\
x_4' &= \hat{d}_3 x_3 - (\tilde{d}_4 + \tilde{\mu}_4)x_4, \\
x_5' &= \hat{d}_4 x_4 - (\tilde{d}_5 + \tilde{\mu}_5(0))x_5, \\
x_6' &= \hat{d}_5 x_5 - (\tilde{d}_6 + \tilde{\mu}_6)x_6, \\
x_7' &= \hat{d}_6 x_6 - (\tilde{d}_7 + \tilde{\mu}_7)x_7, \\
x_8' &= \hat{d}_7 x_7 - (\tilde{d}_8 + \tilde{\mu}_8(0))x_8, \\
x_9' &= \hat{d}_8 x_8 - (\tilde{d}_9 + \tilde{\mu}_9)x_9, \\
x_{10}' &= \hat{d}_9 x_9 - (\tilde{d}_{10} + \tilde{\mu}_{10})x_{10}, \\
x_{11}' &= \tfrac{1}{2}\hat{d}_{10}x_{10} - (\tilde{d}_{11} + \tilde{\mu}_{11}(x_{11}))x_{11}, \\
x_{12}' &= \hat{d}_{11}x_{11} - (\tilde{d}_{12} + \tilde{\mu}_{12})x_{12}.
\end{aligned}
\tag{3.2.3}
$$

The system (3.2.3) is a cooperative and irreducible system. Using the same argument as those in section 2.2.1 of Chapter 2, we obtain that either zero equilibrium or a unique endemic equilibrium of the system (3.2.3) is globally asymptotically stable. Hence, the comparison principle implies that every solution $x(t)$ of system (3.2.1) with nonnegative initial value is bounded for all $t \in [0, \infty)$. □

3.2.2 Uniform persistence of positive periodic solutions

In this section, we show the existence of positive solutions of the system (3.2.1). We start to derive the basic reproductive ratio ($\mathcal{R}_0^{v,p}$) to classify the tick population dynamics. The basic reproductive ratio $\mathcal{R}_0^{v,p}$ determines the threshold value at which the tick population model exhibits the change of stability of the tick-free state and the change of population dynamics from persistence to extinction [21, 99]. More precisely, $\mathcal{R}_0^{v,p} > 1$ implies the instability of the tick-free state and the persistence of ticks, while $\mathcal{R}_0^{v,p} < 1$ implies the stability of the tick-free state and hence the extinction of the ticks. Hartemink et al. [36] presented an approach to estimate the $\mathcal{R}_0^{v,p}$ of tick-borne infections by obtaining the dominant eigenvalue of the next generation matrix of their model equations. This technique is applicable to the case where parameters of the system are constant. Here, we used a recently developed general approach [8, 99] to evaluate $\mathcal{R}_0^{v,p}$ for time periodic systems.

3.2.2.1 Basic reproductive ratio ($\mathcal{R}_0^{v,p}$)

In the approaches recently developed by [8, 99], the calculation of $\mathcal{R}_0^{v,p}$ is determined by the system (3.2.1) linearized at the tick-free state given below:

$$\begin{aligned}
x_1' &= d_{12}(t)x_{12} - \mu_1(t)x_1,\\
x_2' &= p(t)f(0)x_1 - (d_2(t) + \mu_2(t))x_2,\\
x_3' &= d_2(t)x_2 - (d_3(t) + \mu_3(t))x_3,\\
x_4' &= d_3(t)x_3 - (d_4(t) + \mu_4(t))x_4,\\
x_5' &= d_4(t)x_4 - (d_5(t) + \mu_5(t,0))x_5,\\
x_6' &= d_5(t)x_5 - (d_6(t) + \mu_6(t))x_6,\\
x_7' &= d_6(t)x_6 - (d_7(t) + \mu_7(t))x_7,\\
x_8' &= d_7(t)x_7 - (d_8(t) + \mu_8(t,0))x_8,\\
x_9' &= d_8(t)x_8 - (d_9(t) + \mu_9(t))x_9,\\
x_{10}' &= d_9(t)x_9 - (d_{10}(t) + \mu_{10}(t))x_{10},\\
x_{11}' &= \tfrac{1}{2}d_{10}(t)x_{10} - (d_{11}(t) + \mu_{11}(t,0))x_{11},\\
x_{12}' &= d_{11}(t)x_{11} - (d_{12}(t) + \mu_{12}(t))x_{12}.
\end{aligned} \tag{3.2.4}$$

The basic reproductive ratio describes the net reproduction (birth rate minus death rate) per generation when the tick population is small (near the tick-free state). However, since the tick population is stratified by development stages, the calculation of $\mathcal{R}_0^{v,p}$ requires the separation of the processes of birth, development and death. As such, we first introduce the birth matrix $F(t) = (f_{ij}(t))_{12\times 12}$, where $f_{2,1}(t) = p(t)f(0)$ and $f_{i,j}(t) = 0$ if $(i,j) \neq (2,1)$. We also need to introduce the progressive matrix $V(t) = V^-(t) - V^+(t)$, with $V^+(t)$ and $V^-(t) := [V_1^-(t)|V_2^-(t)]$

denoting the input and output to a particular tick stage due to development or natural death. These are given by

$$V^{+}(t) = \begin{pmatrix} 0 & 0 & 0 & 0 & 0 & 0 & 0 & 0 & 0 & 0 & 0 & d_{12}(t) \\ 0 & 0 & 0 & 0 & 0 & 0 & 0 & 0 & 0 & 0 & 0 & 0 \\ 0 & d_2(t) & 0 & 0 & 0 & 0 & 0 & 0 & 0 & 0 & 0 & 0 \\ 0 & 0 & d_3(t) & 0 & 0 & 0 & 0 & 0 & 0 & 0 & 0 & 0 \\ 0 & 0 & 0 & d_4(t) & 0 & 0 & 0 & 0 & 0 & 0 & 0 & 0 \\ 0 & 0 & 0 & 0 & d_5(t) & 0 & 0 & 0 & 0 & 0 & 0 & 0 \\ 0 & 0 & 0 & 0 & 0 & d_6(t) & 0 & 0 & 0 & 0 & 0 & 0 \\ 0 & 0 & 0 & 0 & 0 & 0 & d_7(t) & 0 & 0 & 0 & 0 & 0 \\ 0 & 0 & 0 & 0 & 0 & 0 & 0 & d_8(t) & 0 & 0 & 0 & 0 \\ 0 & 0 & 0 & 0 & 0 & 0 & 0 & 0 & d_9(t) & 0 & 0 & 0 \\ 0 & 0 & 0 & 0 & 0 & 0 & 0 & 0 & 0 & d_{10}(t) & 0 & 0 \\ 0 & 0 & 0 & 0 & 0 & 0 & 0 & 0 & 0 & 0 & d_{11}(t) & 0 \end{pmatrix},$$

$$V_1^{-}(t) = \begin{pmatrix} \mu_1(t) & 0 & 0 & 0 & 0 & 0 \\ 0 & d_2(t)+\mu_2(t) & 0 & 0 & 0 & 0 \\ 0 & 0 & d_3(t)+\mu_3(t) & 0 & 0 & 0 \\ 0 & 0 & 0 & d_4(t)+\mu_4(t) & 0 & 0 \\ 0 & 0 & 0 & 0 & d_5(t)+\mu_5(t,0) & 0 \\ 0 & 0 & 0 & 0 & 0 & d_6(t)+\mu_6(t) \\ 0 & 0 & 0 & 0 & 0 & 0 \\ 0 & 0 & 0 & 0 & 0 & 0 \\ 0 & 0 & 0 & 0 & 0 & 0 \\ 0 & 0 & 0 & 0 & 0 & 0 \\ 0 & 0 & 0 & 0 & 0 & 0 \\ 0 & 0 & 0 & 0 & 0 & 0 \end{pmatrix},$$

and

$$V_2^-(t) = \begin{pmatrix} 0 & 0 & 0 & 0 & 0 & 0 \\ 0 & 0 & 0 & 0 & 0 & 0 \\ 0 & 0 & 0 & 0 & 0 & 0 \\ 0 & 0 & 0 & 0 & 0 & 0 \\ 0 & 0 & 0 & 0 & 0 & 0 \\ 0 & 0 & 0 & 0 & 0 & 0 \\ d_7(t)+\mu_7(t) & 0 & 0 & 0 & 0 & 0 \\ 0 & d_8(t)+\mu_8(t,0) & 0 & 0 & 0 & 0 \\ 0 & 0 & d_9(t)+\mu_9(t) & 0 & 0 & 0 \\ 0 & 0 & 0 & d_{10}(t)+\mu_{10}(t) & 0 & 0 \\ 0 & 0 & 0 & 0 & d_{11}(t)+\mu_{11}(t,0) & 0 \\ 0 & 0 & 0 & 0 & 0 & d_{12}(t)+\mu_{12}(t) \end{pmatrix}.$$

In the above progressive matrices, $V_{i,j}^+(t)$ is the input (development) rate of the ticks from the x_j-stage to the x_i-stage, and $V_{i,j}^-(t)$ is the output rate at which ticks at the x_j-stage move out to the x_i-stage, or die.

With these matrix notations, we can rewrite the linear system (3.2.4) as

$$\frac{dx(t)}{dt} = (F(t) - V(t))x(t).$$

Whether the tick population grows or decays over time is determined by how the population is (dynamically) transferred from the beginning to the end of a year. The growth or decay rate of the tick population is determined by the transfer rate. To calculate this transfer rate, we need to study the so-called fundamental matrix solution of the above linear periodic system. These are the solutions of the linear system with special initial conditions (see [33]) so that all other solutions

with arbitrarily given initial condition can be expressed analytically in terms of the fundamental matrix solution and the initial condition. The work in [8, 99] develops a general approach that ties the fundamental matrix solution of the above linear system and the growth or decay rate of tick population to the evolution operator $Y(t,s)$, $t \geq s$, of the linear periodic system $y' = -V(t)y$. This operator is defined as follows: for each $s \in \mathbb{R}$, the 12×12 matrix $Y(t,s)$ satisfies

$$\frac{d}{dt}Y(t,s) = -V(t)Y(t,s) \quad \forall t \geq s, \quad Y(s,s) = I,$$

where I is the 12×12 identity matrix. To relate to the basic reproductive ratio, we let C_ω denote the collection of all possible initial tick populations distributed over the period $[0,\omega]$-the set of all continuous periodic functions from $[0,\omega]$ to R^{12} equipped with certain mathematical structures such as the supremum norm. For a fixed initial tick population distribution $\phi \in C_\omega$, $F(s)\phi(s)$ is the rate of new ticks produced by the initial ticks who were introduced at time s, and $Y(t,s)F(s)\phi(s)$ represents the distribution of those ticks who were newly produced at time s and remained alive at time t for $t \geq s$. Hence,

$$\psi(t) = \int_{-\infty}^{t} Y(t,s)F(s)\phi(s)ds = \int_{0}^{\infty} Y(t,t-a)F(t-a)\phi(t-a)da$$

is the distribution of accumulated ticks at time t produced by all those ticks $\phi(s)$ introduced at the previous time. This naturally leads to the linear operator L :

$C_\omega \to C_\omega$ given by

$$(L\phi)(t) = \int_0^\infty Y(t, t-a)F(t-a)\phi(t-a)da \quad \forall t \in \mathbb{R}, \quad \phi \in C_\omega.$$

It then follows from [99] that L is the next generation operator, and the basic reproductive ratio is $\mathcal{R}_0^{v,p} := \rho(L)$, the spectral radius of L.

3.2.2.2 Uniform persistence of tick population

Based on the basic reproductive ratio, we have the following two Theorems, which show that the tick population dies out if the basic reproductive ratio is less than unity while remains endemic in the habitat if the ratio exceeds one.

Theorem 3.2.2. *If the basic reproductive ratio $\mathcal{R}_0^{v,p} < 1$, then the zero solution is globally asymptotically stable.*

Proof. By [99, Theorem 2.2], we know that if $\mathcal{R}_0^{v,p} < 1$, then zero is locally asymptotically stable. It is sufficient to prove that zero is also globally attractive if $\mathcal{R}_0^{v,p} < 1$. Consider the linear system (3.2.4), that is

$$\frac{dx(t)}{dt} = (F(t) - V(t))x(t).$$

Denote $\Phi_{F-V}(t)$ and $\rho(\Phi_{F-V}(\omega))$ be the monodromy matrix of linear ω-periodic system (3.2.4) and the spectral radius of $\Phi_{F-V}(\omega)$, respectively. Since $\mathcal{R}_0^{v,p} < 1$, we have $\rho(\Phi_{F-V}(\omega)) < 1$. However the solution map of (3.2.4) is not strongly

monotone when $t > 0$, but it is eventually strongly monotone when $t \geq 11\omega$. The reason will be clear in Theorem 4.3.2 of Chapter 4. It then follows from [107, lemma 2.1] that there exists a positive, 11ω-periodic (also ω-periodic) function $h(t)$ such that

$$e^{\frac{1}{11\omega}ln(\rho(\Phi_{F-V}(11\omega)))t}h(t) = e^{\frac{1}{11\omega}ln(\rho(\Phi_{F-V}(\omega)))^{11}t}h(t) = e^{\frac{1}{\omega}ln(\rho(\Phi_{F-V}(\omega)))t}h(t)$$

is a solution of (3.2.4). Since $\rho(\Phi_{F-V}(\omega)) < 1$, $e^{\frac{1}{\omega}ln(\rho(\Phi_{F-V}(\omega)))t}h(t) \to 0$ as $t \to \infty$. For any nonnegative initial value x^0, there is a sufficiently large M such that $x^0 \leq Mh(0)$. Since system (3.2.1) can be controlled by the linear system (3.2.4), applying the comparison principle, we have $x(t, x^0) \leq Me^{\frac{1}{\omega}ln(\rho(\Phi_{F-V}(\omega)))t}h(t)$. Therefore, we obtain $x(t, x^0) \to 0$ as $t \to \infty$. □

Theorem 3.2.3. *If the basic reproductive ratio $\mathcal{R}_0^{v,p} > 1$, then there exists an $\epsilon > 0$ such that every solution $x(t, x^0)$ of system (3.2.1) with initial value $x^0 \neq 0$ satisfies*

$$\liminf_{t\to\infty} x_i(t, x^0) > \epsilon,$$

and system (3.2.1) admits at least one positive periodic solution.

Proof. Let $\hat{p} = \max_{t\in[0,\omega]} p(t)$, $D_i = \max_{t\in[0,\omega]} d_i(t)$ for $i \in \{2, \cdots, 12\}$, $\Delta_j = \min_{t\in[0,\omega]} \mu_j(t)$ for $j \in \{1, \cdots, 12\} \setminus \{5, 8, 11\}$, $\Delta_5 = \min_{t\in[0,\omega]} \mu_5(t, 0)$, $\Delta_8 = \min_{t\in[0,\omega]} \mu_8(t, 0)$ and $\Delta_{11} =$

$\min_{t\in[0,\omega]} \frac{\partial \mu_{11}(t,0)}{\partial x_{11}}$. Then the original system (3.2.1) can be controlled by the following

$$
\begin{aligned}
x_1' &= D_{12}x_{12} - \Delta_1 x_1,\\
x_2' &= \hat{p}f(0)x_1 - \Delta_2 x_2,\\
x_3' &= D_2 x_2 - \Delta_3 x_3,\\
x_4' &= D_3 x_3 - \Delta_4 x_4,\\
x_5' &= D_4 x_4 - \Delta_5 x_5,\\
x_6' &= D_5 x_5 - \Delta_6 x_6,\\
x_7' &= D_6 x_6 - \Delta_7 x_7,\\
x_8' &= D_7 x_7 - \Delta_8 x_8,\\
x_9' &= D_8 x_8 - \Delta_9 x_9,\\
x_{10}' &= D_9 x_9 - \Delta_{10} x_{10},\\
x_{11}' &= \tfrac{1}{2} D_{10} x_{10} - \Delta_{11} x_{11}^2,\\
x_{12}' &= D_{11} x_{11} - \Delta_{12} x_{12}.
\end{aligned}
\tag{3.2.5}
$$

It is easy to see that system (3.2.5) has a positive equilibrium x^*. Hence, this positive equilibrium is globally asymptotically stable with respect to $\mathbb{R}_+^{12} \setminus \{0\}$ according to [109, Corollary 3.2]. Moreover, an application of the comparison principle yields $\limsup_{t\to\infty} x(t,x^0) \leq x^*$, where $x(t,x^0)$ is the unique solution of (3.2.1) with $x(0,x^0) = x^0$ for $x^0 \in \mathbb{R}_+^{12}$. This indicates that system (3.2.1) is point dissipative.

Let $\Psi(t)$ be the solution map associated with system (3.2.1), that is

$$\Psi(t)(x^0) = x(t,x^0),\ \forall x^0 \in \mathbb{R}_+^{12},$$

where $x(t, x^0)$ is the unique solution of (3.2.1) with $x(0, x^0) = x^0$. Let $P : \mathbb{R}^{12}_+ \to \mathbb{R}^{12}_+$ be the Poincaré map associated with system (3.2.1), that is

$$P(x^0) = \Psi(\omega)(x^0), \ \forall x^0 \in \mathbb{R}^{12}_+.$$

Define $X = \mathbb{R}^{12}_+$, $X_0 = Int\mathbb{R}^{12}_+ = \{x \in \mathbb{R}^{12}_+ : x_i > 0, i = 1, 2, \ldots, 12\}$. Then ∂X_0 $:= X \setminus X_0 = \{x \in \mathbb{R}^{12}_+ : \Pi^{12}_{i=1} x_i = 0\}$. We first prove that P is uniformly persistent with respect to $(X_0, \partial X_0)$. By the form of (3.2.1), it is easy to see that both X and X_0 are positively invariant. Clearly, ∂X_0 is relatively closed in X. Furthermore, system (3.2.1) is point dissipative. Set $M_\partial = \{x \in \mathbb{R}^{12}_+ : P^m(x) \in \partial X_0, \forall m > 0\}$, then it is easy to see that $M_\partial = \{0\}$. Since $\mathcal{R}_0^{v,p} > 1$, then $\rho(\Phi_{F-V}(\omega)) > 1$. Hence, there exists a small $\delta > 0$ such that $\rho(\Phi_{F(\delta)-V}(\omega)) > 1$, where $F(\delta)$ is generated by replacing $f(0)$ with $f(\delta)$ in the matrix $F(t)$. It then follows from [99, Theorem 2.2] and [109, Theorem 2.2 and Lemma 2.1] that system (3.2.1) with $f(x_{11})$ replaced by $f(\delta)$ has a positive periodic solution $x^*(t, \delta)$, which is globally asymptotically stable with respect to $\mathbb{R}^{12}_+ \setminus \{0\}$. Suppose $x^*(t, 0)$ is the positive solution associated with system (3.2.1) with $f(x_{11})$ replaced by $f(0)$. Since $x^*(t, \delta) \to x^*(t, 0) \gg 0$ as $\delta \to 0$. We can choose a $\delta_0 < \delta$ small enough such that $x^*_{11}(t, \delta_0) > \delta_0$, $\forall t \geq 0$. Since

$$\lim_{x \to 0} \Psi(t)x = 0$$

uniformly for $t \in [0, \omega]$, there exists $\delta_1 > 0$ such that

$$\|\Psi(t)x\| < \delta_0/2, \ \forall t \in [0, \omega], \ \|x\| < \delta_1.$$

Our next claim shows that $\{0\}$ is a uniform weak repeller for X_0.

Claim: $\limsup_{n\to\infty} \|P^n(x)\| \geq \delta_1$ for all $x \in X_0$.

Suppose, by contradiction, that $\limsup_{n\to\infty} \|P^n x_0\| < \delta_1$ for some $x_0 \in X_0$. Let $A = \limsup_{n\to\infty} \|P^n x_0\|$, then $A < \delta_1$. Let $\varepsilon = \frac{\delta_1 - A}{2} > 0$. Since we know $\limsup_{n\to\infty} \|P^n x_0\| = A$, then there exists $n_1 > 0$, such that

$$\begin{aligned} \|P^n x_0\| &\leq A + \varepsilon = A + \varepsilon \\ &= A + \frac{\delta_1 - A}{2} = \frac{\delta_1}{2} + \frac{A}{2} \\ &< \frac{\delta_1}{2} + \frac{\delta_1}{2} = \delta_1. \end{aligned}$$

Let $t \geq n_1\omega$, there exists a $n_2 > 0$ such that $n_2 \geq n_1$ and $t - n_2\omega \in [0, \omega]$, therefore

$$\|\Psi(t)x_0\| = \|\Psi(t - n_2\omega)\Psi(n_2\omega)x_0\| = \|\Psi(t - n_2\omega)P^{n_2}x_0\| < \delta_0/2.$$

Since f is decreasing function along with $x_{11}(t) \leq \delta_0/2 < \delta_0$ when $t \geq n_1\omega$, we have

$$f(x_{11}(t)) \geq f(\delta_0/2) > f(\delta_0).$$

That is, there exists a $n_1 > 0$ such that $\|\Psi(t)(x_0)\| \leq \delta_0/2$ and $\frac{dx_2}{dt} \geq x_1 p(t) f(\delta_0) - (d_2(t) + \mu_2(t))x_2$, $\forall t \geq n_1\omega$. By the comparison principle, we have

$$\limsup_{t\to\infty} x_{11}(t, x_0) \geq x_{11}^*(t, \delta_0) > \delta_0,$$

a contradiction to $\|\Psi(t)(x_0)\| \leq \delta_0/2$ for all $t \geq n_1\omega$.

Note that every orbit in M_∂ approaches to $\{0\}$, and $\{0\}$ is acyclic in M_∂. By [108, Theorem 1.3.1], it follows that P is uniformly persistent with respect to $(X_0, \partial X_0)$. It then follows from [108, Theorem 3.1.1] that the solutions of system (3.2.1) are uniformly persistent with respect to $(X_0, \partial X_0)$, that is, there exists an $\epsilon > 0$ such that any solution $x(t, x^0)$ of system (3.2.1) with initial value $x^0 \neq 0$ satisfies

$$\liminf_{t\to\infty} x_i(t, x^0) > \epsilon.$$

Furthermore, [108, Theorem 1.3.6] implies that P has a fixed point $x^* \in X_0$. Thus, $x(t, x^*)$, the solution through x^*, is a positive periodic solution. □

3.3 Model parameterization and validation

The aim of this section is to provide the values of $\mathcal{R}_0^{v,p}$, defined in subsection 3.2.2.1, at each of 30 locations in southeastern Canada. Then we obtain a threshold of monthly temperature conditions for *I. scapularis* establishment, compare the results with the mechanistic model of [68]. To achieve this aim, we will first parameterize the model as described below.

3.3.1 Materials and methods

All model parameter values (3.2.1) are the same as for the model of [68], i.e. they are derived from laboratory and field studies in the Lyme-endemic woodlands of Long Point, Ontario, by Lindsay and collaborators [52, 51]. The host population is fixed at 200 rodents and 20 deer as in [68]. The hosts in the model are a considerable simplification of the community of hosts of *I. scapularis*, but this approach has been found to be adequate in field validation of the previous mechanistic version of the model (e.g. [75]). Specifically, all parameter values are the same as those in Table 2.1 of Chapter 2 except the development rates of POP, PEP, larva-to-nymph, nymph-to adult and questing activity. How to estimate these values will to be clear below (section 3.3.1.1). The estimated detailed formulas in one specific location over 1971-2000 period are shown in Appendix A. We adopt the method, outlined in Bacaër 2007 [5] and Wang and Zhao 2008 [99], to evaluate $\mathcal{R}_0$. This is based on the Floquet theory and a standard dichotomy argument.

3.3.1.1 Estimation of the development rates

For the study of [68] temperature data from the Port Dover weather station were used, this station being the closest to Long Point Ontario where the field data used in model calibration were collected, and where field studies on tick season-

ality allowed validation. However, Port Dover weather station has closed, so in this study we shall use temperature data from the Delhi CDA station (obtained from the Environment Canada website: www.climate.weatheroffice.gc.ca), which is the currently functioning weather station that is closest to Long Point (latitude: $42^0 36' N$; longitude: $80^0 05' W$), so that we can provide simulations with more recent temperature data (temperature normal for 1971-2000). The distance from the Delhi CDA station to Long point is 28.254 km, obtained by the city distance calculator from the website: www.javascripter.net/math/calculators/distancecalculator.htm. Some early studies of ticks in the field suggest that as far as air temperatures affecting development are concerned, this spatial resolution is adequate [71].

As described in the literature [51, 71], we assume that the development rates of POP, PEP and larva-to-nymph are temperature-dependent and development rates of nymph-to-adult are influenced by both temperature and temperature-independent diapause induced by photoperiodicity. Similarly questing activity is assumed to vary with temperature and as in [68] the host finding probabilities is varied according to host densities.

As in [68] we use the relationships between temperature and tick stage specific

development duration derived from field-validated laboratory observations [71]:

$$D_1(T) = 1300 \times T^{-1.42} \quad \text{(time delay for the pre-oviposition period)} \tag{3.3.6}$$

$$D_2(T) = 34234 \times T^{-2.27} \quad \text{(time delay for the pre-eclosion period of eggs)} \tag{3.3.7}$$

$$D_3(T) = 101181 \times T^{-2.55} \text{ (time delay for engorged larva to questing nymph)} \tag{3.3.8}$$

$$D_4(T) = 1596 \times T^{-1.21} \quad \text{(time delay for engorged nymph to questing adult)} \tag{3.3.9}$$

where T is the temperature in Celsius (°C). Nymph-to-adult development rates are only determined by temperature for those nymphs that fed before mid-June; all nymphs that feed after mid-June enter diapause (which is temperature independent and likely daylength-induced [71]) and molt on the same day of the next year, a day predicted by the temperature-development relationship, for nymphs feeding on December 31st of that year.

A key simplification here, compared to the model of [68], is that rather than accumulating daily proportions of development from one stage to another, the proportion of development for a particular day of the year (being the reciprocal of the relationship between duration of development and temperature on that day) becomes the proportion of ticks in a particular life stage that move to the next life stage on that day, i.e. this becomes the coefficient (that varies for each day of the year according to temperature) for the rate of movement from engorged to

molted ticks, engorged to egg-laying females and eggs to hatched larvae ($d_{12}(t)$, $d_2(t)$, $d_6(t)$ and $d_9(t)$). For the daily development rate ($d_9(t)$) of nymph-to-adult after the summer solstice, when temperature-independent diapause determines development time, the coefficient is the reciprocal of the estimated length of diapause for each day of the duration of diapause. As in [68] development is set at zero for all temperatures of 0°C and below. While this method is not biologically accurate (no tick of any stage develops to the next stage without undergoing the full process of development lasting weeks to months), this simplification would allow development of a differential equation model, and in our validation we aim to investigate whether this model is adequate or not.

Observations against field data [68] suggest that this method does not produce realistic seasonality of nymphal ticks, so a modified method of calculating the daily rate ($d_6(t)$) at which ticks move from the engorged larva state to the questing nymph state is used as described in the following. To estimate the larvae-to-nymph development rate for a specific day, temperature data points on that day and subsequent days are used. Suppose the temperature for day i is T_i, then the development duration from engorged larvae to molted nymphs under condition of subsequent constant temperature for day i is $D_3(T_i)$, which is calculated by the relationship between development and temperature (formula (3.3.8)). Therefore, the development proportion for day i is $1/D_3(T_i)$. Similarly, the development pro-

portion for day $i+1$ is $1/D_3(T_{i+1})$. When the sum of the accumulative proportion for subsequent n days:

$$\sum_{j=i}^{i+n} \frac{1}{D_3(T_j)}$$

equals unity, we obtain a number n and then $1/n$ is defined as the development rate of larva-to-nymph at the particular day i.

The 1971-2000 temperature normals used are averages of 30 years data and present as monthly means. While this is adequate for the mechanistic model of [68] we smooth the temperature-driven periodic coefficients for development by Fourier analysis as shown in Figure 3.1.

3.3.1.2 Sensitivity analysis

To assess the sensitivity of model outcomes to variations in each parameter we carry out a global sensitivity analysis with the Monte Carlo-based Latin Hypercube Sampling (LHS) variance method [61, 58] using the $\mathcal{R}_0^{v,p}$ as the outcome variable. All the parameters in the investigation are changed by 20% from their start values and then 600 simulations are run. Sensitivity to each given parameter is measured by the partial rank correlation coefficient (PRCC) between the parameter and the outcome variable ($\mathcal{R}_0^{v,p}$).

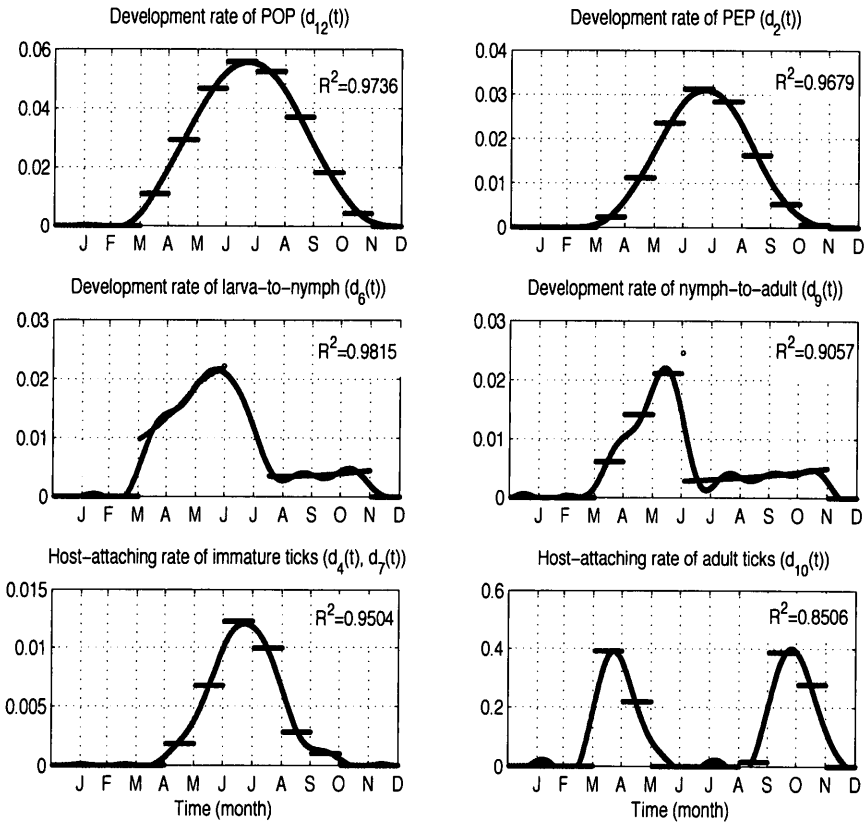

Figure 3.1: Development rates and host-attaching rates of *I. scapularis* ticks in a one year period. Blue lines represent development rates or host-attaching rates at each day of the year, calculated from the mean monthly normal temperature data of Delhi CDA for 1971-2000 periods. Red lines represent the development rates and host-attaching rates at each day of the year after smoothing by Fourier series. R^2 are shown.

3.3.1.3 Simulation and validation

We perform model simulations using temperature data (mean monthly temperature normal data for the period 1971-2000) from 16 meteorological stations in southern Ontario and 14 meteorological stations in Quebec. In each case $\mathcal{R}_0^{v,p}$ is calculated and these are compared with the data obtained in simulations of the model of [68]. From these latter data, Ogden et al. [68] produced a graph of the relationship between the cumulative degree days above 0°C for each meteorological station and an index of the numbers of ticks at model equilibrium. By finding the x-axis intercept of the fitted regression line the temperature conditions at which the number of ticks was zero in the model were determined. This graph is reproduced and compares with the $\mathcal{R}_0^{v,p}$ values obtained for the same locations using simulations of the model developed here. We also compare the seasonality of tick activity produced by the new model and the model in [68].

3.3.1.4 Mapping

A map of $\mathcal{R}_0^{v,p}$ values > 1 in Canada east of the Rocky Mountains (a different tick species transmits Lyme west of this) is prepared using the relationship between $\mathcal{R}_0^{v,p}$ and temperature conditions (using cumulative annual degree-days > 0°C $[DD > 0$°C] as an index) estimated from the simulations for meteorological stations in

Quebec (which provides a more cautious assessment of risk of *I. scapularis* invasion- see results section) as described above. The method used is similar to that described in [75]: $DD > 0$°C values are obtained for 2368 meteorological stations that have data for > 15 years during the period 1971-2000 and these values are converted to $\mathcal{R}_0^{v,p}$ values according to the relationship described above, and then $\mathcal{R}_0^{v,p}$ values are interpolated by inverse distance weighting across a 4×4 km pixelated landscape with pixel size 4×4 km.

3.4 Results

3.4.1 Model simulations

There is considerable concurrence in the outcomes of simulations by the modified model and the model of [68]. $\mathcal{R}_0^{v,p}$ for *I. scapularis* at Long Point, Point Pelee and Chatham, sites where *I. scapularis* populations are known to be established during the period 1971-2000, is estimated at 1.5, 3.19 and 3.65 respectively (Table 3.1). The temperature conditions identified by the two models as being those at which $\mathcal{R}_0^{v,p} = 1$ (i.e. threshold conditions for tick population persistence) are effectively identical at 3100 $DD > 0$°C (Figure 3.2). The relationship between $\mathcal{R}_0^{v,p}$ and $DD > 0$°C is essentially linear and, as in [68] slightly different for Ontario and Quebec ($\mathcal{R}_0^{v,p} = 0.0033DD > 0°C - 9.358$ and $\mathcal{R}_0^{v,p} = 0.003DD > 0°C - 7.551$ respectively).

Based on the aforementioned relationship between $\mathcal{R}_0^{v,p}$ and temperature conditions estimated from the simulations for meteorological stations, an $\mathcal{R}_0^{v,p}$ map for Canada is developed (Figure 3.3). Simulated seasonality of ticks by the two models are also similar (Figure 3.4).

3.4.2 Sensitivity analysis

Figure 3.5 presents the Partial Rank Correlation Coefficients (PRCC) for each parameter used in the sensitivity analysis that, in turn, explains the sensitivity of the $\mathcal{R}_0^{v,p}$ value to each parameter. The model is particularly sensitive (absolute PRCC > 0.7) to changes in summer (July, August, June) mean temperatures and host abundance of immature ticks. $\mathcal{R}_0^{v,p}$ is moderately sensitive to development rates of feeding ticks and mortalities of immature questing ticks. $\mathcal{R}_0^{v,p}$ is particularly insensitive to mean temperatures in April/October/November, mortalities of engorged/questing adults, mortalities of hardening larvae, number of deer (absolute PRCC < 0.2). Table 3.3 lists parameters in a descending order of importance.

3.5 Discussion

Our study applies a new mathematical approach to predict the survival and occurrence of the tick vector of Lyme disease, and by inference the spread of Lyme disease risk, using a direct $\mathcal{R}_0^{v,p}$-based approach.

Table 3.1: Outcomes of simulations of the current model and that in [68] (respectively $\mathcal{R}_0^{v,p}$ and numbers of feeding adult ticks at equilibrium). The locations of meteorological stations from Ontario where temperature data are used in the simulations.

Station	Location	Mean $DD > 0°C$	Resident tick (Y/N)	Maximum no. of FA at equilibrium	$\mathcal{R}_0^{v,p}$
Ontario					
Point Pelee	$41^0 57' N$, $82^0 31' W$	3791	Y	383	3.19
Chatham WCPC	$42^0 23' N$, $82^0 12' W$	3911	N	409	3.65
New Glasgow	$42^0 31' N$, $81^0 38' W$	3536	N	205	2.06
Port Stanley	$42^0 40' N$, $81^0 13' W$	3315	N	104	1.50
Courtright	$42^0 45' N$, $82^0 27' W$	3734	N	358	3.04
Delhi CDA	$42^0 52' N$, $80^0 33' W$	3441	N	N.A	2.04
London Airport	$43^0 02' N$, $81^0 09' W$	3355	N	104	1.73
Exeter	$43^0 21' N$, $81^0 29' W$	3336	N	100	1.71
Blyth	$43^0 43' N$, $81^0 23' W$	3221	N	54	1.30
Hanover	$44^0 07' N$, $81^0 00' W$	3100	N	23	1.01
Wiarton Airport	$44^0 45' N$, $81^0 06' W$	2959	N	0	0.71
South Baymouth	$45^0 35' N$, $82^0 01' W$	2733	N	0	0.52
Timmins Airport	$48^0 34' N$, $81^0 23' W$	2351	N	0	0.20
Cochrane	$49^0 04' N$, $81^0 02' W$	2256	N	0	0.17
Kapuskasing CDA	$49^0 24' N$, $82^0 26' W$	2317	N	0	0.19
Smoky Falls	$50^0 04' N$, $82^0 10' W$	2283	N	0	0.19

DD: Degree days; FA: Feeding adults; $\mathcal{R}_0^{v,p}$: The basic reproductive ratio; N.A: Not available in [68].

Table 3.2: Outcomes of simulations of the current model and that in [68] (respectively $\mathcal{R}_0^{v,p}$ and numbers of feeding adult ticks at equilibrium). The locations of meteorological stations from Quebec where temperature data are used in the simulations.

Station	Location	Mean $DD > 0°C$	Resident tick (Y/N)	Maximum no. of FA at equilibrium	$\mathcal{R}_0^{v,p}$
Quebec					
Hemmingford	$45^0 04' N$, $73^0 43' W$	3076	N	87	1.61
St Anicet	$45^0 08' N$, $74^0 21' W$	3167	N	126	1.86
Iberville	$45^0 20' N$, $73^0 15' W$	3131	N	117	1.80
Montreal McGill	$45^0 30' N$, $73^0 35' W$	3409	N	288	2.84
Ste Thérèse Ouest	$45^0 39' N$, $73^0 53' W$	3000	N	70	1.50
St Janvier	$45^0 44' N$, $73^0 53' W$	2860	N	24	1.19
Fleury	$45^0 48' N$, $73^0 00' W$	2969	N	54	1.37
Sorel	$46^0 02' N$, $73^0 07' W$	3095	N	129	1.94
St Côme	$46^0 17' N$, $73^0 45' W$	2417	N	0	0.38
St Zenon	$46^0 37' N$, $73^0 52' W$	2236	N	0	0.20
St Michel des Saints	$46^0 41' N$, $73^0 55' W$	2392	N	0	0.35
Grande Anse	$47^0 06' N$, $72^0 56' W$	2575	N	0	0.60
La Dore	$48^0 46' N$, $72^0 43' W$	2264	N	0	0.26
Chapais 2	$49^0 47' N$, $74^0 51' W$	2001	N	0	0.11

DD: Degree days; FA: Feeding adults; $\mathcal{R}_0^{v,p}$: The basic reproductive ratio; N.A: Not available in [68].

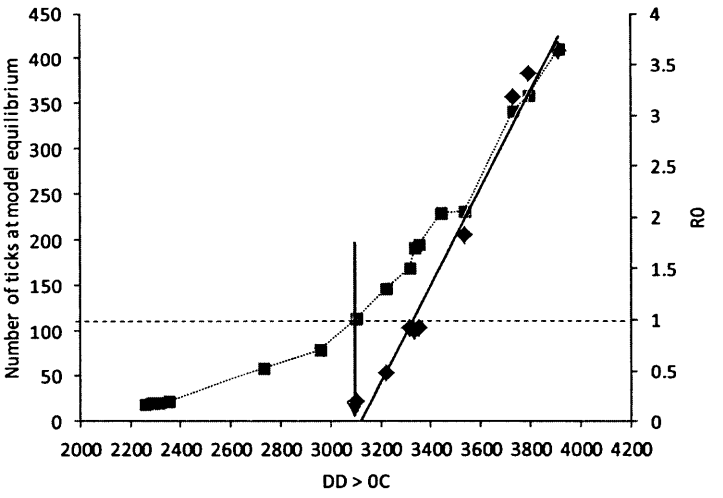

Figure 3.2: Model validation. $\mathcal{R}_0^{v,p}$ calculated in this study (light gray squares), as well as the maximum numbers of feeding adult ticks at equilibrium using the model of [68] (dark gray lozenges with linear trend line), are plotted against the mean annual number of degree-days > 0°C ($DD > 0$°C) for the meteorological stations in Ontario that provided temperature data for the simulations. The horizontal dashed line indicates $\mathcal{R}_0^{v,p} = 1$ on the secondary axis and the arrow indicates the value of $DD > 0$°C at which $\mathcal{R}_0^{v,p}$ is estimated at 1 by both models.

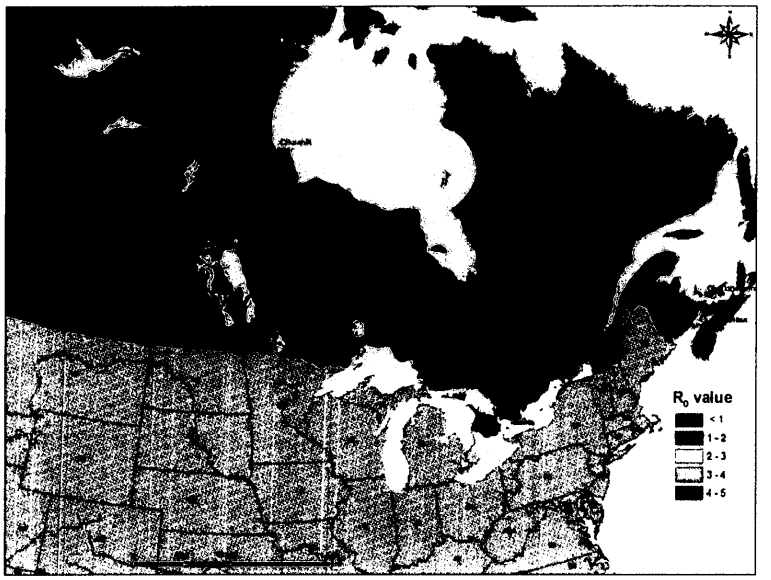

Figure 3.3: A map of $\mathcal{R}_0^{v,p}$ values for *I. scapularis* for Canada east of the Rocky Mountains. Assuming that all model parameter values other than those affected by temperature conditions are the same as those used in model simulations in this model.

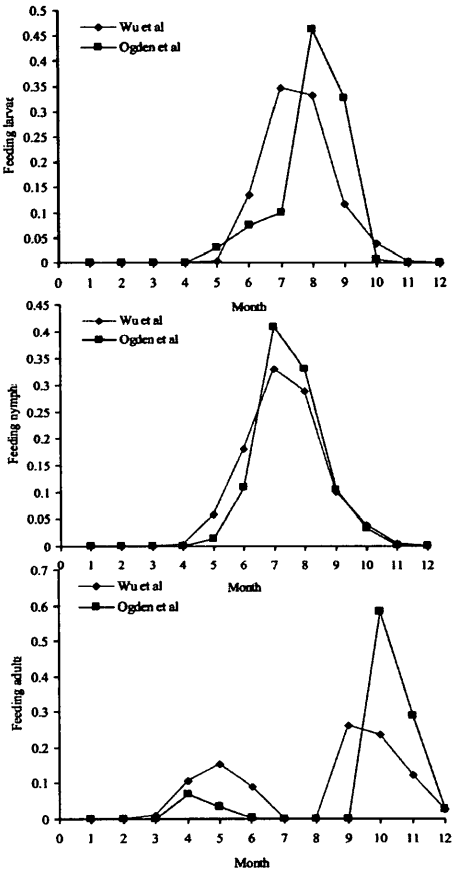

Figure 3.4: Comparison of model simulations of the seasonality of ticks (lozenges) generated by our model using mean monthly temperatures from Delhi CDA, Ontario meterorological station, and the seasonality simulated in [68] (square). The numbers of y-axis are the proportion of ticks of that instar feeding on the same day as field observations, against presented as a proportion of the total annual number of ticks feeding on the same dates in the simulation.

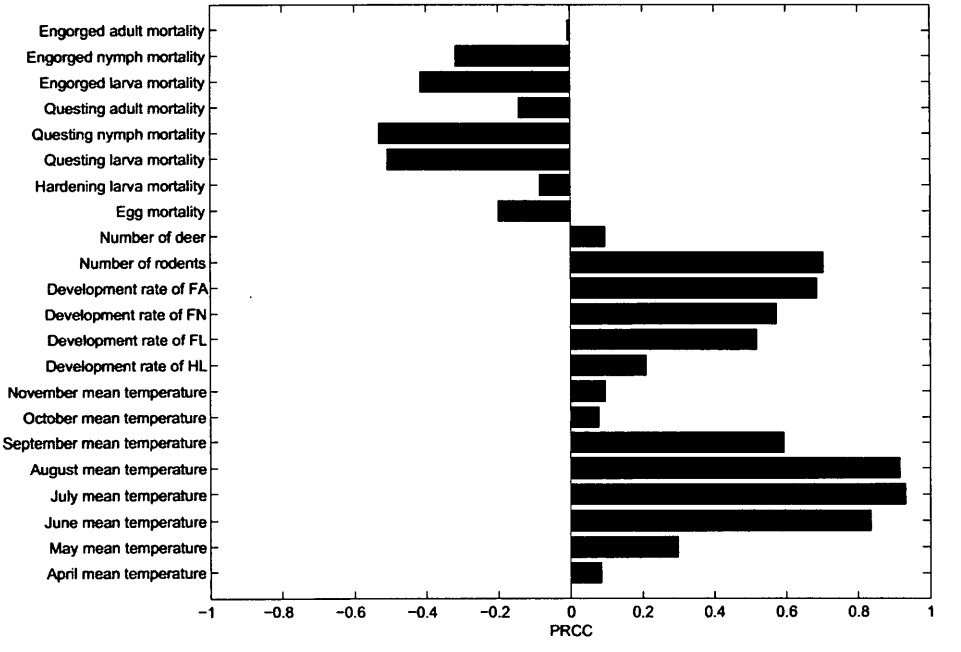

PRCC: Partial rank correlation coefficient

Figure 3.5: Global sensitivity analysis of $\mathcal{R}_0^{v,p}$. The graph is obtained by 20% change in the value of in the chosen different parameters and by 600 simulations.

Table 3.3: PRCC results for each parameter in the LHS/PRCC sensitivity analysis.

Parameter description	**PRCC**	**p-value**	**Significant** ($p < 0.01$)
July mean monthly temperature	0.93103	$8.9284e-255$	*
August mean monthly temperature	0.91524	$5.8975e-230$	*
June mean monthly temperature	0.83477	$1.1508e-151$	*
Number of rodents (R)	0.70357	$1.1792e-087$	*
Development rate of feeding adults (d_{11})	0.68585	$1.1092e-081$	*
September mean monthly temperature	0.5938	$1.861e-056$	*
Development rate of feeding nymphs (d_8)	0.57262	$9.5196e-052$	*
Questing nymph mortality (μ_7)	-0.53144	$1.6233e-043$	*
Development rate of feeding larvae (d_5)	0.51807	$4.4421e-041$	*
Questing larva mortality (μ_4)	-0.50762	3.0201e-039	*
Engorged larva mortality (μ_6)	-0.41474	$1.7793e-025$	*
Engorged nymph mortality (μ_9)	-0.31698	$5.5725e-015$	*
May mean monthly temperature	0.29966	$1.7717e-13$	*
Development rate of hardening larvae (d_3)	0.21037	$3.2498e-007$	*
Egg mortality (μ_2)	-0.20051	$1.1513e-006$	*
Questing adult mortality (μ_{10})	-0.14358	0.00052924	*
November mean monthly temperature	0.096436	0.020294	
Number of deer (D)	0.09592	0.020977	
Hardening larva mortality (μ_3)	-0.086626	0.037175	
April mean monthly temperature	0.08569	0.039279	
October mean monthly temperature	0.078827	0.058012	
Engorged adult mortality (μ_{12})	-0.0076705	0.85388	

This table summarizes results in terms of PRCC and p-value when changing model parameter values by 20% from their start values. The start values of mean monthly temperature are adapted from Delhi CDA weather station over 1971-2000 period, and all other parameters are the same as those in Table 2.1 in this study. The sign of PRCC represents the positive (+) or negative (-) response of $\mathcal{R}_0^{v,p}$ to the changed parameter values. The parameters are listed in descending order of the magnitude of the sensitivity of $\mathcal{R}_0^{v,p}$ to changes in their values. *: Significant at the $p < 0.01$.

Models of vectors and vector-borne diseases (including ticks and tick-borne pathogens) include those that aim to explore theoretically the behaviors of the systems, which may or may not use $\mathcal{R}_0^{v,p}$ as an index of the relative contributions or effects of different model parameters (e.g. [66, 85, 83, 82, 80, 16, 31, 29, 36]); and simulation models that aim to explicitly simulate aspects of the biology of vectors and vector-borne disease systems as accurately as possible (e.g. [63, 64, 79, 68, 24]). The outcomes of the latter models have been used to produce predictive and risk assessment tools for practical animal health and public health decision-making. Examples include risk maps for Lyme disease, Bluetonge virus and Leishmaniasis (e.g. [36, 35, 34]), but none to date have been able to produce maps using a dynamical version of $\mathcal{R}_0^{v,p}$.

Here we have developed a relatively highly parameterized model that employs the next generation matrix approach to obtain values for $\mathcal{R}_0^{v,p}$ in complex systems with multiple differential equations [23, 36, 34]. Special attention has to be made to ensure that the simplification of the mechanistic model of [68] allows retention of a key feature-a realistic modelling of the effect of temperature on total tick mortality indirectly induced by variations in the length of the tick lifecycle. Both models produce near identical results in terms of identifying the temperature conditions at which $\mathcal{R}_0^{v,p}$ falls below unity, i.e. they identify threshold environmental conditions for survival of the tick *I. scapularis*, which is a prerequisite for Lyme disease risk

emergence. However using the model developed here we can obtain and map direct estimates for $\mathcal{R}_0^{v,p}$ for *I. scapularis*. As a consequence we could produce an $\mathcal{R}_0^{v,p}$ map for *I. scapularis* for regions of Canada east of the Rocky Mountains (although this assumes habitat in terms of host community and off-host tick survival is constant). The geographic extent of territory where $\mathcal{R}_0^{v,p} > 1$ is similar to that for the map generated by the model of [68] although the $\mathcal{R}_0^{v,p}$ map immediately provides a gradient of suitability above $\mathcal{R}_0^{v,p} = 1$. To our knowledge this is the first $\mathcal{R}_0^{v,p}$ map for an arthropod tick vector.

Sensitivity analysis produces expected results. Because *I. scapularis* is an obligate parasite, host densities have a strong effect on tick abundance although deer abundance must fall below a certain threshold before the abundance of ticks falls significantly [69]. Also, variations in temperature conditions during the warmer months have a greater effect on $\mathcal{R}_0^{v,p}$ than changes during the coolest months because of the non-linear relationship between temperature and tick development rates [71]. This is also the reason why the relationships between $\mathcal{R}_0^{v,p}$ and $DD > 0°C$ are slightly different for simulations in southern Quebec and southern Ontario: summers are shorter but warmer in southern Quebec and $\mathcal{R}_0^{v,p}$ is rather higher than in southern Ontario for locations having the same $DD > 0°C$ values.

The accuracy of the model developed here is demonstrated by the model's ability to identify a threshold temperature condition for tick population persistence of

3100 $DD > 0$°C, which is the same as that identified by the model of [68]. This value has been extensively validated in the field against the locations of confirmed endemic populations of *I. scapularis* [75]. The appropriateness of our approach is also demonstrated by the ability of the model to simulate tick seasonality expected in northeastern North America [68]. The model is also, however, able to quantify relationships between temperature and $\mathcal{R}_0^{v,p}$. When $DD > 0$°C is greater than the threshold condition for $\mathcal{R}_0^{v,p} = 1$, $\mathcal{R}_0^{v,p}$ increases by approximately 0.5 for every 100 increase in $DD > 0$°C (see Fig 3.2) although this will vary with a number of model parameters such as host finding rates and host densities [68]. Subsequent empirical and field-observation studies have underlined the importance of temperature as a driver of establishment of *I. scapularis* ([70, 46]), and future studies must aim to precisely model effects of climate change on $\mathcal{R}_0^{v,p}$ for *I. scapularis*. Nevertheless, we have developed here a methodology for estimating $\mathcal{R}_0^{v,p}$ for ticks that can be used for practical animal and public health purposes.

The model presented here is parameterized in mostly the same way, and with the same values, as the model in [68], and the impact of variation in these on tick survival and abundance are explored in that paper as well as here. The factors affecting the threshold temperature conditions for $\mathcal{R}_0^{v,p} \geq 1$ are the relationship between temperature and development rates, and the per-capita daily mortality rates of free-living ticks [68]. As mentioned in [68] variations in the former could

occur with different genotypes of *I. scapularis* although we have no evidence for that. Variations in the latter could occur due to the characteristics of the habitats in which the ticks live, so for some locations the map in Fig 3.3 may rather over or under estimate risk (see [67] for details). Above the threshold conditions for $\mathcal{R}_0^{v,p} \geq 1$, the magnitude of the relationship between $\mathcal{R}_0^{v,p}$ and $DD > 0°C$ (and the abundance of ticks at equilibrium in [68]) depend on parameters such as host finding rates and host densities and these will vary from one location to the next according to different ecological conditions, but these factors will vary at a scale that is too fine for visualization at a national scale. They may well be very significant at a local, operational scale, however. Stochastic effects are not included in the model because of lack of information on which to parameterize them. Therefore, the model in this chapter estimates the main macroclimatic influence on possible tick population occurrence in Canada upon which more local variations in ecological conditions will be superimposed to determine $\mathcal{R}_0^{v,p}$ at these more precise locations. It would be expected that at marginal temperature conditions, stochastic events could drive recently established populations to extinction, but ticks are constantly re-introduced by migratory birds and other hosts to re-establish populations [72, 75] so stochastic fade out of tick populations would likely be only temporary in southern Canada. Furthermore, tick populations are resilient to wide temperature and humidity variations on a short (day-to-year) time scale because ticks actively

seek effective refugia from climatic extremes in the surface layers of the forest floor, and there is latency in changes in development rates in response to fluctuations in temperatures [71].

The methodology developed here can be expanded to directly model the effects on $\mathcal{R}_0^{v,p}$ for the agent of Lyme disease, *Borrelia burgdorferi*, of a greater range of environmental factors that determine Lyme disease risk establishment such as host densities, community structure, habitat effects on tick mortality, and immigration rates for ticks and *B. burgdorferi*. It could also be adapted for other tick species in other parts of the world.

3.6 Conclusion

We have developed a methodology for modelling the biology of the tick vector of Lyme disease to produce a value for $\mathcal{R}_0^{v,p}$ according to ambient temperature conditions. It can also be adapted to investigate how $\mathcal{R}_0^{v,p}$ may vary with other environmental variables such as host densities and habitat effects on tick mortality. The model can be used directly to assess the risk from emerging Lyme disease in Canada (and elsewhere) that will allow more effective planning of public health policy, and development/evaluation of preventive and control strategies. While the precise parameterizations of the model is relevant for Canada and the northeastern USA, the methodology is applicable to other tick species elsewhere in the world.

This tool is particularly powerful by providing a value for $\mathcal{R}_0^{v,p}$, which is the universally accepted value translatable to all branches of epidemiology including those involved in vector borne diseases (The malERA Consultative Group on Modeling [57]) and emerging infectious diseases (e.g. [100, 32, 28, 89, 26]). In the process we have produced estimates of $\mathcal{R}_0^{v,p}$ for locations in Canada where *I. scapularis* are established, and produced the first $\mathcal{R}_0^{v,p}$ map for an arthropod vector.

4 Spatial spread of tick population with seasonality

4.1 Introduction

Periodic systems arise very naturally in population dynamics when relevant biological activities are regulated by seasonality. When state variables of such systems correspond to the densities of the population at different development stages, we obtain certain positive feedback systems which generate monotone or order-preserving periodic processes/discrete dynamical systems. Interestingly, the associated periodic maps are usually not strongly monotone.

This lack of strong monotonicity of the periodic (solution) map for a system [91] has been previously observed by Smith [90] in a completely different setting of functional differential equations with constant coefficients, where the solution operators are not strongly monotone but eventually strongly monotone due to the involved time lags. We observe similar phenomena here for periodic systems even

without time lags, where model parameters such as birth and developmental rates are periodic in time but can be positive only during particular seasons of the year or the life cycle of the species considered. For this reason, it will take a few cycles for two ordered initial points to be strongly separated along their solutions and hence we can only expect the strong order-preserving property for some iterations of the periodic map. Existing results for strongly monotone maps can of course be applied to these iterations of the periodic map to yield such qualitative results as the threshold dynamics, existence of non-trivial fixed points, heteroclinic orbits, and traveling waves (if spatial movement involved), but only for the considered iteration of the period map. Although some qualitative aspects such as persistence/extinction can and have been addressed for discrete maps whose iterations are eventually strongly order-preserving, how to derive fine qualitative properties for the periodic map itself rather than its iterations remains an issue. For example, how do we know the minimal period of a stable positive periodic solution once if the periodic solution is established by applying general theories to an iteration of the periodic map? If this is a spatially homogeneous periodic solution of a corresponding reaction-diffusion system that corresponds to the persistence state of a transition (wavefront) from the trivial solution, how do we calculate the propagation speed/minimal wave speed of the periodic map when corresponding results are obtained by applying using general results to an iteration of the periodic map?

In this chapter, we develop some techniques to address the aforementioned questions, using a reaction-diffusion system modeling the range expansion of blacklegged tick *I. scapularis*. As discussed in the earlier chapters, the range expansion of *I. scapularis* is of importance for relevant tick-borne diseases control and prevention, and tick dispersal is a major reason for its northward spread in Canada. Though ticks ability of self-directed horizontal or long-range movement is very limited [19], the lifestyle of *I. scapularis* indicates that it is perfectly possible for the tick vector to disperse in a number of ways. Firstly, when engorged adult females lay eggs on the ground at the site where they detached from their hosts, the light-weighted eggs may have small movement due to the strong wind or the floating water. Secondly, *I. scapularis* can crawl no more than a few meters during any of its life stages [27, 56]. Feeding ticks move as far as their hosts during its lifetime. Furthermore, the relatively long feeding period (larvae feed for 3-5 days, nymphs feed for 3-4 days and adults feed for 5-7 days [94]) and the firm attachment once ticks attach to the host boost dispersal of the tick when the host moves in the environment. Finally, many studies [75, 87, 93] demonstrate that *I. scapularis* are carried into Canada by migratory birds in spring either from endemic foci in the United States or from existing Canadian habitats. How to model the effect of the mobility of ticks in their different development stages on the range expansion is the focus of this chapter.

In the rest of the chapter, we consider the range expansion of ticks in an isolated

unbounded 1-dimensional domain and we model the tick movement by diffusion. Our approach in analyzing the model is guided by applying some recent results in monotone reaction-diffusion equations with periodic coefficients [48, 49, 50, 55] to our specific setting, and we focus on how to move further beyond direct application of these results to an iteration of the periodic map so we can draw conclusions about the periodic map itself.

4.2 Model formulation

We capture some key stages of the tick life cycle, explicitly incorporating 7 mutually exclusive stages, and this yields a minor simplification of the model developed in [68]. In what follows, all variables are functions of space variable $x \in \mathbb{R}$ and the time variable t. These variables are the numbers of eggs ($E(t,x)$), questing larvae ($L_Q(t,x)$), feeding larvae ($L_F(t,x)$), questing nymphs ($N_Q(t,x)$), feeding nymphs ($N_F(t,x)$), questing adults ($A_Q(t,x)$) and feeding adults ($A_F(t,x)$).

We assume the birth rate of eggs per day is given by a periodic function (of time) $b(t)$, and we use $d_i(t)$ $(i = E, L, N)$ to denote respective development rates per day from eggs to larvae, from larvae to nymphs, and from nymphs to adults. We denote by $a_i(i = L, N, A)$ the attachment rate of questing larvae, nymphs and adults per day, respectively and these rates may depend on corresponding host densities (in our consideration, R is the number of rodents and D is the number of deers,

both assumed to be constants). Finally, we use $\mu_e, \mu_{ql}, \mu_{fl}, \mu_{qn}, \mu_{fn}, \mu_{qa}, \mu_{fa}$ to denote the death rates of ticks in respective stages. We emphasize that we use three density-dependent death rates $\mu_{fl}(L_F), \mu_{fn}(N_F), \mu_{fa}(A_F)$, and we assume each of these functions is strictly increasing, differentiable and goes to infinity when its argument goes to infinity with. In the following, all coefficients, if written as functions of the time variable t, will be assumed to be continuous and periodic with the period $\omega = 365$ days. As for spatial movements, we let $D_i (i = E, L_Q, L_F, N_Q, N_F, A_Q, A_F)$ be the diffusion coefficients of the ticks in respective stages, and we assume all coefficients are positive. We will use random diffusion to model the spatial movement of ticks and assume ticks move with different rates in different stages.

With these assumptions, we have the following system of reaction-diffusion equations with periodic coefficients:

$$
\begin{aligned}
\frac{\partial E}{\partial t} &= b(t)A_F - d_E(t)E - \mu_e E + D_E \frac{\partial^2 E}{\partial x^2}, \\
\frac{\partial L_Q}{\partial t} &= d_E(t)E - a_L(t,R)L_Q - \mu_{ql} L_Q + D_{L_Q} \frac{\partial^2 L_Q}{\partial x^2}, \\
\frac{\partial L_F}{\partial t} &= a_L(t,R)L_Q - d_L(t)L_F - \mu_{fl}(L_F)L_F + D_{L_F} \frac{\partial^2 L_F}{\partial x^2}, \\
\frac{\partial N_Q}{\partial t} &= d_L(t)L_F - a_N(t,R)N_Q - \mu_{qn} N_Q + D_{N_Q} \frac{\partial^2 N_Q}{\partial x^2}, \\
\frac{\partial N_F}{\partial t} &= a_N(t,R)N_Q - d_N(t)N_F - \mu_{fn}(N_F)N_F + D_{N_F} \frac{\partial^2 N_F}{\partial x^2}, \\
\frac{\partial A_Q}{\partial t} &= d_N(t)N_F - a_A(t,D)A_Q - \mu_{qa} A_Q + D_{A_Q} \frac{\partial^2 A_Q}{\partial x^2}, \\
\frac{\partial A_F}{\partial t} &= a_A(t,D)A_Q - \mu_{fa}(A_F)A_F + D_{A_F} \frac{\partial^2 A_F}{\partial x^2}.
\end{aligned}
\tag{4.2.1}
$$

The corresponding periodic systems of ordinary differential equations is

$$\begin{aligned}
\tfrac{dE}{dt} &= b(t)A_F - d_E(t)E - \mu_e E,\\
\tfrac{dL_Q}{dt} &= d_E(t)E - a_L(t,R)L_Q - \mu_{ql}L_Q,\\
\tfrac{dL_F}{dt} &= a_L(t,R)L_Q - d_L(t)L_F - \mu_{fl}(L_F)L_F,\\
\tfrac{dN_Q}{dt} &= d_L(t)L_F - a_N(t,R)N_Q - \mu_{qn}N_Q,\\
\tfrac{dN_F}{dt} &= a_N(t,R)N_Q - d_N(t)N_F - \mu_{fn}(N_F)N_F,\\
\tfrac{dA_Q}{dt} &= d_N(t)N_F - a_A(t,D)A_Q - \mu_{qa}A_Q,\\
\tfrac{dA_F}{dt} &= a_A(t,D)A_Q - \mu_{fa}(A_F)A_F,
\end{aligned} \tag{4.2.2}$$

and this system can be rewritten as

$$\frac{du}{dt} = G(t,u) \tag{4.2.3}$$

with initial data

$$u(0) = u^0 \in \mathbb{R}^7, \tag{4.2.4}$$

where,

$$\begin{aligned}
u(t) &= (u_1(t); u_2(t); u_3(t); u_4(t); u_5(t); u_6(t); u_7(t))\\
&= (E(t); L_Q(t); L_F(t); N_Q(t); N_F(t); A_Q(t); A_F(t))\,,
\end{aligned}$$

$$G(t,u) = \begin{pmatrix} b(t)u_7 - (d_E(t) + \mu_e)u_1 \\ d_E(t)u_1 - (a_L(t,R) + \mu_{ql})u_2 \\ a_L(t,R)u_2 - (d_L(t) + \mu_{fl}(u_3))u_3 \\ d_L(t)u_3 - (a_N(t,R) + \mu_{qn})u_4 \\ a_N(t,R)u_4 - (d_N(t) + \mu_{fn}(u_5))u_5 \\ d_N(t)u_5 - (a_A(t,D) + \mu_{qa})u_6 \\ a_A(t,D)u_6 - \mu_{fa}(u_7)u_7 \end{pmatrix}. \tag{4.2.5}$$

Since R and D are constants in this chapter, in what follows, we will write $a_L(t,R) = a_L(t)$, $a_N(t,R) = a_N(t)$ and $a_A(t,D) = a_A(t)$.

4.3 The spatially homogeneous system

We first show our mathematical model is biologically well-posed. Namely we show that the model (4.2.3) with initial condition (4.2.4) has a unique globally defined, differentiable solution which remains non-negative and bounded.

Proposition 4.3.1. *For system (4.2.3) with initial data (4.2.4), we have $u(t) \geq 0$ for all $t \geq 0$, that is, $\mathbb{R}^7_+$ is positively invariant. Moreover, the system (4.2.3) exists a unique and bounded solution $u(t,u^0)$ for every initial value $u^0 \in \mathbb{R}^7_+$.*

Proof. The nonnegativity of each $u_i(t)$ follows immediately from [92, Theorem 5.2.1]. Hence $\mathbb{R}^7_+$ is positively invariant for the system (4.2.3). It is easy to

check $G(t,u)$ is continuous, differentiable and locally Lipschitzian in u on each compact subset of $\mathbb{R}^7_+$. Hence, there is a unique solution $u(t,u^0)$ for system (4.2.3) through the initial value $u^0 \in \mathbb{R}^7_+$ in its maximal interval of the existence. Since $\mu_{fl}(u_3), \mu_{fn}(u_5), \mu_{fa}(u_7)$ are strictly increasing functions with respect to their arguments u_3, u_5, and u_7, system (4.2.3) can be controlled by the following linear system

$$\begin{aligned}
u_1' &= b(t)u_7 - (d_E(t) + \mu_e)u_1, \\
u_2' &= d_E(t)u_1 - (a_L(t) + \mu_{ql})u_2, \\
u_3' &= a_L(t)u_2 - (d_L(t) + \mu_{fl}(0))u_3, \\
u_4' &= d_L(t)u_3 - (a_N(t) + \mu_{qn})u_4, \\
u_5' &= a_N(t)u_4 - (d_N(t) + \mu_{fn}(0))u_5, \\
u_6' &= d_N(t)u_5 - (a_A(t) + \mu_{qa})u_6, \\
u_7' &= a_A(t)u_6 - \mu_{fa}(0)u_7.
\end{aligned} \tag{4.3.6}$$

Note that solutions for linear system (4.3.6) exist on $[0,\infty)$. By the comparison theorem [92, Theorem 5.1.1], every solution $u(t)$ of system (4.2.3) exists globally.

Next we establish the boundedness of solutions. For any periodic nonnegative function $f(t)$ with period ω, we denote $\hat{f} = \max_{t\in[0,\omega]} f(t)$. It is easy to see that system (4.2.3) can be controlled by the following cooperative and irreducible system with

constant coefficients:

$$\begin{aligned}
u_1' &= \hat{b}u_7 - \mu_e u_1, \\
u_2' &= \hat{d}_E u_1 - \mu_{ql} u_2, \\
u_3' &= \hat{a}_L u_2 - \mu_{fl}(0) u_3, \\
u_4' &= \hat{d}_L u_3 - \mu_{qn} u_4, \\
u_5' &= \hat{a}_N u_4 - \mu_{fn}(0) u_5, \\
u_6' &= \hat{d}_N u_5 - \mu_{qa} u_6, \\
u_7' &= \hat{a}_A u_6 - \mu_{fa}(u_7) u_7.
\end{aligned} \tag{4.3.7}$$

Clearly, when $\frac{\hat{a}_A}{\mu_{fa}(0)}\frac{\hat{d}_N}{\mu_{qa}}\frac{\hat{a}_N}{\mu_{fn}(0)}\frac{\hat{d}_L}{\mu_{qn}}\frac{\hat{a}_L}{\mu_{fl}(0)}\frac{\hat{d}_E}{\mu_{ql}}\frac{\hat{b}}{\mu_E} \leq 1$, only one nonnegative equilibrium 0 exists for system (4.3.7), which is globally asymptotically stable according to [109, Corollary 3.2]. If $\frac{\hat{a}_A}{\mu_{fa}(0)}\frac{\hat{d}_N}{\mu_{qa}}\frac{\hat{a}_N}{\mu_{fn}(0)}\frac{\hat{d}_L}{\mu_{qn}}\frac{\hat{a}_L}{\mu_{fl}(0)}\frac{\hat{d}_E}{\mu_{ql}}\frac{\hat{b}}{\mu_E} > 1$, system (4.3.7) admits a unique positive equilibrium, which is also globally asymptotically stable for all nonzero solutions by [109, Corollary 3.2]. Hence, the comparison principle implies that every solution $u(t)$ of system (4.2.3) with nonnegative initial value u^0 is bounded for all $t \in [0, \infty)$. □

4.3.1 Existence and stability of nonnegative periodic solutions

In this section, we show the existence and stability of two types of periodic solutions of system (4.2.3). Namely, the tick-free periodic solution and a tick-persistent periodic solution. We start with some notations.

Let $\mathcal{C}$ be the set of all bounded and continuous functions from $\mathbb{R}$ to $\mathbb{R}^7$ and $\mathcal{C}_+ = \{\varphi \in \mathcal{C} : \varphi(x) \geq 0, \forall x \in \mathbb{R}\}$. For $\varphi = (\varphi_1, \cdots, \varphi_7)^T$, $\psi = (\psi_1, \cdots, \psi_7)^T$ in $\mathcal{C}$, we write $\varphi \geq \psi$ ($\varphi \gg \psi$) provided $\varphi_i(x) \geq \psi_i(x)$ ($\varphi_i(x) > \psi_i(x)$), for any $i = 1, \cdots, 7$, $x \in \mathbb{R}$; $\varphi > \psi$ provided $\varphi \geq \psi$ but $\varphi \neq \psi$. It is easy to see that $\mathcal{C}_+$ is a closed cone of $\mathcal{C}$. In what follows, we will also identify a vector in $\mathbb{R}^7$ as a constant map with the vector value. For any $r \gg 0$, we define $[0, r] := \{u \in \mathbb{R}^7 : 0 \leq u \leq r\}$ and $\mathcal{C}_r := \{\varphi \in \mathcal{C} : 0 \leq \varphi \leq r\}$. We equip $\mathcal{C}$ with the compact open topology, i.e. $\varphi^m \to \varphi$ in $\mathcal{C}$ means that the sequence of $\varphi^m(x)$ converges to $\varphi(x)$ as $m \to \infty$ uniformly for x in any compact set in $\mathbb{R}$. Define

$$\|\varphi\|_{\mathcal{C}} = \sum_{k=1}^{\infty} \frac{\max_{|x| \leq k} |\varphi(x)|}{2^k}, \quad \forall \varphi \in \mathcal{C}, \tag{4.3.8}$$

where $|\cdot|$ denotes the usual norm in $\mathbb{R}^7$. Then $(\mathcal{C}, \|\cdot\|_{\mathcal{C}})$ is a normed space. Let $d_{\mathcal{C}}(\cdot, \cdot)$ be the distance induced by the norm $\|\cdot\|_{\mathcal{C}}$. It follows that the topology in the metric space $(\mathcal{C}, d_{\mathcal{C}})$ is the same as the compact open topology in $\mathcal{C}$. Moreover, $(\mathcal{C}_r, d_{\mathcal{C}})$ is a complete metric space.

Note that it is easy to see that 0 is an ω-periodic solution of system (4.2.3), and the corresponding linearized system for (4.2.3) at the zero solution is

$$\frac{dz}{dt} = D_u G(t, 0) z \tag{4.3.9}$$

with $D_u G(t,0)$ given by

$$\begin{pmatrix} -(\mu_e + d_E(t)) & 0 & 0 & 0 & 0 & 0 & b(t) \\ d_E(t) & -(a_L(t) + \mu_{ql}) & 0 & 0 & 0 & 0 & 0 \\ 0 & a_L(t) & -(d_L(t) + \mu_{fl}(0)) & 0 & 0 & 0 & 0 \\ 0 & 0 & d_L(t) & -(a_N(t) + \mu_{qn}) & 0 & 0 & 0 \\ 0 & 0 & 0 & a_N(t) & -(d_N(t) + \mu_{fn}(0)) & 0 & 0 \\ 0 & 0 & 0 & 0 & d_N(t) & -(a_A(t) + \mu_{qa}) & 0 \\ 0 & 0 & 0 & 0 & 0 & a_A(t) & -(\mu_{fl}(0)) \end{pmatrix}.$$

We follow ideas of [8, 99] to define the basic reproduction ratio for system (4.2.3). Let

$$F(t) = (f_{ij}(t))_{7\times 7}, \tag{4.3.10}$$

where $f_{1,7}(t) = b(t)$ and $f_{i,j}(t) = 0$ if $(i,j) \neq (1,7)$. In addition, we define $V(t)$ as

$$\begin{pmatrix} \mu_e + d_E(t) & 0 & 0 & 0 & 0 & 0 & 0 \\ -d_E(t) & a_L(t) + \mu_{ql} & 0 & 0 & 0 & 0 & 0 \\ 0 & -a_L(t) & d_L(t) + \mu_{fl}(0) & 0 & 0 & 0 & 0 \\ 0 & 0 & -d_L(t) & a_N(t) + \mu_{qn} & 0 & 0 & 0 \\ 0 & 0 & 0 & -a_N(t) & d_N(t) + \mu_{fn}(0) & 0 & 0 \\ 0 & 0 & 0 & 0 & -d_N(t) & a_A(t) + \mu_{qa} & 0 \\ 0 & 0 & 0 & 0 & 0 & -a_A(t) & \mu_{fl}(0) \end{pmatrix}.$$

Then we can rewrite (4.3.9) as

$$\frac{dz(t)}{dt} = (F(t) - V(t))z(t).$$

Let $\Phi_V(t)$ and $\rho(\Phi_V(\omega))$ be the monodromy matrix of the linear ω-periodic system $z'(t) = V(t)z$ and the spectral radius of $\Phi_V(\omega)$, respectively. Assume $Y(t,s)$, $t \geq s$, is the evolution operator of the linear periodic system

$$\frac{dy}{dt} = -V(t)y.$$

That is, for each $s \in \mathbb{R}$, the 7×7 matrix $Y(t,s)$ satisfies

$$\frac{d}{dt}Y(t,s) = -V(t)Y(t,s) \quad \forall t \geq s, \quad Y(s,s) = I,$$

where I is the 7×7 identity matrix.

Let C_ω be the Banach space of all ω-periodic functions from $\mathbb{R}$ to $\mathbb{R}^7$, equipped with the supremum norm. Suppose $w(s) \in C_\omega$ is the initial distribution at time s of ticks in this periodic environment. Then $F(s)w(s)$ is the rate of new ticks produced by the initial ticks who were introduced at time s, and $Y(t,s)F(s)w(s)$ represents the distribution of those ticks newly produced at time s and remain alive at time t for $t \geq s$. Hence,

$$\psi(t) = \int_{-\infty}^{t} Y(t,s)F(s)w(s)ds = \int_{0}^{\infty} Y(t,t-a)F(t-a)w(t-a)da \quad (4.3.11)$$

is the distribution of accumulative ticks at time t produced by all those ticks $w(s)$ introduced at the previous time. We then define the linear operator $\mathcal{L} : C_\omega \to C_\omega$ by

$$(\mathcal{L}w)(t) = \int_{0}^{\infty} Y(t,t-a)F(t-a)w(t-a)da \quad \forall t \in \mathbb{R}, \quad w \in C_\omega. \quad (4.3.12)$$

It then follows from [8, 99] that $\mathcal{L}$ is the next generation operator, and the basic reproduction ratio, denoted by $\mathcal{R}_0^{s_1v,p}$, is the spectral radius of $\mathcal{L}$, i.e., $\mathcal{R}_0^{s_1v,p} := \rho(\mathcal{L})$.

We denote by $P_t : \mathbb{R}^7_+ \to \mathbb{R}^7_+$, the solution map of system (4.2.3). That is if $u(t,u^0) = (u_1(t), u_2(t), \cdots, u_7(t))^T$ is the solution of (4.2.3) with initial value

$u^0 = (u_1^0, u_2^0, \cdots, u_7^0)^T \in \mathbb{R}_+^7$, here T is transpose of a matrix or vector, then $P_t(u^0) = u(t, u^0)$.

It is natural to try to employ [108, Theorem 2.3.4] for monotone discrete dynamical systems to establish the existence of a unique positive periodic solution of system (4.2.3). Unfortunately, the map P_ω is not strongly monotone for reasons to be clear below. Therefore, we start with $P_{6\omega}$ (which is strongly monotone) to obtain the existence and uniqueness of a positive periodic solution with a period 6ω, and we will then show that the minimal period of this solution must be ω.

Theorem 4.3.2. *The solution map P_t is strongly order-preserving (monotone) for all $t \geq 6\omega$. In particular, $P_{6\omega}$ is strongly monotone. That is, for any u^0, $v^0 \in \mathbb{R}_+^7$ with $u^0 < v^0$, we have $P_t(u^0) \ll P_t(v^0)$ for all $t \geq 6\omega$.*

Proof. Denote $X(t) = \frac{\partial P_t}{\partial w}(w) = \frac{\partial u}{\partial w}(t, w)$ and $A(t) = D_u(G(t, u(t, w))) = (a_{ij}(t))_{7\times 7}$. Since

$$X'(t) = \frac{\partial}{\partial t}(\frac{\partial P_t}{\partial w}(w)) = \frac{\partial}{\partial w}(\frac{\partial P_t}{\partial t}(w)) = \frac{\partial}{\partial w}(G(t, u(t, w))) = D_u G(t, u(t, w))\frac{\partial P_t}{\partial w}(w),$$

we have that $X(t) = (x_{ij}(t))_{7\times 7}$ satisfies

$$X'(t) = A(t)X(t), \quad X(0) = I. \tag{4.3.13}$$

Since $\frac{\partial G_i}{\partial u_j}(t, u) = a_{ij}(t) \geq 0$, for all $i \neq j$, $(t, u) \in \mathbb{R}_+ \times \mathbb{R}_+^7$, the Kamke's theorem (see page 425 of [37]) implies $x_{ij}(t) \geq 0$ for all $i, j \in \{1, \cdots, 7\}$ and $t \geq 0$, and

$x'_{ij}(t) \geq a_{ii}(t)x_{ij}(t)$ for any $i, j \in \{1, \cdots, 7\}$ and $t \geq 0$. If there exists $t_0 > 0$ such that $x_{ij}(t_0) > 0$, then it follows that $x_{ij}(t) > 0$ for all $t \geq t_0$. Since $x_{ii}(0) = 1$, we have $x_{ii}(t) > 0$ for all $t \geq 0$, $i \in \{1, \cdots, 7\}$.

We now prove that $x_{ij}(t) > 0$ for all $t \geq 6\omega$, $i, j \in \{1, \cdots, 7\}$. Note that $A(t) = D_u G(t, u(t, w))$ is given by

$$\begin{pmatrix} -(\mu_e + d_E(t)) & 0 & 0 & 0 & 0 & 0 & b(t) \\ d_E(t) & -(a_L(t) + \mu_{ql}) & 0 & 0 & 0 & 0 & 0 \\ 0 & a_L(t) & a_{33}(t) & 0 & 0 & 0 & 0 \\ 0 & 0 & d_L(t) & -(a_N(t) + \mu_{qn}) & 0 & 0 & 0 \\ 0 & 0 & 0 & a_N(t) & a_{55}(t) & 0 & 0 \\ 0 & 0 & 0 & 0 & d_N(t) & -(a_A(t) + \mu_{qa}) & 0 \\ 0 & 0 & 0 & 0 & 0 & a_A(t) & a_{77}(t) \end{pmatrix},$$

where

$$a_{33}(t) = -(d_L(t) + \mu'_{fl}(w_3)w_3 + \mu_{fl}(w_3)),$$

$$a_{55}(t) = -(d_N(t) + \mu'_{fn}(w_5)w_5 + \mu_{fn}(w_5)),$$

$$a_{77}(t) = -(\mu'_{fa}(w_7)w_7 + \mu_{fa}(w_7)).$$

Assume, by contradiction, that there is an element $x_{i(i-1)}(t) \equiv 0$ for all $t \in [0, \omega]$ with $i \in \{2, \cdots, 7\}$. Then from equation (4.3.13) we have

$$x'_{i(i-1)}(t) = \sum_{l=1}^{7} a_{il}(t)x_{l(i-1)}(t) = a_{i(i-1)}(t)x_{(i-1)(i-1)}(t) + a_{ii}(t)x_{i(i-1)}(t)$$

$$= a_{i(i-1)}(t)x_{(i-1)(i-1)}(t) \equiv 0, \forall t \in [0, \omega].$$

Immediately, we obtain $a_{i(i-1)}(t) \equiv 0, \forall t \in [0, \omega]$ by using the fact $x_{(i-1)(i-1)}(t) > 0, \forall t \geq 0$. This contradicts with $a_{i(i-1)}(t) \geq 0$ but $a_{i(i-1)}(t) \not\equiv 0$, $\forall t \in [0, \omega]$. So,

$x_{i(i-1)} > 0$ for some $t \in [0, \omega]$. Once $x_{i(i-1)(t)}$ is strictly positive it remains so, and therefore $x_{i(i-1)}(t) > 0$ for all $t \geq \omega$, $i \in \{2, \cdots, 7\}$.

Similarly, if $x_{i(i-2)}(t) \equiv 0$ for all $t \in [\omega, 2\omega]$ with $i \in \{3, \cdots, 7\}$, then from equation (4.3.13) we have

$$x'_{i(i-2)}(t) = a_{i(i-1)}(t)x_{(i-1)(i-2)}(t) + a_{ii}(t)x_{i(i-2)}(t) = a_{i(i-1)}(t)x_{(i-1)(i-2)}(t) \equiv 0, \forall t \in [\omega, 2\omega].$$

But from $x_{(i-1)(i-2)}(t) > 0$ for all $t \in [\omega, 2\omega]$, it follows that $a_{i(i-1)}(t) \equiv 0$ for all $t \in [\omega, 2\omega]$. This contradicts with $a_{i(i-1)}(t) \not\equiv 0$, $t \in [\omega, 2\omega]$. So, $x_{i(i-2)}(t) > 0$ for all $t \geq 2\omega$, $i \in \{3, \cdots, 7\}$.

Using the same argument, we can obtain

(1) If $i > j$, then $x_{ij}(t) > 0$ for all $t \geq k\omega$ provided $i - j = k$, $i \in \{2, \cdots, 7\}$;

(2) If $i < j$, then $x_{ij}(t) > 0$ for all $t \geq (7-k)\omega$ provide $j - i = k$, $j \in \{2, \cdots, 7\}$.

Therefore, we get $X(t) \gg 0$ for all $t \geq 6\omega$, that is, $\frac{\partial P_t}{\partial w}(w) \gg 0$ for all $t \geq 6\omega$. Furthermore, if $u^0, v^0 \in \mathbb{R}^7_+$ satisfy $u^0 < v^0$, then for all $t \geq 6\omega$, we have

$$P_t(v^0) - P_t(u^0) = \int_0^1 \frac{\partial P_t}{\partial w}(u^0 + r(v^0 - u^0))(v^0 - u^0)dr \gg 0.$$

Hence, we have $P_t(u^0) \ll P_t(v^0), \forall t \geq 6\omega$. That is, P_t is strongly monotone whenever $t \geq 6\omega$. In particular, $P_{6\omega}$ is strongly monotone. □

Theorem 4.3.3. *The following statements hold:*

(1) If the basic reproduction ratio $\mathcal{R}_0^{s_1v,p} \leq 1$, then zero is globally asymptotically stable for system (4.2.3) in $\mathbb{R}^7_+$;

(2) If the basic reproduction ratio $\mathcal{R}_0^{s_1v,p} > 1$, then system (4.2.3) admits a unique positive ω-periodic solution $u^*(t) = (E^*(t), L_Q^*(t), L_F^*(t), N_Q^*(t), N_F^*(t), A_Q^*(t), A_F^*(t))$, which is globally asymptotically stable for system (4.2.3) with initial values in $\mathbb{R}^7_+ \setminus \{0\}$.

Proof. We have shown that $P_{6\omega}$ is strongly monotone. Furthermore, $P_{6\omega}(0) = 0$, $DP_{6\omega}(0) = X(6\omega)|_{w=0}$ is compact and strongly positive. Since we have already shown the positivity and boundedness of the solutions of (4.2.3) with the initial data u^0 in $\mathbb{R}^7_+$, the operator $P_{6\omega} : \mathbb{R}^7_+ \to \mathbb{R}^7_+$ is asymptotically smooth and every positive orbit of $P_{6\omega}$ in $\mathbb{R}^7_+$ is bounded.

We also know that $P_{6\omega}$ is strictly subhomogeneous. This can be easily done since $G(t,u)$ is strictly subhomogeneous on u in the sense that $G(t,\alpha u) > \alpha G(t,u)$ for all $u \in \mathbb{R}^7_+ \setminus \{0\}$, $\alpha \in (0,1)$, $t > 0$. Therefore, by [99, Therorem 2.2] and [108, Theorem 2.3.4], we have the following threshold dynamics:

- If $\rho(DP_{6\omega}(0)) \leq 1$, then all solutions of system (4.2.3) with initial data u^0 in $\mathbb{R}^7_+$ converge to zero;

- If $\rho(DP_{6\omega}(0)) > 1$, then system (4.2.3) has a unique positive 6ω-periodic solution $u^*(t)$, and every solution of system (4.2.3) with initial data u^0 in

$\mathbb{R}^7_+ \setminus \{0\}$ converges to $u^*(t)$ as $t \to \infty$.

By the similar argument used already in the last paragraph of the proof of Theorem 3.2 in [102], we have

$$P_\omega(u^*) = P_\omega(P_{6\omega}(u^*)) = P_{6\omega}(P_\omega(u^*)).$$

Since $P_{6\omega}$ has a unique positive fixed point, we conclude that $P_\omega(u^*) = u^*$. Therefore, u^* is a fixed point of P_ω. □

4.4 Spatial dynamics

In this section, we study the spatial dynamics of the model (4.2.1) in the unbounded spatial domain $\mathbb{R}$. We always assume that $\mathcal{R}_0^{s_1 v,p} > 1$ in this section. Therefore according to Theorem 4.3.3 of this chapter, there exist two ω-periodic solutions, 0 and $u^*(t)$, for the spatially homogeneous system (4.2.3).

Now we consider the reaction-diffusion system (4.2.1) on the unbounded spatial domain $\mathbb{R}$. We rewrite (4.2.1) with a given initial data $\varphi \in \mathcal{C}_+$ as

$$\begin{cases} \partial_t u(t,x) = \bar{D}\Delta u(t,x) + G(t,u(t,x)), \quad x \in \mathbb{R}, \quad t > 0, \\ u(0,x) = \varphi(x), \quad x \in \mathbb{R}, \end{cases} \tag{4.4.14}$$

where $u(t,x) = (u_1(t,x), \cdots, u_7(t,x))^T = (E(t,x), L_Q(t,x), L_F(t,x), N_Q(t,x), N_F(t,x), A_Q(t,x), A_F(t,x))^T$, $G : \mathbb{R} \times \mathcal{C} \to \mathbb{R}^7$ is defined in (4.2.5), $\varphi = (\varphi_1, \varphi_2, \cdots, \varphi_7)^T \in$

$\mathcal{C}_+$ is the initial data, Δ is the Laplacian operator on $\mathbb{R}$,

$\bar{D} = (D_E, D_{L_Q}, D_{L_F}, D_{N_Q}, D_{N_F}, D_{A_Q}, D_{A_F})^T$ is the diffusion coefficient.

4.4.1 Existence, uniqueness, positivity and monotonicity of solutions

Let $\mathcal{D}$ be the set of all bounded and continuous functions from $\mathbb{R}$ to $\mathbb{R}$ equipped with the compact open topology. Let $\mathcal{D}_+ = \{\varphi \in \mathcal{D} : \varphi(x) \geq 0, \forall x \in \mathbb{R}\}$. Consider

$$\begin{cases} \partial_t u_i(t,x) = \bar{D}_i \Delta u_i(t,x), \quad t > 0, \quad x \in \mathbb{R}, \\ u_i(0,x) = \varphi_i(x), \quad x \in \mathbb{R}. \end{cases} \tag{4.4.15}$$

The solution of (4.4.15) can be expressed in terms of the heat kernel as:

$$u_i(t,x,\varphi_i) = [T_i(t)\varphi_i](x) = \frac{1}{\sqrt{4\pi \bar{D}_i t}} \int_{-\infty}^{\infty} e^{-\frac{(x-y)^2}{4\bar{D}_i t}} \varphi_i(y) dy, x \in \mathbb{R}, t > 0, i = 1, \cdots, 7.$$

Then $\{T_i(t)\}_{t\geq 0}$ $(i = 1, \cdots, 7)$ is a strongly continuous semigroup (or C_0-semigroup) on $\mathcal{D}$ generated by the infinitesimal generator $\bar{D}_i\Delta$ which satisfies: (a). $T_i(0)\varphi = \varphi$, for all $\varphi \in \mathcal{D}$; (b). $T_i(t+s)\varphi = T_i(t)T_i(s)\varphi$, for all t, $s \geq 0$, $\varphi \in \mathcal{D}$; (c). For any fixed $\varphi \in \mathcal{D}$, $T_i(\cdot)\varphi : [0,\infty) \to \mathcal{D}$ is continuous; (d). $\exists\ \hat{M} \geq 0$ and $\omega \in \mathbb{R}$, such that $||T_i(t)|| = \sup\{||T_i(t)\varphi||_{\mathcal{D}} : |\varphi(x)| \leq 1, x \in \mathbb{R}\} \leq \hat{M}e^{\omega t}$ for all $t \geq 0$. We adapt the similar analysis as in [55, Lemma 2.6] to conclude that $T_i(t)$ is a compact and positive operator on $\mathcal{D}$ for each $t > 0$ (or see Appendix B). By [59, proposition 5.1], $T_i(t)$ is continuous for all $t > 0$. Moreover $T_i(t)\mathcal{D}_+ \subset \mathcal{D}_+$. Therefore, $\{T(t)\}_{t\geq 0} = \{\{T_i(t)\}_{i=1}^7\}_{t\geq 0}$ is compact and positive operator semigroup.

(4.4.14) can be written as an abstract integral equation associated with the initial value problem

$$\begin{cases} u(t,\cdot,\varphi) = T(t)\varphi + \int_0^t T(t-s)G(s,u(s))ds, \\ u(0) = \varphi \in \mathcal{C}_+, \end{cases} \tag{4.4.16}$$

whose solution is called the mild solution of the system (4.4.14). In the next theorem, we establish the existence, uniqueness, positivity and monotonicity of the mild solution of the Cauchy problem (4.4.14).

Theorem 4.4.1. *For any $\varphi \in \mathcal{C}_+$, system (4.4.14) has a unique mild solution $u(t,\cdot,\varphi)$ with $u(0,\cdot,\varphi) = \varphi$, and $u(t,x,\varphi)$ is a classical solution when $t > 0$. Moreover, if $0 \leq \varphi \leq \psi < \infty$, then $0 \leq u(t,\cdot,\varphi) \leq u(t,\cdot,\psi) < \infty$, $\forall t \geq 0$.*

Proof. In order to verify the existence, uniqueness, positivity and monotonicity of the solution of the Cauchy problem (4.4.14), we need to show that G is a quasi-monotone map from $[0,\infty)\times\mathcal{C}_+$ to $\mathbb{R}^7_+$ and locally Lipschitz continuous, as specified in (2.3) on page 18 on [60].

Since for any $k \in \{1,\cdots,7\}$, (t,u), $(t,v) \in [0,\infty)\times\mathbb{R}^7_+$ with $u \leq v$, when $u_k = v_k$ implies $G_k(t,u) \leq G_k(t,v)$, From [60, Remark 1.4], the function G is quasi-monotone on $\mathbb{R}^7_+$. It is easy to show that $G(t,u)$ satisfies the locally Lipschitz continuity, that is, for any $\bar{R} > 0$, there exist a $L_{\bar{R}} > 0$ and a continuous function $\nu_{\bar{R}} : [0,\infty) \to [0,\infty)$ such that $\nu_{\bar{R}}(0) = 0$ and

$$|G(t,u) - G(s,v)| \leq \nu_{\bar{R}}(|t-s|) + L_{\bar{R}}||u-v|| \tag{4.4.17}$$

for all (t,u), $(s,v) \in [0,\infty) \times \mathbb{R}^7_+$ with $||u||$, $||v|| \leq \bar{R}$ and $0 \leq s,t \leq \bar{R}$. By [60, Corollary 5] with $v^+(t,x) = +\infty$, $v^-(t,x) = 0$, and $S(t,s) = T(t,s) = T(t-s), t \geq s \geq 0$, system (4.4.14) has a unique non-continuable mild solution $u(t,\cdot,\varphi)$ on $[0, t_{\max}(\varphi))$ with $t_{\max}(\varphi) > 0$ for any $\varphi \in \mathcal{C}_+$ and $u(t,\cdot,\varphi) \in \mathcal{C}_+$. It then follows from [60, Theorem 1] that $u(t,\cdot,\varphi)$ is a classical solution for all $t \in [0, t_{\max}(\varphi))$. By the theory of continuation of solution (see Theorem 2.3 on page 49 or Theorem 2.6 on page 51 of [103]), we conclude that $t_{\max}(\varphi) = \infty$, this means the solution $u(t,\cdot,\varphi)$ exists globally. Moreover, the comparison principle holds by [60, Corollary 5]. □

4.4.2 Traveling waves of the system

In this subsection, we establish the existence/nonexistence of ω-period traveling waves of system (4.4.14). We say $u(t,x) = U(t, x - tc)$ is an ω-periodic traveling wave of system (4.4.14) if it is a solution of (4.4.14) and $U(t,s)$ is ω-periodic in t.

To study spreading speeds and traveling waves for system (4.4.14), we define the reflection operator $\mathcal{R}$ by $\mathcal{R}[u](x) = u(-x)$. Given any $y \in \mathbb{R}$, define the translation operator T_y by $T_y[u](x) = u(x-y)$.

Let $\beta \in \mathbb{R}^7$ with $\beta \gg 0$ and $Q = (Q_1, \cdots, Q_7) : \mathcal{C}_\beta \to \mathcal{C}_\beta$. In order to use the theory of spreading speeds and traveling waves developed in [48, 49], we introduce the following assumptions on Q:

(A1) $Q[\mathcal{R}[u]] = \mathcal{R}[Q[u]]$, $T_y[Q[u]] = Q[T_y[u]], \forall y \in \mathbb{R}$.

(A2) $Q : \mathcal{C}_\beta \to \mathcal{C}_\beta$ is continuous with respect to the compact open topology.

(A3) $Q[\mathcal{C}_\beta]$ is precompact in $\mathcal{C}_\beta$.

(A4) $Q : \mathcal{C}_\beta \to \mathcal{C}_\beta$ is monotone (order-preserving) in the sense that $Q[u] \geq Q[v]$ whenever $u \geq v$ in $\mathcal{C}_\beta$.

(A5) $Q : [0, \beta] \to [0, \beta]$ admits exactly two fixed points 0 and β, and for any positive number ε, there is $\alpha \in [0, \beta]$ with $||\alpha|| < \varepsilon$ such that $Q[\alpha] \gg \alpha$.

Recall that a family of mappings $\{Q_t\}_{t\geq 0}$ is said to be an ω-periodic semiflow on the metric space $(\mathcal{C}_r, d_C)$ with the metric d_C, provided Q_t satisfies the following properties:

(i) $Q_0[\varphi] = \varphi, \forall \varphi \in \mathcal{C}_r$;

(ii) $Q_{t+\omega}[\varphi] = Q_t[Q_\omega[\varphi]], \forall t \geq 0, \varphi \in \mathcal{C}_r$;

(iii) $Q(t, \varphi) := Q_t(\varphi)$ is continuous in $(t, \varphi) \in [0, \infty) \times \mathcal{C}_r$ with respect to the compact open topology.

Define a family of maps $\{Q_t\}_{t\geq 0}$ from $\mathcal{C}_+$ to $\mathcal{C}_+$ by

$$Q_t(\varphi)(x) = u(t, x, \varphi) = (u_i(t, x, \varphi))_{i=1}^7, \forall t \geq 0, x \in \mathbb{R}, \varphi \in \mathcal{C}_+,$$

where $u(t, x, \varphi)$ is the mild solution of system (4.4.14) with $u(0, \cdot, \varphi) = \varphi$.

Lemma 4.4.2. *The following three statements hold for the solution map Q_t:*

(1) $\{Q_t\}_{t\geq 0}$ is an ω-periodic semiflow on $\mathcal{C}_{u^*(0)}$.

(2) $Q_t[\mathcal{C}_{u^*(0)}]$ is precompact in $\mathcal{C}_{u^*(0)}$ for all $t > 0$.

(3) For each $t > 0$, Q_t is strictly subhomogenous and monotone from $\mathcal{C}_+ \setminus \{0\}$ to $\mathcal{C}_+ \setminus \{0\}$.

Proof. It is easy to know $\{Q_t\}_{t\geq 0}$ satisfy (i) and (ii) on $\mathcal{C}_{u*(0)}$, since for every $t \geq 0$, $\varphi \in \mathcal{C}_{u^*(0)}$,

$$\begin{aligned}
Q_{t+\omega}[\varphi] &= u(t+\omega, \cdot, \varphi) \\
&= T(t+\omega)\varphi + \int_0^{t+\omega} T(t+\omega-s)G(s,u(s))ds \\
&= T(t)T(\omega)\varphi + \int_0^{\omega} T(t+\omega-s)G(s,u(s))ds + \int_{\omega}^{t+\omega} T(t+\omega-s)G(s,u(s))ds \\
&= T(t)[T(\omega)\varphi + \int_0^{\omega} T(\omega-s)G(s,u(s))ds] + \int_0^t T(t-s)G(s+\omega,u(s+\omega))ds \\
&= T(t)Q_\omega(\varphi) + \int_0^t T(t-s)G(s,u(s+\omega))ds \\
&= Q_t[Q_\omega(\varphi)].
\end{aligned}$$

Note that $\{T(t)\}_{t\geq 0}$ is compact on metric space $(\mathcal{C}_{u^*(0)}, d_{\mathcal{C}})$, $T(t)\varphi$ is continuous in $(t,\varphi) \in [0,\infty) \times \mathcal{C}_{u^*(0)}$ and in particular $T(t)$ is continuous for each $t > 0$, by a similar argument as in [59, Theorem 8.5.2], we obtain that $Q_t(\varphi)$ is continuous in $(t,\varphi) \in [0,\infty) \times \mathcal{C}_{u^*(0)}$ with respect to the compact open topology and $Q_t[\mathcal{C}_{u^*(0)}]$ is precompact in $\mathcal{C}_{u^*(0)}$ for all $t > 0$ (see Appendix B).

For any $u \in \mathbb{R}^7_+ \setminus \{0\}$, $G(t,u)$ is strictly subhomogeneous in u. Therefore, for any $(t,\varphi) \in [0,\infty) \times \mathcal{C}_+ \setminus \{0\}$ and any $k \in (0,1)$, we have

$$\begin{aligned} kQ_t(\varphi) = ku(t,\cdot,\varphi) &= kT(t)\varphi + k\int_0^t T(t-r)G(r,u(r))dr \\ &= T(t)k\varphi + \int_0^t T(t-r)[kG(r,u(r))]dr \\ &< T(t)k\varphi + \int_0^t G(r,ku(r))dr \\ &= u(t,x,k\varphi) = Q_t(k\varphi). \end{aligned}$$

Thus, $\{Q_t\}_{t>0}$ is strictly subhomogeneous and monotone by Theorem 4.4.1. □

Lemma 4.4.3. *The map $Q_{6\omega}$ satisfies all hypotheses (A1)-(A5) with $\beta = u^*(0)$ and Q_t satisfies (A1) and (A4) for any $t > 0$.*

Proof. If $u(t,x)$ is a solution for the system (4.4.14), then $u(t,x-y)$, $\forall y \in \mathbb{R}$, is also a solution, and hence (A1) holds. (A2) and (A3) come from Lemma 4.4.2. (A4) follows directly from the comparison principle in Theorem 4.4.1.

Let $\hat{Q}_{6\omega} = Q_{6\omega}|_{[0,u^*(0)]_{\mathcal{R}^7}}$. Then $\hat{Q}_{6\omega} : [0,u^*(0)] \to [0,u^*(0)]$ is the map generated by system (4.2.3). Note that (4.2.3) has a positive 6ω-periodic solution $u^*(t)$ which is globally asymptotically stable in $\mathbb{R}^7_+ \setminus \{0\}$. We see that $\hat{Q}_{6\omega}$ has only two fixed points 0 and $u^*(0)$ in $[0,u^*(0)]$. Thus, by the Dancer-Hess connecting orbit lemma ([108, section 2.2.1]), we obtain that there exists a strictly monotone full orbit $\{a_n\}_{-\infty}^{\infty}$ connecting 0 to $u^*(0)$ and $a_i < a_{i+1}$ for all $i \in \mathbb{Z}$. Since $\hat{Q}_{6\omega}$ is strongly monotone, $a_{i+1} = \hat{Q}_{6\omega}(a_i) \ll \hat{Q}_{6\omega}(a_{i+1}) = a_{i+2}$ for any $i \in \mathbb{Z}$. Therefore, $a_i \ll a_{i+1}$ for any $i \in \mathbb{Z}$. This implies that (A5) holds for $Q_{6\omega}$. □

Remark 4.4.1. $Q_{6\omega}$ satisfies (A1)-(A5) with $\tau = 0$ and $\beta = u^*(0)$, Theorem A ([48]) implies that $Q_{6\omega}$ admits a spreading speed $c^*_{6\omega}$. That is, $Q_{6\omega}$ has the asymptotic speed of spread $c^*_{6\omega}$.

Remark 4.4.2. Theorem 4.3.3 implies that the assumption (A5) in the paper [50] holds for the Poincaré map Q_ω. As a consequence of Theorems 3.1-3.2 and Remark 3.1, Q_ω has the spreading speed c^*_ω. That is, Q_ω has the asymptotic speed of spread c^*_ω.

Next we use Theorem B in [48] to obtain the explicit expression $c^*_{6\omega}$. Consider the linearized system of (4.2.1) at the zero solution

$$\begin{aligned}
\frac{\partial u_1(t,x)}{\partial t} &= b(t)u_7(t,x) - (d_E(t) + \mu_e)u_1(t,x) + D_E\frac{\partial^2 u_1(t,x)}{\partial x^2},\\
\frac{\partial u_2(t,x)}{\partial t} &= d_E(t)u_1(t,x) - (a_L(t) + \mu_{ql})u_2(t,x) + D_{L_Q}\frac{\partial^2 u_2(t,x)}{\partial x^2},\\
\frac{\partial u_3(t,x)}{\partial t} &= a_L(t)u_2(t,x) - (d_L(t) + \mu_{fl}(0))u_3(t,x) + D_{L_F}\frac{\partial^2 u_3(t,x)}{\partial x^2},\\
\frac{\partial u_4(t,x)}{\partial t} &= d_L(t)u_3(t,x) - (a_N(t) + \mu_{qn})u_4(t,x) + D_{N_Q}\frac{\partial^2 u_4(t,x)}{\partial x^2},\\
\frac{\partial u_5(t,x)}{\partial t} &= a_N(t)u_4(t,x) - (d_N(t) + \mu_{fn}(0))u_5(t,x) + D_{N_F}\frac{\partial^2 u_5(t,x)}{\partial x^2},\\
\frac{\partial u_6(t,x)}{\partial t} &= d_N(t)u_5(t,x) - (a_A(t) + \mu_{qa})u_6(t,x) + D_{A_Q}\frac{\partial^2 u_6(t,x)}{\partial x^2},\\
\frac{\partial u_7(t,x)}{\partial t} &= a_A(t)u_6(t,x) - \mu_{fa}(0)u_7(t,x) + D_{A_F}\frac{\partial^2 u_7(t,x)}{\partial x^2}.
\end{aligned} \tag{4.4.18}$$

For any $\mu \in [0,\infty)$, let $u(t,x) = e^{-\mu x}v(t)$, where $u(t,x) = (u_1(t,x),\cdots,u_7(t,x))^T$

and $v(t) = (v_1(t), \cdots, v_7(t))^T$. Substituting $u(t,x)$ into (4.4.18) yields

$$\begin{aligned}
\frac{dv_1(t)}{dt} &= b(t)v_7(t) - (d_E(t) + \mu_e)v_1(t) + D_E\mu^2 v_1(t),\\
\frac{dv_2(t)}{dt} &= d_E(t)v_1(t) - (a_L(t) + \mu_{ql})v_2(t) + D_{L_Q}\mu^2 v_2(t),\\
\frac{dv_3(t)}{dt} &= a_L(t)v_2(t) - (d_L(t) + \mu_{fl}(0))v_3(t) + D_{L_F}\mu^2 v_3(t),\\
\frac{dv_4(t)}{dt} &= d_L(t)v_3(t) - (a_N(t) + \mu_{qn})v_4(t) + D_{N_Q}\mu^2 v_4(t),\\
\frac{dv_5(t)}{dt} &= a_N(t)v_4(t) - (d_N(t) + \mu_{fn}(0))v_5(t) + D_{N_F}\mu^2 v_5(t),\\
\frac{dv_6(t)}{dt} &= d_N(t)v_5(t) - (a_A(t) + \mu_{qa})v_6(t) + D_{A_Q}\mu^2 v_6(t),\\
\frac{dv_7(t)}{dt} &= a_A(t)v_6(t) - \mu_{fa}(0)v_7(t) + D_{A_F}\mu^2 v_7(t).
\end{aligned} \tag{4.4.19}$$

So, if $v(t)$ is a solution of (4.4.19), then $u(t,x) = e^{-\mu x}v(t)$ is a solution of (4.4.18).

Let $\{M_t\}_{t\geq 0}$ be the linear solution map associated with (4.4.18), define

$$B_\mu^t(\varphi) := M_t(\varphi e^{-\mu x})(0) = v(t,\varphi), \quad \forall \varphi \in \mathbb{R}_+^7, \quad t \geq 0,$$

where $v(t,\varphi)$ is the solution of (4.4.19) with initial data $v(0,\varphi) = \varphi$. Therefore, B_μ^t is just the solution map of linear ordinary differential equation (4.4.19) on $\mathbb{R}_+^7$.

We rewrite (4.4.19) as

$$\frac{dv(t)}{dt} = H(t,\mu)v(t), \tag{4.4.20}$$

where $H(t,\mu) = (H_1(t,\mu)|H_2(t,\mu))$ with

$$H_1(t,\mu) = \begin{pmatrix}
D_E\mu^2 - (\mu_e + d_E(t)) & 0 & 0 & 0\\
d_E(t) & D_{L_Q}\mu^2 - (a_L(t) + \mu_{ql}) & 0 & 0\\
0 & a_L(t) & D_{L_F}\mu^2 - (d_L(t) + \mu_{fl}(0)) & 0\\
0 & 0 & d_L(t) & D_{N_Q}\mu^2 - (a_N(t) + \mu_{qn})\\
0 & 0 & 0 & a_N(t)\\
0 & 0 & 0 & 0\\
0 & 0 & 0 & 0
\end{pmatrix}$$

and

$$H_2(t,\mu)=\begin{pmatrix} 0 & 0 & b(t) \\ 0 & 0 & 0 \\ 0 & 0 & 0 \\ 0 & 0 & 0 \\ D_{N_F}\mu^2-(d_N(t)+\mu_{fn}(0)) & 0 & 0 \\ d_N(t) & D_{A_Q}\mu^2-(a_A(t)+\mu_{qa}) & 0 \\ 0 & a_A(t) & D_{A_F}\mu^2-\mu_{fl}(0) \end{pmatrix}.$$

Note that $H(t,\mu)$ is a continuous, cooperative and ω-periodic 7×7 matrix function. In fact, B_μ^t is the fundamental solution matrix of the linear ordinary differential system (4.4.20). Let $\rho(\mu)$ be spectral radius of the 6ω-periodic solution map $B_\mu^{6\omega}$ associated with (4.4.20). It follows from the similar argument in Theorem 4.3.2 that B_μ^t is strongly monotone for all $t \geq 6\omega$ in the sense that $B_\mu^t[v_0] \gg 0$ for all $v_0 > 0$. By the Krein-Rutman theorem, $\rho(\mu)$ is the principle eigenvalue of $B_\mu^{6\omega}$ in the sense that it is simple and positive with a strongly positive eigenvector v^*. Define a function

$$\Phi(\mu) := \frac{\ln\rho(\mu)}{\mu}, \quad \forall \mu > 0. \tag{4.4.21}$$

In order to use [48, Theorem B], we have to show $\Phi(\infty) = \infty$. The following result is used to prove $\Phi(\infty) = \infty$.

Lemma 4.4.4. *Let $\lambda(\mu) = \frac{1}{6\omega} ln\rho(\mu) = \frac{1}{6\omega} ln\rho(B_\mu^{6\omega})$. Then there exists a positive 6ω-periodic function $w(t)$ such that $e^{\lambda(\mu)t}w(t)$ is a solution of $v' = H(t,\mu)v$.*

Proof. We will use the similar argument developed in [107, Lemma 2.1]. Let $w^* \gg 0$ be an eigenvector associated with the principal eigenvalue $\rho(B_\mu^{6\omega})$, that is, $B_\mu^{6\omega} w^* = \rho(B_\mu^{6\omega}) w^*$. Substituting $v(t) = e^{\lambda(\mu)t} w(t)$ into the linear system $v' = H(t,\mu)v$ gives

$$w' = (H(t,\mu) - \lambda(\mu)I)w. \tag{4.4.22}$$

Thus, $w(t) = \phi_{(H(\cdot,\mu)-\lambda(\mu)I)}(t)w^*$ is a positive solution of (4.4.22), where $\phi_{(H(\cdot,\mu)-\lambda(\mu)I)}(t)$ is the fundamental solution matrix of (4.4.22), and

$$e^{\lambda(\mu)t}\phi_{(H(\cdot,\mu)-\lambda(\mu)I)}(t) = \phi_{H(\cdot,\mu)}(t) = B_\mu^t.$$

Moreover,

$$\begin{aligned} w(6\omega) &= \phi_{(H(\cdot,\mu)-\lambda(\mu)I)}(6\omega)w^* = e^{-\lambda(\mu)6\omega}\phi_{H(\cdot,\mu)}(6\omega)w^* \\ &= e^{-\lambda(\mu)6\omega}\rho(\phi_{H(\cdot,\mu)}(6\omega))w^* = w^* = w(0). \end{aligned}$$

Therefore, $w(t)$ is a positive 6ω-periodic solution of (4.4.22), and hence, $v(t) = e^{\lambda(\mu)t}w(t)$ is a solution of $v' = H(t,\mu)v$. □

Proposition 4.4.5. *Let $c^*_{6\omega}$ be the spreading speed of $Q_{6\omega}$, then $c^*_{6\omega} = \inf_{\mu>0} \Phi(\mu)$.*

Proof. When $\mu = 0$, (4.4.20) becomes (4.3.9). Since in this section, we assume $\mathcal{R}_0^{s_1 v,p} > 1$, then we have $\rho(0) = \rho(B_0^{6\omega}) = (\rho(B_0^\omega))^6 > 1$, where B_0^ω is the Poincaré map associated with (4.3.9). Hence (C7) in [49] is satisfied. Now we need to prove $\Phi(\infty) = \infty$. By Lemma 4.4.4, we have

$$v_1'(t) = (D_E\mu^2 - \mu_e - d_E(t))v_1(t) + b(t)v_7(t) \geq (D_E\mu^2 - \mu_e - d_E(t))v_1(t),$$

and hence

$$\frac{w_1'(t)}{w_1(t)} \geq D_E\mu^2 - \mu_e - d_E(t) - \lambda(\mu).$$

Then

$$\begin{aligned} 0 = \int_0^{6\omega} \frac{w_1'(t)}{w_1(t)}dt &\geq \int_0^{6\omega} (D_E\mu^2 - \mu_e - d_E(t) - \lambda(\mu))dt \\ &= (D_E\mu^2 - \mu_e - \lambda(\mu))6\omega - 6\int_0^{\omega} d_E(t)dt, \end{aligned}$$

which implies that

$$\lambda(\mu)6\omega \geq (D_E\mu^2 - \mu_e)6\omega - 6\int_0^{\omega} d_E(t)dt.$$

Thus, we have

$$\Phi(\mu) = \frac{\ln\rho(\mu)}{\mu} = \frac{6\omega\lambda(\mu)}{\mu} \geq 6\omega D_E\mu - \frac{6\omega\mu_e + 6\int_0^{\omega} d_E(t)dt}{\mu}.$$

Letting $\mu \to \infty$, we obtain $\Phi(\infty) = \infty$. Therefore, $\Phi(\mu)$ can attain the infimum at some value $\mu^* \in (0, \infty)$.

Note that $M_{6\omega}$ and $B_\mu^{6\omega}$ satisfy (C1)-(C7) in [49]. Since $\mu_{fi}(x)(i = l, n, a)$ are strictly increasing functions on $\mathbb{R}_+$, we have $-\mu_{fi}(x)x \leq -\mu_{fi}(0)x \quad (i = l, n, a)$ for all $x \in \mathbb{R}_+$. Then by the comparison theorem, we have $Q_{6\omega}[\varphi] \leq M_{6\omega}[\varphi]$ for each $\varphi \in \mathcal{C}_{u^*(0)}$. Consequently, [49, Theorem 3.10] implies that $C_{6\omega}^* \leq \inf_{\mu>0} \frac{\ln\rho(\mu)}{\mu} = \inf_{\mu>0} \frac{\ln\rho(B_\mu^{6\omega})}{\mu}$.

Let $\{M_t^\epsilon\}_{t\geq 0}$ be the solution map associated with the linear system

$$\begin{aligned}
\frac{\partial u_1(t,x)}{\partial t} &= b(t)u_7(t,x) - (d_E(t)+\mu_e)u_1(t,x) + D_E\frac{\partial^2 u_1(t,x)}{\partial x^2},\\
\frac{\partial u_2(t,x)}{\partial t} &= d_E(t)u_1(t,x) - (a_L(t)+\mu_{ql})u_2(t,x) + D_{L_Q}\frac{\partial^2 u_2(t,x)}{\partial x^2},\\
\frac{\partial u_3(t,x)}{\partial t} &= a_L(t)u_2(t,x) - d_L(t)u_3(t,x) - (1-\epsilon)\mu_{fl}(0)u_3(t,x) + D_{L_F}\frac{\partial^2 u_3(t,x)}{\partial x^2},\\
\frac{\partial u_4(t,x)}{\partial t} &= d_L(t)u_3(t,x) - (a_N(t)+\mu_{qn})u_4(t,x) + D_{N_Q}\frac{\partial^2 u_4(t,x)}{\partial x^2},\\
\frac{\partial u_5(t,x)}{\partial t} &= a_N(t)u_4(t,x) - d_N(t)u_5(t,x) - (1-\epsilon)\mu_{fn}(0)u_5(t,x) + D_{N_F}\frac{\partial^2 u_5(t,x)}{\partial x^2},\\
\frac{\partial u_6(t,x)}{\partial t} &= d_N(t)u_5(t,x) - (a_A(t)+\mu_{qa})u_6(t,x) + D_{A_Q}\frac{\partial^2 u_6(t,x)}{\partial x^2},\\
\frac{\partial u_7(t,x)}{\partial t} &= a_A(t)u_6(t,x) - (1-\epsilon)\mu_{fa}(0)u_7(t,x) + D_{A_F}\frac{\partial^2 u_7(t,x)}{\partial x^2},
\end{aligned} \tag{4.4.23}$$

$\rho^\epsilon(\mu)$ be spectral radius of the 6ω-periodic solution map associated with the following linear periodic cooperative system

$$\begin{aligned}
\frac{dv_1(t)}{dt} &= b(t)v_7(t) - (d_E(t)+\mu_e)v_1(t) + D_E\mu^2 v_1(t),\\
\frac{dv_2(t)}{dt} &= d_E(t)v_1(t) - (a_L(t)+\mu_{ql})v_2(t) + D_{L_Q}\mu^2 v_2(t),\\
\frac{dv_3(t)}{dt} &= a_L(t)v_2(t) - d_L(t)v_3(t) - (1-\epsilon)\mu_{fl}(0)v_3(t) + D_{L_F}\mu^2 v_3(t),\\
\frac{dv_4(t)}{dt} &= d_L(t)v_3(t) - (a_N(t)+\mu_{qn})v_4(t) + D_{N_Q}\mu^2 v_4(t),\\
\frac{dv_5(t)}{dt} &= a_N(t)v_4(t) - d_N(t)v_5(t) - (1-\epsilon)\mu_{fn}(0)v_5(t) + D_{N_F}\mu^2 v_5(t),\\
\frac{dv_6(t)}{dt} &= d_N(t)v_5(t) - (a_A(t)+\mu_{qa})v_6(t) + D_{A_Q}\mu^2 v_6(t),\\
\frac{dv_7(t)}{dt} &= a_A(t)v_6(t) - (1-\epsilon)\mu_{fa}(0)v_7(t) + D_{A_F}\mu^2 v_7(t).
\end{aligned} \tag{4.4.24}$$

Since $-\mu_{fi}(x)x \quad (i=l,n,a)$ is subhomogeneous in x on $\mathbb{R}_+$, it follows from [108, Lemma 2.3.2] that $-\mu_{fi}(x)x \leq -\mu_{fi}(0)x$, $i=l,n,a$, $x\geq 0$. Then for any $\epsilon\in(0,1)$,

there is a $x_\epsilon > 0$ such that

$$-\mu_{fi}(x)x \geq -(1-\epsilon)\mu_{fi}(0)x, \quad \forall x \in [0, x_\epsilon], \quad i = l, n, a.$$

We rewrite (4.4.23) as

$$\partial_t u(t,x) = \bar{G}(t,\epsilon)u(t,x) + \bar{D}\Delta u(t,x), \tag{4.4.25}$$

and note that for any $\epsilon \in (0,1)$, there exists $\delta > 0$ such that $G(t,u) > \bar{G}(t,\epsilon)u$, for any $(t,u) \in \mathbb{R}_+ \times [0,\delta]$. Moreover, there exists $\eta = \eta(\delta)$ such that for any $\varphi \in \mathcal{C}_\eta$, we have

$$0 \leq Q_t[\varphi](x) \leq Q_t[\eta] \ll \delta, \forall x \in \mathbb{R}, \quad t \in [0, 6\omega].$$

Then the comparison principle implies

$$M_t^\epsilon[\varphi] \leq Q_t[\varphi], \quad \forall \varphi \in \mathcal{C}_\eta, \quad t \in [0, 6\omega]. \tag{4.4.26}$$

In particular, $M_{6\omega}^\epsilon[\varphi] \leq Q_{6\omega}[\varphi]$, for all $\varphi \in \mathcal{C}_\eta$. Define

$$\Phi_\epsilon(\mu) := \frac{\ln \rho^\epsilon(\mu)}{\mu}, \quad \forall \mu > 0.$$

By an analysis for M_t^ϵ similar to that of M_t, we conclude by [49, Theorem 3.10] that $c_{6\omega}^* \geq \inf_{\mu>0} \Phi_\epsilon(\mu), \forall \epsilon \in (0,1)$. Combining $c_{6\omega}^* \leq \inf_{\mu>0} \Phi(\mu)$ and letting $\epsilon \to 0$, we obtain $c_{6\omega}^* = \inf_{\mu>0} \Phi(\mu)$. □

Then the following results shows that c^* is the spreading speed of the ω-periodic system (4.2.1) and that this c^* is also the minimum wave speed for the ω-periodic traveling waves with initial functions having compact support.

Theorem 4.4.6. *Let $u(t,x,\varphi) = u(t,\varphi)(x)$ be the solution of system (4.2.1) with initial function φ. Then $c^* := \frac{c^*_\omega}{\omega} = \frac{c^*_{6\omega}}{6\omega}$ and the following two statements are valid:*

(i) For any $c > c^*$, if $\varphi \in \mathcal{C}_{u^*(0)}$ with $0 \le \varphi \ll u^*(0)$ and $\varphi(x) = 0$ for x outside a bounded interval, then

$$\lim_{t\to\infty, |x|\ge tc} u(t,x,\varphi) = 0.$$

(ii) For any $c < c^*$, if $\varphi \in \mathcal{C}_{u^*(0)}$ with $\varphi \not\equiv 0$, then

$$\lim_{t\to\infty, |x|\le tc} [u(t,x,\varphi) - u^*(t)] = 0.$$

Proof. Conclusion (i) follows from Lemma 4.4.3 and [48, Theorem 2.1]. Moreover, both $\frac{c^*_\omega}{\omega}$ and $\frac{c^*_{6\omega}}{6\omega}$ are the spreading speeds for the system (4.2.1) and both are also the minimum wave speeds for the system (4.2.1). Then, $c^* := \frac{c^*_\omega}{\omega} = \frac{c^*_{6\omega}}{6\omega}$. By Lemma 4.4.3 and [48, Theorem 2.1], for any $c < c^* := \frac{c^*_\omega}{\omega} = \frac{c^*_{6\omega}}{6\omega}$, there is a positive number σ such that if $\varphi \in \mathcal{C}_{u^*(0)}$ and $\varphi(x) > 0$ for x on an interval of length 2σ, then $\lim_{t\to\infty, |x|\le tc}[u(t,x,\varphi) - u^*(t)] = 0$. For any $\varphi \in \mathcal{C}_{u^*(0)}$ with $\varphi \not\equiv 0$, there exists $\hat{\varphi} \in [0, u^*(0)]$ with $\hat{\varphi} \not\equiv 0$, $\hat{Q}_t(\hat{\varphi}) \gg 0$ for all $t \ge 6\omega$. We fix $t_0 \ge 6\omega$ and take $\hat{Q}_{t_0}(\hat{\varphi})$ as a new initial value for $u(t,x,\varphi)$. Then by the above analysis, conclusion (ii) is valid. □

By [48, Theorems 2.2 and 2.3], we have the following result about traveling waves of system (4.2.1).

Theorem 4.4.7. *Let* $c^* := \frac{c^*_\omega}{\omega} = \frac{c^*_{6\omega}}{6\omega}$. *Then for any* $c \geq c^*$, *system (4.2.1) has an* ω*-periodic traveling wave solution* $U(t, x - tc)$ *connecting* $u^*(t)$ *to* 0 *such that* $U(t, s)$ *is continuous and nonincreasing in* $s \in \mathbb{R}$, *and* $\lim_{s\to-\infty} U(t, s) = u^*(t)$ *and* $\lim_{s\to\infty} U(t, s) = 0$. *Moreover, for any* $c < c^*$, *(4.2.1) has no* ω*-periodic traveling wave* $U(t, x - tc)$ *connecting* $u^*(t)$ *to* 0.

Proof. Following Theorem 2.2-2.3 in [48], when $c \geq c^*$, $\{Q_t\}_{t\geq 0}$ has a 6ω-periodic (ω-periodic too) traveling wave which connects $u^*(t)$ to 0; when $c < c^*$, $\{Q_t\}_{t\geq 0}$ has no ω-periodic traveling wave which connects $u^*(t)$ to 0. □

5 Lyme disease pathogen transmission in seasonal tick populations with multiple host species

5.1 Introduction

Lyme disease can be transmitted to humans or animals during *B.burgdorferi*-infected blacklegged ticks (*I. scapularis*) feeding. The pathogen has a complex life history because it must colonize both hosts and vectors for successful transmission, involving three ecological and epidemiological processes: nymphal ticks infected in the previous year appear first; these ticks transmit the pathogen to their susceptible vertebrate hosts during feeding period; the next generation larvae acquire infection by sucking recently infected hosts' blood later in the same year and these larvae develop into nymphs in the next year, which completes the transmission cycle. Understanding the transmission cycle that regulates the abundance and distribution of the Lyme pathogen is crucial for the effective control and prevention of the

infection.

Among many factors for Lyme risk [77] are host diversity [83, 66, 69, 82], stage structure of ticks [16, 81, 80, 68, 69, 65, 3, 105] and climate effects [80, 68, 69, 31, 4]. Modelling disease transmission incorporating multiple life stages, tick seasonality and host community composition is crucial to understanding the pathogen transmission. There have been some modeling efforts (e.g., [4, 68, 104, 105, 83, 82, 31]), but many of these modeling studies incorporating some of the aforementioned facts do not permit analytic investigation rather than simulations.

Host diversity affects the dilution and/or amplification of the Lyme disease risk. Dilution effect is defined as "the pathogen population becomes less abundant or less likely to persist than in the present of one highly competent reservoir host species alone when one or more host species are added to a community" [11]. The opposite side of dilution is amplification. Many efforts for measuring dilution/amplification effect of Lyme disease have been made [53, 85, 14, 73]. Some researchers considered the nymphal infection prevalence (NIP) as an index to identify the dilution/amplification effect (e.g., [53]); some used the actual number of infected host-seeking nymphal *I. scapularis* per unit area of habitat (the density of infected nymphs or DIN) as another index (e.g., [73]). However, these frequency-dependent and density-dependent indexes have not been widely adapted by the public health community so far, moreover "cast-iron support of a dilution effect in

nature is still not clear" [11]. Here, we suggest that the basic reproduction ratio of pathogen combined with NIP and DIN can provide an effective joint measure of the potential risk of Lyme disease. The basic reproduction ratio is the most important and useful measure in the field of ecology and infectious disease epidemiology. In epidemiology, it is defined as the average number of secondary cases produced by one infectious primary case in a totally susceptible population [2, 21] and in ecology it is defined as the total number of new borne females produced by a female member. For complex disease systems described by ordinary differential equations with constant coefficients, the construction of next generation matrix is an efficient way to define the basic reproductive ratio and overcome the complex transmission process [98, 36, 22]. In this study we use extended ideas proposed in [8, 99] to define the basic reproduction ratio by formulating a next generation operator [22] for the ordinary differential systems with periodic coefficients.

In this chapter, we develop a modeling framework to investigate the impact of multiple tick life stages, tick seasonality and host diversity on the infection cycle of the Lyme disease agent, and this model seems to be mathematically tractable. In this study, we follow the framework proposed by Randolph and Rogers [81], and we divide the vector population into 7 stages with 12 subclasses, as illustrated in Figure 5.1. This scheme can account for the following key features in tick development and the pathogen transmission: (1) temperature-dependent/temperature-

independent development rate; (2) temperature-dependent host seeking rates; (3) density-dependent mortality, caused by the hosts' responses during the feeding period; (4) density-independent/constant mortality induced by the influence of abiotic factors acting on the off-host development stages. Our aim in this modeling study is to answer the following two questions on Lyme transmission from a theoretical point of view: Could climate change distribute the disease pathogen? Could the change of host diversity by adding alternative host species into the community dilute/amplify the Lyme pathogen?

5.2 Mathematical models and analysis

Our model uses periodic differential equations to account for the effects of temperature variations on tick development and pathogen transmission. The ticks, *I. scapularis*, pass through four stages which are labeled as E, L, N, A for the eggs, larvae, nymphs and adults, respectively. Each postegg stage is subdivided into questing and feeding phases according to the activity. We use E to denote the number of eggs, i_{FS}/i_{FI} denote the number of susceptible/infected ticks of feeding phase in the i stage ($i = L, N, A$), and i_{QS}/i_{QI} be the number of susceptible/infected ticks of questing phase in the i stage ($i = L, N, A$), respectively. The host population is considered as two types: hosts for immature ticks (which include the white-footed mouse H_1 and an alternative host H_2) and host for adult ticks

(deer D). The host death rates are μ_{H1} and μ_{H2} respectively. We assume that the total number of each host species (susceptible plus infected) in the isolated habitat is constant. To consider Lyme disease transmission between *I. scapularis* and rodents, we denote H_{1I} and H_{2I} the number of infected mice and the number of infected alternative host individuals. Eggs hatch to larvae at a development rate $d_E(t)$, while feeding larvae and nymphs will go through to the next stage (nymphs and adults, respectively) at the development rates $d_L(t)$ and $d_N(t)$. Host-finding rates $F_L(t)$, $F_N(t)$ and $F_A(t)$ between questing ticks and hosts of each class are reported in [68], as described in section 2.2 of Chapter 2. Due to the host resistance to the feeding ticks, we also consider density-dependent mortality of each feeding stage as a quadratic function with coefficient $D_i(t)$ $(i = L, N, A)$ respectively. We use μ_{Qi} and μ_{Fi} $(i = L, N, A)$ to denote the natural death rates of larvae, nymphs and adults at respective questing and feeding phases. We also suppose eggs are produced by feeding adult ticks at a rate $b(t)$ and die at a rate $\mu_E(t)$.

For the host-pathogen-tick transmission cycle, susceptible larvae can be infected by sucking blood from the infected hosts, after a duration of developmental delay, the infected nymphs developed from infected larvae then transmit the pathogen to their new host in the nymphal feeding period. In order to identify the different biting rates on two host species for immature ticks, we use the biting bias coefficients [40, 43] to describe the competence of different host species. We assume p_1 (p_2)

represents larval (nymphal) ticks biting bias for the alternative host. The biting bias coefficient $p_1 > 1$ ($p_2 > 1$) indicates larvae (nymphs) bias for the alternative host; on the other hand, $0 < p_1 < 1$ ($0 < p_2 < 1$) means larvae (nymphs) bias for the main immature host (*Peromyscus leucopus*). Using the method as described in [12], $F_L(t)\frac{H_1}{H_1+p_1H_2}\frac{H_{1I}(t)}{H_1}$ is the average rate at which a susceptible questing larva finds and attaches successfully onto the infected mice, and $\beta_{H1L}F_L(t)\frac{H_1}{H_1+p_1H_2}\frac{H_{1I}(t)}{H_1}$ is the average infection rate at which a susceptible larva gets infected from mice, where β_{H1L} is the transmission probability per bite from infectious mice (H_1) to susceptible larvae. Using the same idea to account the infection rate of larvae from the infected alternative host (H_2), the larval infection rate is given by

$$\begin{aligned} & \beta_{H1L}F_L(t)\frac{H_1}{H_1+p_1H_2}\frac{H_{1I}(t)}{H_1}L_Q(t) + \beta_{H2L}F_L(t)\frac{p_1H_2}{H_1+p_1H_2}\frac{H_{2I}(t)}{H_2}L_Q(t) \\ = \; & (\beta_{H1L}\frac{H_{1I}(t)}{H_1+p_1H_2} + \beta_{H2L}\frac{p_1H_{2I}(t)}{H_1+p_1H_2})F_L(t)L_Q(t). \end{aligned}$$

Similarly the newly infected feeding nymphs which come from the contact of questing susceptible nymphs and infectious hosts are given by

$$\begin{aligned} & \beta_{H1N}F_N(t)\frac{H_1}{H_1+p_2H_2}\frac{H_{1I}(t)}{H_1}N_{QS}(t) + \beta_{H2N}F_N(t)\frac{p_2H_2}{H_1+p_2H_2}\frac{H_{2I}(t)}{H_2}N_{QS}(t) \\ = \; & (\beta_{H1N}\frac{H_{1I}(t)}{H_1+p_2H_2} + \beta_{H2N}\frac{p_2H_{2I}(t)}{H_1+p_2H_2})F_N(t)N_{QS}(t). \end{aligned}$$

The susceptible hosts can get infected when they are bitten by infected questing nymphs. The conservation of bites requires that the numbers of bites made by ticks and received by hosts should be conserved. The disease incidence rate for mice

Peromyscus leucopus is therefore given by

$$\begin{aligned} & F_N(t)\beta_{NH1}(N_{QI}(t)+N_{QS}(t))\frac{N_{QI}(t)}{N_{QI}(t)+N_{QS}(t)}\frac{H_1}{H_1+p_2H_2}\frac{H_1-H_{1I}(t)}{H_1} \\ = \; & F_N(t)\beta_{NH1}N_{QI}(t)\frac{H_1-H_{1I}(t)}{H_1+p_2H_2}. \end{aligned}$$

Similarly, the alternative host is infected by the infectious nymphal biting at a rate

$$F_N(t)\beta_{NH2}N_{QI}(t)\frac{p_2(H_2-H_{2I}(t))}{H_1+p_2H_2}.$$

Therefore, the disease transmission process between ticks and their hosts can

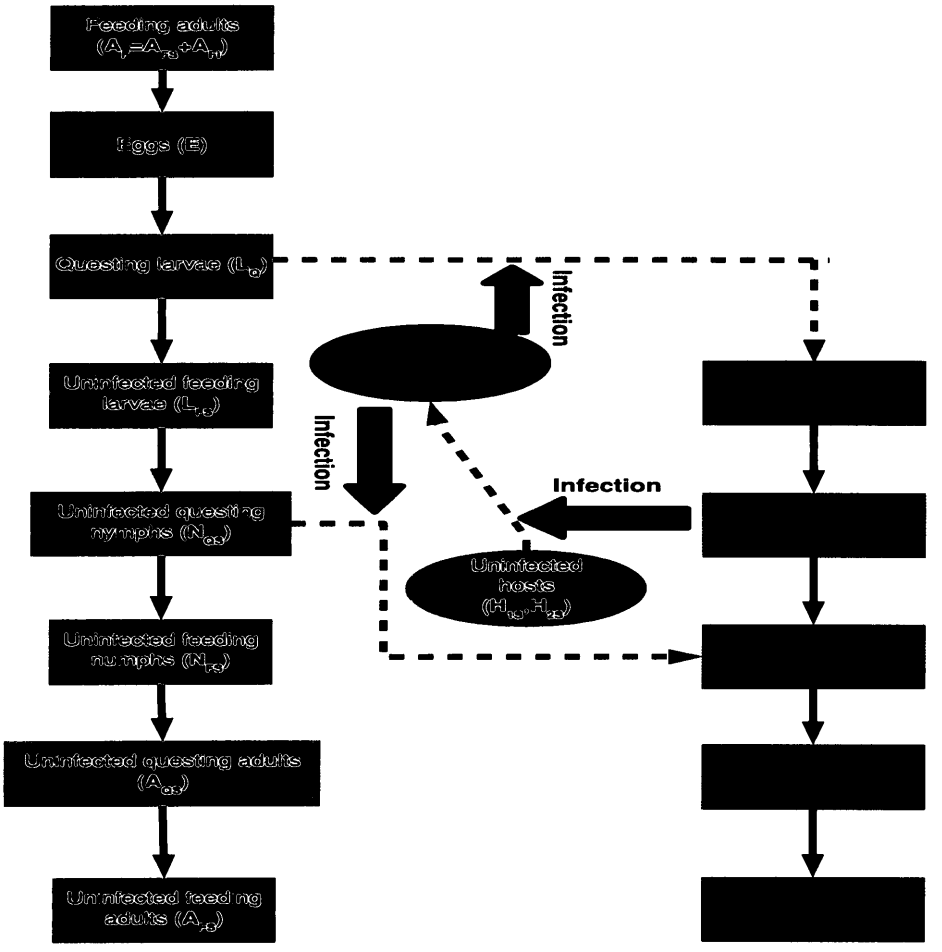

Figure 5.1: A diagram for the Lyme disease transmission. To describe the tick development and biting activities, the tick population is divided into 7 stages, with the uninfected or infected epidemiological classes for postegg stages. Immature ticks can feed on two host species, the mice (H_1) and an alternative host (H_2), while adult ticks mainly feed on deer.

be described by the following system

$$
\begin{aligned}
\frac{dE}{dt} &= b(t)(A_{FS}(t)+A_{FI}(t)) - \mu_E(t)E(t) - d_E(t)E(t),\\
\frac{dL_Q}{dt} &= d_E(t)E(t) - \mu_{QL}(t)L_Q(t) - F_L(t)L_Q(t),\\
\frac{dL_{FS}}{dt} &= (1-(\beta_{H1L}\frac{H_{1I}(t)}{H_1+p_1H_2}+\beta_{H2L}\frac{p_1H_{2I}(t)}{H_1+p_1H_2}))F_L(t)L_Q(t)\\
&\quad -\mu_{FL}(t)L_{FS}(t) - D_L(t)(L_{FS}(t)+L_{FI}(t))L_{FS}(t) - d_L(t)L_{FS}(t),\\
\frac{dL_{FI}}{dt} &= (\beta_{H1L}\frac{H_{1I}(t)}{H_1+p_1H_2}+\beta_{H2L}\frac{p_1H_{2I}(t)}{H_1+p_1H_2})F_L(t)L_Q(t)\\
&\quad -\mu_{FL}(t)L_{FI}(t) - D_L(t)(L_{FS}(t)+L_{FI}(t))L_{FI}(t) - d_L(t)L_{FI}(t),\\
\frac{dN_{QS}}{dt} &= d_L(t)L_{FS}(t) - \mu_{QN}(t)N_{QS}(t) - F_N(t)N_{QS}(t),\\
\frac{dN_{QI}}{dt} &= d_L(t)L_{FI}(t) - \mu_{QN}(t)N_{QI}(t) - F_N(t)N_{QI}(t),\\
\frac{dN_{FS}}{dt} &= (1-(\beta_{H1N}\frac{H_{1I}(t)}{H_1+p_2H_2}+\beta_{H2N}\frac{p_2H_{2I}(t)}{H_1+p_2H_2}))F_N(t)N_{QS}(t)\\
&\quad -\mu_{FN}(t)N_{FS}(t) - D_N(t)(N_{FS}(t)+N_{FI}(t))N_{FS}(t) - d_N(t)N_{FS}(t),\\
\frac{dN_{FI}}{dt} &= F_N(t)N_{QI}(t) + (\beta_{H1N}\frac{H_{1I}(t)}{H_1+p_2H_2}+\beta_{H2N}\frac{p_2H_{2I}(t)}{H_1+p_2H_2})F_N(t)N_{QS}(t)\\
&\quad -\mu_{FN}(t)N_{FI}(t) - D_N(t)(N_{FS}(t)+N_{FI}(t))N_{FI}(t) - d_N(t)N_{FI}(t),\\
\frac{dA_{QS}}{dt} &= d_N(t)N_{FS}(t) - \mu_{QA}(t)A_{QS}(t) - F_A(t)A_{QS}(t),\\
\frac{dA_{QI}}{dt} &= d_N(t)N_{FI}(t) - \mu_{QA}(t)A_{QI}(t) - F_A(t)A_{QI}(t),\\
\frac{dA_{FS}}{dt} &= F_A(t)A_{QS}(t) - \mu_{FA}(t)A_{FS}(t) - D_A(t)(A_{FS}(t)+A_{FI}(t))A_{FS}(t),\\
\frac{dA_{FI}}{dt} &= F_A(t)A_{QI}(t) - \mu_{FA}(t)A_{FI}(t) - D_A(t)(A_{FS}(t)+A_{FI}(t))A_{FI}(t),\\
\frac{dH_{1I}}{dt} &= F_N(t)\beta_{NH1}N_{QI}(t)\frac{H_1-H_{1I}(t)}{H_1+p_2H_2} - \mu_{H1}H_{1I}(t),\\
\frac{dH_{2I}}{dt} &= F_N(t)\beta_{NH2}N_{QI}(t)\frac{p_2(H_2-H_{2I}(t))}{H_1+p_2H_2} - \mu_{H2}H_{2I}(t).
\end{aligned}
\tag{5.2.1}
$$

We assume all the coefficients in the system are nonnegative and ω-periodic with period $\omega = 365$ days and the detailed parameter definitions are summerized in Table 5.1.

5.2.1 Positivity and boundedness of solutions

Our first task is to show that the mathematical model is biologically meaningful. Theoretically, we have the following theorem to ensure that all solutions through nonnegative initial values remain nonnegative and bounded.

Theorem 5.2.1. *System (5.2.1) has a unique nonnegative and bounded solution with the initial value*

$$x^0 \in X := \{x \in \mathbb{R}^{14}_+ : H_{1I} \leq H_1, H_{2I} \leq H_2\}.$$

Moreover, the solution $x(t, x^0)$ through $x^0 \in X$ remains in X for any $t \geq 0$.

Proof. It follows from [92, Theorem 5.2.1] that for any initial value $x^0 \in X$, system (5.2.4) admits a unique nonnegative solution $x(t, x^0)$ through this initial value with the maximal interval of existence $[0, \sigma)$ for some $\sigma > 0$.

Let $L_F = L_{FS} + L_{FI}$, $N_Q = N_{QS} + N_{QI}$, $N_F = N_{FS} + N_{FI}$, $A_Q = A_{QS} + A_{QI}$ and $A_F = A_{FS} + A_{FI}$. Then we can see that the tick growth is governed by the

Table 5.1: Model parameter definitions and values (all rates are per day unless otherwise stated).

Parameter	Meaning	Value	Resource
μ_E	basal mortality rate of an egg	0.002	[68]
μ_{QL}	basal mortality rate of questing larvae	0.0365	[82]
μ_{QN}	basal mortality rate of questing nymphs	0.015	[82]
μ_{QA}	basal mortality rate of questing adults	0.00625	[82]
μ_{FL}	basal mortality rate of feeding larvae	0.0365	[82]
μ_{FN}	basal mortality rate of feeding nymphs	0.015	[82]
μ_{FA}	basal mortality rate of feeding adults	0.00625	[82]
μ_{H_1}	death rate of white-footed mice	0.0075	[1]
μ_{H_2}	death rate of the alternative host H_2	variable	[1]
p	maximum number of eggs produced by per feeding adult female	3000	[68]
$b(t)$	time-dependent birth rate of eggs produced by feeding adult females	$0.5 * p * \frac{1}{\frac{1}{EAdel(t)}+10}$	[104]
$d_E(t)$	time-dependent development rate of eggs	$\frac{1}{\frac{1}{Edel(t)}+21}$	[104]
$d_L(t)$	time-dependent development rate of larvae	$\frac{1}{\frac{1}{Ldel(t)}+3}$	[104]
$d_N(t)$	time-dependent development rate of nymphs	$\frac{1}{\frac{1}{Ndel(t)}+5}$	[104]
H_1	number of white-footed mice	200	[68]
H_2	number of alternative host H_2	variable	N/A
D	number of deer	20	[68]
p_1	larval biting bias for host 2	see table 2	N/A
p_2	nymphal biting bias for host 2	see table 2	N/A
$F_L(t)$	time and density dependent host-finding rate of larvae	$0.0013(H_1 + p_1 H_2)^{0.515}\theta^i(t)$	[68]
$F_N(t)$	time and density dependent host-finding rate of nymphs	$0.0013(H_1 + p_2 H_2)^{0.515}\theta^i(t)$	[68]
$F_A(t)$	time and density dependent host-finding rate of adults	$0.086(D)^{0.515}\theta^a(t)$	[68]
$D_L(t)$	density-dependent mortality rate of feeding larvae on hosts	$\frac{0.001084}{H_1+p_1H_2}$	E
$D_N(t)$	density-dependent mortality rate of feeding nymphs on hosts	$\frac{0.001084}{H_1+p_2H_2}$	E
$D_A(t)$	density-dependent mortality rate of feeding adults on hosts	$\frac{0.001084}{D}$	E
β_{H_1L}	transmission probability from infected host species H_1 to susceptible larvae	0.914	[13]
β_{NH_1}	transmission probability from infected nymphs to susceptible host species H_1	1	[13]
β_{H_2L}	transmission probability from infected host species H_2 to susceptible larvae	see table 2	[13]
β_{NH_2}	transmission probability from infected nymphs to susceptible host species H_2	see table 2	[13]

E: Estimated from published data in [47].

following system:

$$\begin{aligned}
\frac{dE}{dt} &= b(t)A_F(t) - \mu_E(t)E(t) - d_E(t)E(t),\\
\frac{dL_Q}{dt} &= d_E(t)E(t) - \mu_{QL}(t)L_Q(t) - F_L(t)L_Q(t),\\
\frac{dL_F}{dt} &= F_L(t)L_Q(t) - \mu_{FL}(t)L_F(t) - D_L(t)L_F^2(t) - d_L(t)L_F(t),\\
\frac{dN_Q}{dt} &= d_L(t)L_F(t) - \mu_{QN}(t)N_Q(t) - F_N(t)N_Q(t),\\
\frac{dN_F}{dt} &= F_N(t)N_Q(t) - \mu_{FN}(t)N_F(t) - D_N(t)N_F^2(t) - d_N(t)N_F(t),\\
\frac{dA_Q}{dt} &= d_N(t)N_F(t) - \mu_{FA}(t)A_Q(t) - F_A(t)A_Q(t),\\
\frac{dA_F}{dt} &= F_A(t)A_Q(t) - \mu_{FA}(t)A_F(t) - D_A(t)A_F^2(t).
\end{aligned} \tag{5.2.2}$$

For any periodic nonnegative function $f(t)$ with period ω, denote $\widehat{f} = \max_{t\in[0,\omega]} f(t)$ and $\widetilde{f} = \min_{t\in[0,\omega]} f(t)$. It is easy to see that system (5.2.2) can be controlled by the following cooperative system:

$$\begin{aligned}
\frac{du_1}{dt} &= \widehat{b}u_7(t) - \widetilde{\mu_E}u_1(t),\\
\frac{du_2}{dt} &= \widehat{d_E}u_1(t) - \widetilde{\mu_{QL}}u_2(t),\\
\frac{du_3}{dt} &= \widehat{F_L}u_2(t) - \widetilde{\mu_{FL}}u_3(t),\\
\frac{du_4}{dt} &= \widehat{d_L}u_3(t) - \widetilde{\mu_{QN}}u_4(t),\\
\frac{du_5}{dt} &= \widehat{F_N}u_4(t) - \widetilde{\mu_{FN}}u_5(t),\\
\frac{du_6}{dt} &= \widehat{d_N}u_5(t) - \widetilde{\mu_{QA}}u_6(t),\\
\frac{du_7}{dt} &= \widehat{F_A}u_6(t) - \widetilde{\mu_{FA}}u_7(t) - \widetilde{D_A}u_7^2(t).
\end{aligned} \tag{5.2.3}$$

Clearly, there is only one nonnegative equilibrium zero for system (5.2.3) when

$$\widehat{F_A}\frac{\widehat{d_N}}{\widetilde{\mu_{QA}}}\frac{\widehat{F_N}}{\widetilde{\mu_{FN}}}\frac{\widehat{d_L}}{\widetilde{\mu_{QN}}}\frac{\widehat{F_L}}{\widetilde{\mu_{FL}}}\frac{\widehat{d_E}}{\widetilde{\mu_{QL}}}\frac{\widehat{b}}{\widetilde{\mu_E}} \le \widetilde{\mu_{FA}}.$$

If $\widehat{F_A}\frac{\widehat{d_N}}{\widehat{\mu_{QA}}}\frac{\widehat{F_N}}{\widehat{\mu_{FN}}}\frac{\widehat{d_L}}{\widehat{\mu_{QN}}}\frac{\widehat{F_L}}{\widehat{\mu_{FL}}}\frac{\widehat{d_E}}{\widehat{\mu_{QL}}}\frac{\widehat{b}}{\widehat{\mu_E}} > \widehat{\mu_{FA}}$, system (5.2.3) admits another positive equilibrium. It then follows from [109, Corollary 3.2] that either zero is globally asymptotically stable or the positive equilibrium is globally asymptotically stable for all nonzero solutions. Hence the comparison principle implies that $(E(t), L_Q(t), L_F(t), N_Q(t), N_F(t), A_Q(t), A_F(t))$ is bounded for any $t \in [0, \sigma)$. Thus, we see that $\sigma = \infty$ and the solution for model (5.2.3) is eventually bounded and exists globally for any nonnegative initial value. □

Using change of variables $L_F = L_{FS} + L_{FI}$, $N_Q = N_{QS} + N_{QI}$, $N_F = N_{FS} + N_{FI}$,

$A_Q = A_{QS} + A_{QI}$ and $A_F = A_{FS} + A_{FI}$, system (5.2.1) can be reduced into

$$\begin{aligned}
\frac{dE}{dt} &= b(t)A_F(t) - (\mu_E(t) + d_E(t))E(t), \\
\frac{dL_Q}{dt} &= d_E(t)E(t) - (\mu_{QL}(t) + F_L(t))L_Q(t), \\
\frac{dL_F}{dt} &= F_L(t)L_Q(t) - D_L(t)L_F^2(t) - (\mu_{FL}(t) + d_L(t))L_F(t), \\
\frac{dN_Q}{dt} &= d_L(t)L_F(t) - (\mu_{QN}(t) + F_N(t))N_Q(t), \\
\frac{dN_F}{dt} &= F_N(t)N_Q(t) - D_N(t)N_F^2(t) - (\mu_{FN}(t) + d_N(t))N_F(t), \\
\frac{dA_Q}{dt} &= d_N(t)N_F(t) - (\mu_{QA}(t) + F_A(t))A_Q(t), \\
\frac{dA_F}{dt} &= F_A(t)A_Q(t) - \mu_{FA}(t)A_F(t) - D_A(t)A_F^2(t), \\
\frac{dL_{FI}}{dt} &= (\beta_{H1L}\frac{H_{1I}(t)}{H_1+p_1H_2} + \beta_{H2L}\frac{p_1H_{2I}(t)}{H_1+p_1H_2})F_L(t)L_Q(t) \\
&\quad -D_L(t)L_F(t)L_{FI}(t) - (\mu_{FL}(t) + d_L(t))L_{FI}(t), \\
\frac{dN_{QI}}{dt} &= d_L(t)L_{FI}(t) - (\mu_{QN}(t) + F_N(t))N_{QI}(t), \\
\frac{dH_{1I}}{dt} &= F_N(t)\beta_{NH1}N_{QI}(t)\frac{H_1-H_{1I}(t)}{H_1+p_2H_2} - \mu_{H1}H_{1I}(t), \\
\frac{dH_{2I}}{dt} &= F_N(t)\beta_{NH2}N_{QI}(t)\frac{p_2(H_2-H_{2I}(t))}{H_1+p_2H_2} - \mu_{H2}H_{2I}(t).
\end{aligned} \tag{5.2.4}$$

In fact, we have three other equations for infected feeding nymphs (N_{FI}), questing adults (A_{QI}) and feeding adults (A_{FI}), which can be decoupled from the above system. Biologically, we are more concerned about the population size of infected questing nymphs whose bites are the main courses of human Lyme disease. We will then focus on system (5.2.4) in the remaining part of the chapter .

5.2.2 Tick population dynamics

We first consider the following stage-structured system for the tick population growth:

$$\begin{aligned}
\frac{dE}{dt} &= b(t)A_F(t) - (\mu_E(t) + d_E(t))E(t), \\
\frac{dL_Q}{dt} &= d_E(t)E(t) - (\mu_{QL}(t) + F_L(t))L_Q(t), \\
\frac{dL_F}{dt} &= F_L(t)L_Q(t) - D_L(t)L_F^2(t) - (\mu_{FL}(t) + d_L(t))L_F(t), \\
\frac{dN_Q}{dt} &= d_L(t)L_F(t) - (\mu_{QN}(t) + F_N(t))N_Q(t), \\
\frac{dN_F}{dt} &= F_N(t)N_Q(t) - D_N(t)N_F^2(t) - (\mu_{FN}(t) + d_N(t))N_F(t), \\
\frac{dA_Q}{dt} &= d_N(t)N_F(t) - (\mu_{QA}(t) + F_A(t))A_Q(t), \\
\frac{dA_F}{dt} &= F_A(t)A_Q(t) - \mu_{FA}(t)A_F(t) - D_A(t)A_F^2(t).
\end{aligned} \tag{5.2.5}$$

Linearization of system (5.2.5) at zero leads to the following linear system

$$\begin{aligned}
\frac{dE}{dt} &= b(t)A_F(t) - (\mu_E(t) + d_E(t))E(t), \\
\frac{dL_Q}{dt} &= d_E(t)E(t) - (\mu_{QL}(t) + F_L(t))L_Q(t), \\
\frac{dL_F}{dt} &= F_L(t)L_Q(t) - (\mu_{FL}(t) + d_L(t))L_F(t), \\
\frac{dN_Q}{dt} &= d_L(t)L_F(t) - (\mu_{QN}(t) + F_N(t))N_Q(t), \\
\frac{dN_F}{dt} &= F_N(t)N_Q(t) - (\mu_{FN}(t) + d_N(t))N_F(t), \\
\frac{dA_Q}{dt} &= d_N(t)N_F(t) - (\mu_{QA}(t) + F_A(t))A_Q(t), \\
\frac{dA_F}{dt} &= F_A(t)A_Q(t) - \mu_{FA}(t)A_F(t).
\end{aligned} \tag{5.2.6}$$

Following ideas proposed in [8, 99], we can define basic reproduction ratio for the

ticks. We introduce

$$F(t) = (f_{ij}(t))_{7\times 7}, \tag{5.2.7}$$

where $f_{1,7}(t) = b(t)$ and $f_{i,j}(t) = 0$ if $(i,j) \neq (1,7)$. Denote $V(t) =$

$$\begin{pmatrix}
\mu_E(t)+d_E(t) & 0 & 0 & 0 & 0 & 0 & 0 \\
-d_E(t) & \mu_{QL}(t)+F_L(t) & 0 & 0 & 0 & 0 & 0 \\
0 & -F_L(t) & \mu_{FL}(t)+d_L(t) & 0 & 0 & 0 & 0 \\
0 & 0 & -d_L(t) & \mu_{QN}(t)+F_N(t) & 0 & 0 & 0 \\
0 & 0 & 0 & -F_N(t) & \mu_{FN}(t)+d_N(t) & 0 & 0 \\
0 & 0 & 0 & 0 & -d_N(t) & \mu_{QA}(t)+F_A(t) & 0 \\
0 & 0 & 0 & 0 & 0 & -F_A(t) & \mu_{FA}(t)
\end{pmatrix},$$

and assume the evolutionary process $Y(t,s)$ satisfying

$$\frac{d}{dt}Y(t,s) = -V(t)Y(t,s) \quad \forall t \geq s, \quad Y(s,s) = I, \quad s \in \mathbb{R},$$

where I is the 7×7 identity matrix.

Let C_ω be the Banach space of all ω-periodic functions from $\mathbb{R}$ to $\mathbb{R}^7$, equipped with the supremum norm. Suppose $\phi \in C_\omega$ is the initial distribution of tick individuals in this periodic environment. We then define the linear operator $G : C_\omega \to C_\omega$ by

$$(G\phi)(t) = \int_0^\infty Y(t, t-a)F(t-a)\phi(t-a)da \quad \forall t \in \mathbb{R}, \quad \phi \in C_\omega. \tag{5.2.8}$$

Following [99] G is the next generation operator, and the basic reproduction ratio for ticks, denoted by $\mathcal{R}_0^{sv,p}$, is the spectral radius of G, i.e., $\mathcal{R}_0^{sv,p} := \rho(G)$.

Note that the Poincaré map associated with system (5.2.5) is not strongly monotone as observed in Chapter 4, but it is eventually strongly monotone after taking a few cycles as the same idea in Theorem 4.3.2 of Chapter 4. Using [99, Theorem 2.2], [108, Theorem 2.3.4], we have

Theorem 5.2.2. *The following statements are valid:*

(1) If $\mathcal{R}_0^{sv,p} \leq 1$, *then zero is globally asymptotically stable for system (5.2.5) in* $\mathbb{R}_+^7$;

(2) If $\mathcal{R}_0^{sv,p} > 1$, *then system (5.2.5) admits a unique* ω*-positive periodic solution*

$$(E^*(t), L_Q^*(t), L_F^*(t), N_Q^*(t), N_F^*(t), A_Q^*(t), A_F^*(t)),$$

and it is globally asymptotically stable for system (5.2.5) with initial values in $\mathbb{R}_+^7 \setminus \{0\}$.

5.2.3 Global dynamics of the model

If the basic reproduction ratio for ticks $\mathcal{R}_0^{sv,p} > 1$, then there exists a positive periodic solution, $(E^*(t), L_Q^*(t), L_F^*(t), N_Q^*(t), N_F^*(t), A_Q^*(t), A_F^*(t))$, for system (5.2.5) such that

$$\lim_{t\to\infty}((E(t), L_Q(t), L_F(t), N_Q(t), N_F(t), A_Q(t), A_F(t))$$
$$-(E^*(t), L_Q^*(t), L_F^*(t), N_Q^*(t), N_F^*(t), A_Q^*(t), A_F^*(t))) = 0.$$

In this case, equations for the infected populations in system (5.2.4) give rise to the following limiting system:

$$\begin{aligned}
\frac{dL_{FI}}{dt} &= (\beta_{H1L}\frac{H_{1I}(t)}{H_1+p_1H_2} + \beta_{H2L}\frac{p_1H_{2I}(t)}{H_1+p_1H_2})F_L(t)L_Q^*(t) \\
&\quad -D_L(t)L_F^*(t)L_{FI}(t) - (d_L(t)+\mu_{FL}(t))L_{FI}(t), \\
\frac{dN_{QI}}{dt} &= d_L(t)L_{FI}(t) - (\mu_{QN}(t)+F_N(t))N_{QI}(t), \\
\frac{dH_{1I}}{dt} &= F_N(t)\beta_{NH1}N_{QI}(t)\frac{H_1-H_{1I}(t)}{H_1+p_2H_2} - \mu_{H1}H_{1I}(t), \\
\frac{dH_{2I}}{dt} &= F_N(t)\beta_{NH2}N_{QI}(t)\frac{p_2(H_2-H_{2I}(t))}{H_1+p_2H_2} - \mu_{H2}H_{2I}(t).
\end{aligned} \tag{5.2.9}$$

As proceed in the definition of $\mathcal{R}_0^{sv,p}$ in the previous section, we can define the basic reproduction ratio for the pathogen denoted by $\mathcal{R}_0^{d,p}$. Let

$\widetilde{F}(t) =$

$$\begin{pmatrix}
0 & 0 & \frac{\beta_{H1L}F_L(t)L_Q^*(t)}{H_1+p_1H_2} & \frac{p_1\beta_{H2L}F_L(t)L_Q^*(t)}{H_1+p_1H_2} \\
0 & 0 & 0 & 0 \\
0 & \frac{F_N(t)\beta_{NH1}H_1}{H_1+p_2H_2} & 0 & 0 \\
0 & \frac{p_2F_N(t)\beta_{NH2}H_2}{H_1+p_2H_2} & 0 & 0
\end{pmatrix},$$

and $\widetilde{V}(t) =$

$$\begin{pmatrix}
D_L(t)L_F^*(t)+d_L(t)+\mu_{FL}(t) & 0 & 0 & 0 \\
-d_L(t) & \mu_{QN}(t)+F_N(t) & 0 & 0 \\
0 & 0 & \mu_{H1} & 0 \\
0 & 0 & 0 & \mu_{H2}
\end{pmatrix}.$$

Introduction of evolutionary process $\widetilde{Y}(t,s)$ satisfying

$$\frac{d}{dt}\widetilde{Y}(t,s) = -\widetilde{V}(t)\widetilde{Y}(t,s) \quad \forall t \geq s, \quad \widetilde{Y}(s,s) = I, \quad s \in \mathbb{R}$$

where I is the 4×4 identity matrix.

Let $\widetilde{C}_\omega$ be the Banach space of all ω-periodic functions from $\mathbb{R}$ to $\mathbb{R}^4$, equipped with the supremum norm. Suppose $\phi \in \widetilde{C}_\omega$ is the initial distribution of infectious tick and host individuals in this periodic environment.

We define the linear operator $\widetilde{G} : \widetilde{C}_\omega \to \widetilde{C}_\omega$ by

$$(\widetilde{G}(\phi))(t) = \int_0^\infty \widetilde{Y}(t, t-a)\widetilde{F}(t-a)\phi(t-a)da \quad \forall t \in \mathbb{R}, \quad \phi \in \widetilde{C_\omega}. \quad (5.2.10)$$

is the distribution of accumulative infectious ticks and hosts at time t produced by all those infectious individuals $\phi(s)$ introduced at the previous time s. $\widetilde{G}$ is the next generation operator by [99], and the basic reproduction ratio for pathogen is $\mathcal{R}_0^{d,p} := \rho(\widetilde{G})$, the spectral radius of $\widetilde{G}$.

Using the same argument as in the previous section, we have the following results:

Theorem 5.2.3. *The following statements are valid:*

(1) If $\mathcal{R}_0^{d,p} \leq 1$, then zero is globally asymptotically stable for system (5.2.9) in $\mathbb{R}^4_+$;

(2) If $\mathcal{R}_0^{d,p} > 1$, then system (5.2.9) admits a unique positive periodic solution

$$(L^*_{FI}(t), N^*_{QI}(t), H^*_{1I}(t), H^*_{2I}(t))$$

and it is globally asymptotically stable for system (5.2.9).

Based on two reproduction ratios, the ratio for ticks ($\mathcal{R}_0^{sv,p}$) and ratio for the pathogen ($\mathcal{R}_0^{d,p}$), we can completely determine the global dynamics of the model system (5.2.4).

Theorem 5.2.4. *Let $x(t, x^0)$ be the solution of system (5.2.4) through x^0. Then the following statements are valid:*

(1) If $\mathcal{R}_0^{sv,p} \leq 1$, then zero is globally attractive for system (5.2.4);

(2) If $\mathcal{R}_0^{sv,p} > 1$ and $\mathcal{R}_0^{d,p} \leq 1$, then

$$\begin{aligned} &\lim_{t\to\infty}((x_1(t), x_2(t), x_3(t), x_4(t), x_5(t), x_6(t), x_7(t)) \\ - \ &(E^*(t), L_Q^*(t), L_F^*(t), N_Q^*(t), N_F^*(t), A_Q^*(t), A_F^*(t))) = 0, \end{aligned}$$

and $\lim_{t\to\infty} x_i(t) = 0$ for $i \in [8, 11]$;

(3) If $\mathcal{R}_0^{sv,p} > 1$ and $\mathcal{R}_0^{d,p} > 1$, then there exists a positive periodic solution $x^*(t)$, and it is globally attractive for system (5.2.4) with respect to all positive solutions.

Proof. We first consider the ω-periodic system as a 11ω-periodic system. Let P be the Poincaré map of system (5.2.4), that is,

$$P(x^0) = x(11\omega, x^0)$$

where $x(t, x^0)$ is the solution of system (5.2.4) through x^0. Then P is compact. Let $\omega = \omega(x^0)$ be the omega limit set of $P(x^0)$. It then follows from [38, Lemma 2.1] (see also [108, Lemma 1.2.1]) that ω is an internally chain transitive set for P.

(1) In the case where $\mathcal{R}_0^{sv,p} \leq 1$, we have $\lim_{t\to\infty} x_i(t) = 0$ for $i \in [1, 9]$. Hence, $\omega = \{(0,0,0,0,0,0,0,0,0)\} \times \omega_1$ for some $\omega_1 \subset \mathbb{R}^2$. It is easy to see that

$$P|_\omega(0,0,0,0,0,0,0,0,0,H_{1I}(0),H_{2I}(0)) = (0,0,0,0,0,0,0,0,0,P_1(H_{1I}(0),H_{2I}(0))),$$

where P_1 is the Poincaré map associated with the following equation:

$$\begin{aligned} \frac{dH_{1I}}{dt} &= -\mu_{H1}H_{1I}, \\ \frac{dH_{2I}}{dt} &= -\mu_{H2}H_{2I}. \end{aligned} \tag{5.2.11}$$

Since ω is an internally chain transitive set for P, it easily follows that ω_1 is an internally chain transitive set for P_1. Since $\{0\}$ is globally asymptotically stable for system (5.2.11), [38, Theorem 3.2] implies that $\omega_1 = \{(0,0)\}$. Thus, we have $\omega = \{0\}$, which proves that every solution converges to zero.

(2) In the case where $\mathcal{R}_0^{sv,p} > 1$, then there exists a positive periodic solution, $(E^*(t), L_Q^*(t), L_F^*(t), N_Q^*(t), N_F^*(t), A_Q^*(t), A_F^*(t))$, for system (5.2.5) such that for any x^0 with $\sum_{i=1}^7 x_i^0 > 0$, we have

$$\begin{aligned} &\lim_{t\to\infty}((x_1(t),x_2(t),x_3(t),x_4(t),x_5(t),x_6(t),x_7(t)) \\ &-(E^*(t),L_Q^*(t),L_F^*(t),N_Q^*(t),N_F^*(t),A_Q^*(t),A_F^*(t))) = 0. \end{aligned}$$

Thus, $\omega = \{(E^*(0),L_Q^*(0),L_F^*(0),N_Q^*(0),N_F^*(0),A_Q^*(0),A_F^*(0))\} \times \omega_2$ for some $\omega_2 \subset$

$\mathbb{R}^4$, and

$$P|_\omega(E^*(0), L_Q^*(0), L_F^*(0), N_Q^*(0), N_F^*(0), A_Q^*(0), A_F^*(0), x_8, x_9, x_{10}, x_{11})$$
$$= (E^*(0), L_Q^*(0), L_F^*(0), N_Q^*(0), N_F^*(0), A_Q^*(0), A_F^*(0), P_2(x_8, x_9, x_{10}, x_{11})),$$

where P_2 is the Poincaré map associated with system (5.2.9). Since ω is an internally chain transitive set for P, then ω_2 is an internally chain transitive set for P_2. Since $\mathcal{R}_0^{d,p} \leq 1$, then $\{(0,0,0,0)\}$ is globally asymptotically stable for system (5.2.9) according to Theorem 5.2.3. It then follows from [38, Theorem 3.2] that $\omega_2 = \{0\}$. This proves

$$\omega = \{(E^*(0), L_Q^*(0), L_F^*(0), N_Q^*(0), N_F^*(0), A_Q^*(0), A_F^*(0), 0, 0, 0, 0)\}.$$

Therefore, statement (2) holds.

(3) In the case where $\mathcal{R}_0^{sv,p} > 1$ and $\mathcal{R}_0^{d,p} > 1$, then there exists a positive periodic solution, $(E^*(t), L_Q^*(t), L_F^*(t), N_Q^*(t), N_F^*(t), A_Q^*(t), A_F^*(t))$, for system (5.2.5) such that for any x^0 with $\sum_{i=1}^7 x_i^0 > 0$, we have

$$\lim_{t\to\infty}((x_1(t), x_2(t), x_3(t), x_4(t), x_5(t), x_6(t), x_7(t))$$
$$-(E^*(t), L_Q^*(t), L_F^*(t), N_Q^*(t), N_F^*(t), A_Q^*(t), A_F^*(t))).$$

It then follows that $\omega = \{(E^*(0), L_Q^*(0), L_F^*(0), N_Q^*(0), N_F^*(0), A_Q^*(0), A_F^*(0)))\} \times \omega_3$ for some $\omega_3 \subset \mathbb{R}^4$, and

$$P|_\omega(E^*(0), L_Q^*(0), L_F^*(0), N_Q^*(0), N_F^*(0), A_Q^*(0), A_F^*(0), x_8, x_9, x_{10}, x_{11})$$
$$= (E^*(0), L_Q^*(0), L_F^*(0), N_Q^*(0), N_F^*(0), A_Q^*(0), A_F^*(0), P_2(x_8, x_9, x_{10}, x_{11})),$$

where P_2 is the solution semiflow of system (5.2.9). Since ω is an internally chain transitive set for P, it follows that ω_3 is an internally chain transitive set for P_2. We claim that $\omega_3 \neq \{0\}$ for any $(x_8^0, x_9^0, x_{10}^0, x_{11}^0) > 0$.

Assume that, by contradiction, $\omega_3 = \{0\}$. That is

$$\omega = \{(E^*(0), L_Q^*(0), L_F^*(0), N_Q^*(0), N_F^*(0), A_Q^*(0), A_F^*(0), 0, 0, 0, 0)\}$$

for some $(x_8^0, x_9^0, x_{10}^0, x_{11}^0) > 0$. Then, we have

$$\lim_{t\to\infty}(x(t) - (E^*(t), L_Q^*(t), L_F^*(t), N_Q^*(t), N_F^*(t), A_Q^*(t), A_F^*(t), 0, 0, 0, 0)) = 0. \tag{5.2.12}$$

Since $\mathcal{R}_0^{d,p} > 1$, there exists some $\delta > 0$ such that the spectral radius of the Poincaré map associated with the linearized system of the following one is greater than unity:

$$\begin{aligned}
\frac{dL_{FI}}{dt} &= (\beta_{H1L}\frac{H_{1I}(t)}{H_1+p_1H_2} + \beta_{H2L}\frac{p_1H_{2I}(t)}{H_1+p_1H_2})F_L(t)(L_Q^*(t) - \delta) \\
&\quad -D_L(t)(L_F^*(t) + \delta)L_{FI}(t) - (d_L(t) + \mu_{FL}(t))L_{FI}(t), \\
\frac{dN_{QI}}{dt} &= d_L(t)L_{FI}(t) - (\mu_{QN}(t) + F_N(t))N_{QI}(t), \\
\frac{dH_{1I}}{dt} &= F_N(t)\beta_{NH1}N_{QI}(t)\frac{H_1-H_{1I}(t)}{H_1+p_2H_2} - \mu_{H1}H_{1I}(t), \\
\frac{dH_{2I}}{dt} &= F_N(t)\beta_{NH2}N_{QI}(t)\frac{p_2(H_2-H_{2I}(t))}{H_1+p_2H_2} - \mu_{H2}H_{2I}(t).
\end{aligned} \tag{5.2.13}$$

It then follows from the same argument as in the proof of Theorem 5.2.2 that the

following system

$$\begin{aligned}
\frac{du_1}{dt} &= (\beta_{H1L}\frac{u_3(t)}{H_1+p_1H_2} + \beta_{H2L}\frac{p_1u_4(t)}{H_1+p_1H_2})F_L(t)(L_Q^*(t)-\delta) \\
&\quad -D_L(t)(L_F^*(t)+\delta)u_1(t) - (d_L(t)+\mu_{FL}(t))u_1(t), \\
\frac{du_2}{dt} &= d_L(t)u_1(t) - (\mu_{QN}(t)+F_N(t))u_2(t), \\
\frac{du_3}{dt} &= F_N(t)\beta_{NH1}u_2(t)\frac{H_1-u_3(t)}{H_1+p_2H_2} - \mu_{H1}u_3(t), \\
\frac{du_4}{dt} &= F_N(t)\beta_{NH2}u_2(t)\frac{p_2(H_2-u_4(t))}{H_1+p_2H_2} - \mu_{H2}u_4(t).
\end{aligned}$$

admits a positive periodic $u^*(t)$ such that

$$\lim_{t\to\infty}(u(t)-u^*(t)) = 0,\ \forall u(t) \neq 0.$$

Since there exists some $\omega_0 > 0$ such that

$$\begin{aligned}
&\|(x_1(t),x_2(t),x_3(t),x_4(t),x_5(t),x_6(t),x_7(t)) \\
&-(E^*(t),L_Q^*(t),L_F^*(t),N_Q^*(t),N_F^*(t),A_Q^*(t),A_F^*(t))\| \leq \delta,\ \forall t > \omega_0,
\end{aligned}$$

we have

$$\begin{aligned}
\frac{dx_8}{dt} &\geq (\beta_{H1L}\frac{x_{10}(t)}{H_1+p_1H_2} + \beta_{H2L}\frac{p_1x_{11}(t)}{H_1+p_1H_2})F_L(t)(L_Q^*(t)-\delta) \\
&\quad -D_L(t)(L_F^*(t)+\delta)x_8(t) - (d_L(t)+\mu_{FL}(t))x_8(t), \\
\frac{dx_9}{dt} &= d_L(t)x_8(t) - (\mu_{QN}(t)+F_N(t))x_9(t), \\
\frac{dx_{10}}{dt} &= F_N(t)\beta_{NH1}x_9(t)\frac{H_1-x_{10}(t)}{H_1+p_2H_2} - \mu_{H1}x_{10}(t), \\
\frac{dx_{11}}{dt} &= F_N(t)\beta_{NH2}x_9(t)\frac{p_2(H_2-x_{11}(t))}{H_1+p_2H_2} - \mu_{H2}x_{11}(t).
\end{aligned} \tag{5.2.14}$$

for all $t > \omega_0$. By the comparison principle, we have

$$\liminf_{t\to\infty}((x_8(t),x_9(t),x_{10}(t),x_{11}(t)) - u^*(t)) \geq 0,$$

a contradiction to (5.2.12).

Since $\omega_3 \neq \{0\}$ and the positive periodic solution $(L^*_{FI}(t), N^*_{QI}(t), H^*_{1I}(t), H^*_{2I}(t))$ is globally asymptotically stable for system (5.2.9) in $\mathbb{R}^4_+ \setminus \{0\}$, it follows that

$$\omega_3 \cap W^s((L^*_{FI}(0), N^*_{QI}(0), H^*_{1I}(0), H^*_{2I}(0))) \neq \emptyset,$$

where

$$W^s((L^*_{FI}(0), N^*_{QI}(0), H^*_{1I}(0), H^*_{2I}(0)))$$

is the stable set for $(L^*_{FI}(0),\ N^*_{QI}(0),\ H^*_{1I}(0),\ H^*_{2I}(0))$ with respect to the Poincaré map P_2. By [38, Theorem 3.1], we then get

$$\omega_3 = \{(L^*_{FI}(0), N^*_{QI}(0), H^*_{1I}(0), H^*_{2I}(0))\}.$$

Thus,

$$\omega = \{(E^*(0), L^*_Q(0), L^*_F(0), N^*_Q(0), N^*_F(0), A^*_Q(0), A^*_F(0), L^*_{FI}(0), N^*_{QI}(0), H^*_{1I}(0), H^*_{2I}(0))\},$$

and hence, statement (3) is valid.

At last, using a similar argument as in the proof of Theorem 5.2.2, we can show that the globally attractive 11ω-periodic solution in each case is also ω-periodic solution. □

5.3 Numerical simulation and sensitivity analysis

We now conduct some simulations to examine the influences of climate warming and host diversity on tick population abundance and disease invasion. The parameter values are estimated from the literatures and experiment reports. We simulate the model until the tick population and pathogen level stabilize at an annual cycle. The simulation results show that every solution attains the same stable annual cycle with different initial conditions, which is consistent with the theoretical results in Section 5.2.

We compare various indexes to measure the disease risk to humans: the reproduction ratios for the tick population ($\mathcal{R}_0^{sv,p}$), for the Lyme pathogen ($\mathcal{R}_0^{d,p}$); the total number of questing nymphs (for short, TQN) at equilibrium (which gives the precise description of questing nymphal abundance and seasonality); and the abundance and seasonality of all actually active infected questing nymphs (for short, AIQN) at equilibrium. Here the number of AIQN is the multiplication of the nymphal tick activity proportion and the number of all infected questing nymphs. Actually, the active number of infected questing nymphs is a real risk measure for Lyme disease of public health concern. Finally, we use the infection prevalence in questing nymphs (INP), defined as the quotient of infected questing nymphs divided by questing nymphs at stable state. We adopt the same Floquet-dichotomy

approach outlined in Bacaër 2007 [5] and Wang and Zhao 2008 [99] to calculate the basic reproduction ratios.

5.3.1 Climate warming effects

We firstly investigate the effect of climate change on the seasonal tick abundance and disease risk. Here, we alter the mean monthly temperature data from the 1961-1990 period to 2000-2009 period, collected individually from the two meteorological stations near a tick endemic area in Canada. For both two periods, we numerically compute the reproduction ratios. The reproduction ratio for ticks $\mathcal{R}_0^{sv,p}$ increases from 1.6996 for the 1961-1990 period to 2.1915 for the 2000-2009 period, while the basic reproduction ratio for the pathogen $\mathcal{R}_0^{d,p}$ also increases, from 0.7585 to 1.0867. Our mathematical results (Theorem 5.2.4) predict that the tick population can successfully invade into the habitat under these two temperatures since $\mathcal{R}_0^{sv,p} > 1$. However, the transmission cycle fails to establish under the 1961-1990 temperature data while the cycle establishes for the 2000-2009 temperature data since $\mathcal{R}_0^{d,p}$ is increased from below one to be greater than one. Figure 5.2 shows both the abundance of TQN and infected questing nymphs (for short, IQN) increase with increased temperatures. Figure 5.2(a) shows that the size of TQN is growing when surrounding temperatures rise. Interestingly, Figure 5.2(b) shows that the size of IQN changes substantially, from dying out to remaining endemic in the habitat

solely due to the temperature rising. Moreover, we can show that climate warming could greatly increase the size of infected tick population and influence the potential risk of Lyme disease as well in the regions. Therefore, climate warming would facilitate the invasion of both ticks and the pathogen.

5.3.2 Host diversity effects

In this subsection, we study the impact of host diversity on the risk of Lyme disease with/without interspecific host competition. The temperature data in the 2000-2009 period is used with other parameters listed in Table 5.1, 5.2, 5.3, then the development rates $EAdel(t)$ (development for pre-oviposition period), $Edel(t)$ (development from eggs to larvae), $Ldel(t)$ (development from engorged larvae to questing nymphs), $Ndel(t)$ (development from engorged nymphs to questing adults) and activity proportions $\theta^i(t)$, $\theta^a(t)$ are estimated using methodology introduced in [104]. All the possible alternative species listed in [53] are tested in our simulations with the exception of deer, which are incompetent exclusive hosts for adult ticks in our model.

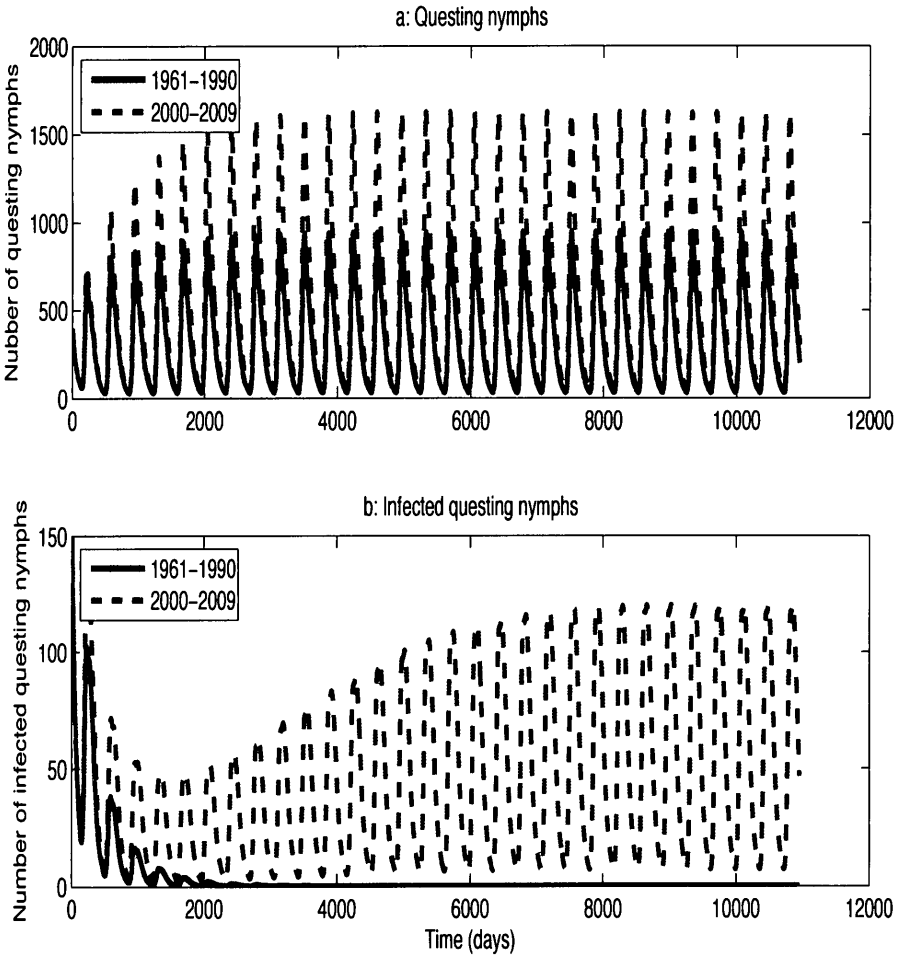

Figure 5.2: The abundance variation of total questing nymphs and infected questing nymphs with increased temperatures. (a): Variations in number of total questing nymphs under two different temperature datasets; (b): Variations in the number of infected questing nymphs under two different temperature scenarios. Red solid lines represent the results by seeding the model with $1961 - 1990$ temperature data ($\mathcal{R}_0^{sv,p} = 1.6996$ and $\mathcal{R}_0^{d,p} = 0.7585$ in this case) while the blue dash lines represent the results by seeding the model with $2000 - 2009$ temperature data ($\mathcal{R}_0^{sv,p} = 2.1915$ and $\mathcal{R}_0^{d,p} = 1.0867$ in this case).

5.3.2.1 Effects of adding alternative hosts without interspecific host competition

As the first step, we assume that only one species of alternative hosts (H_2) is added into the host community while the abundance of the competent host *P. leucopus* population is set as a constant. When 10/20 alternative hosts (*Eastern chipmunk*) are added, both basic reproductive ratios $\mathcal{R}_0^{sv,p}$ for *I. scapularis* (from 2.1915 to 2.3511/2.4978) and $\mathcal{R}_0^{d,p}$ for pathogen (from 1.0867 to 1.1777/1.2579) increase. Figure 5.3 shows that all the numbers of (active) questing nymphs, (active) infected questing nymphs become larger and larger as well. From Figure 5.3(d), *Eastern chipmunk* would amplify the number of active infected questing nymphal ticks, a real concern to public, moreover the peak timing of infected questing nymphs happens in summer times (July and August) which is consistent with the peak human outdoor activity, and thus contributes to a high risk of getting Lyme disease.

Table 5.2 summarizes the results examining the effects of adding some chosen alternative host species on the risk of the disease without interspecific host competition. From the computations for reproduction ratios, adding an alternative host always increases the reproduction ratios for ticks $\mathcal{R}_0^{sv,p}$, which is due to that the alternative host serves as a food supply and promotes tick development. However, adding an alternative host may increase or decrease the reproduction ratio for the

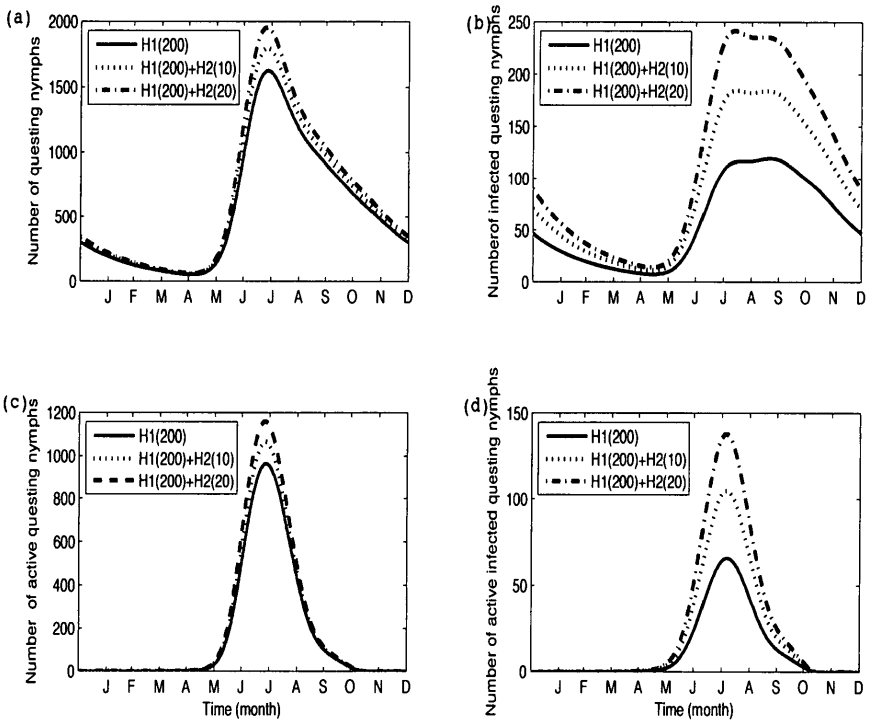

Figure 5.3: Variations of the abundance of total questing nymphal ticks and infected questing nymphal ticks without/with an alternative host *Eastern chipmunk*, where $p_1 = 0.4$, $p_2 = 3.5$. Blue solid lines represent the scenario without any alternative hosts; black dash lines represent the scenario when alternative host *Eastern chipmunk* is 10; red dot-dash lines represent the scenario when alternative host *Eastern chipmunk* is 20. Where $H_1 = 200$, $H_2 = 0$, $\mathcal{R}_0^{sv,p} = 2.1915$, $\mathcal{R}_0^{d,p} = 1.0867$; $H_1 = 200$, $H_2 = 10$, $\mathcal{R}_0^{sv,p} = 2.3511$, $\mathcal{R}_0^{d,p} = 1.1777$; $H_1 = 200$, $H_2 = 20$, $\mathcal{R}_0^{sv,p} = 2.4978$ and $\mathcal{R}_0^{d,p} = 1.2579$.

pathogen $\mathcal{R}_0^{d,p}$ since this value is affected by the tick development and the reservoir competence of the adding host. According to Table 5.2, some host species may amplify the disease risk while others may dilute the disease risk. However, this result largely depends on the host's pathogen-reservoir competence, as well as their densities and tick biting bias coefficients. Moreover, two indexes, the active infected questing nymphs (AIQN) and infected nymphal proportion (INP) may generate conflicting predictions in determining the amplification and dilution effects. For example, adding 20 raccoons into the existing host community may increase the AIQN while decrease the INP. Therefore, different indexes, instead of a single index, should be used to measure the disease risk.

5.3.2.2 Effects of adding alternative hosts with interspecific host competition

In this subsection, we investigate whether the addition of alternative hosts will reduce the abundance of *P. leucopus* through interspecific competition on a one-for-one basis, that is, the total number of hosts (including mice and alternative hosts) in the community remains a constant. This scenario is based on the assumption that the environment can only support a saturated number of rodents. When the reduced number of *P. leucopus* is replaced by an equal number of alternative hosts in the model, dilution/amplification effect will occur for all the simulations (Table

Table 5.2: Effect of adding an alternative hosts without interspecific host competition.

Species	β_{H_2L}	β_{NH_2}	μ_{H_2}	p_1	p_2	Density	AIQN	INP	$\mathcal{R}_0^{sv,p}$	$\mathcal{R}_0^{d,p}$
Eastern chipmunk	0.569	0.971	0.00274	0.4	3.5	20	A	A	2.4978	1.2579
Raccoon	0.017	1.0	0.0005	8.5	5.3	20	A	D	3.3775	1.9705
				18.5	5.6	20	A	D	4.0814	2.6701
				1.3	11.1	20	A	D	3.0456	1.3899
Virginia opossum	0.004	0.261	0.0018	8.6	3.9	10	A	D	2.7542	1.1217
				7.6	8.0	10	A	D	2.8775	1.1184
				7.2	36.9	20	D	D	4.7264	1.0601
Striped skunk	0.191	0.530	0.00274	10.9	8.0	10	A	A	3.0230	1.8792
Short-tailed shrew	0.505	0.831	0.001	2*	1*	20	A	A	2.4612	1.6240
Sorex shrews	0.537	0.701	0.0018	2*	1*	20	A	A	2.4612	1.3724
Red and grey squirrel	0.061	0.831	0.0002	1.8	6.9	10	A	A	2.5475	1.9863
				1.3	4.4	10	A	A	2.4285	1.5788
Resources	[13]	[13]	[1]	[76]	[76]					

The table summarizes the results of dilution/amplification effect and two basic reproductive ratios. Here, A means amplification effect; D means dilution effect. The mean monthly temperatures are adapted from 2000-2009 period, and all other parameter values are the same as those in Table 5.1 in this study.

5.3), which is slightly different from the results induced by ignoring the interspecific competition between different host species.

Figure 5.4 shows that the size of (active) questing nymphs is increasing while that of the (active) infected questing nymphs is contrarily decreasing when we increase the density of the alternative host *Virginia opossum*. The basic reproductive ratio $\mathcal{R}_0^{sv,p}$ for *I. scapularis* increases from 2.1915 to 3.5788/4.1041 when 10/15 *Virginia opossums* are added, but in the meanwhile $\mathcal{R}_0^{d,p}$ for pathogen decreases form 1.0867 to 1.0643/1.0405, on the contrary. In this case, *Virginia opossum*, serving as a blood source for the ticks, can dilute the pathogen of Lyme disease and thus decrease the risk to Lyme disease.

5.3.3 Sensitivity analysis

The Lyme disease transmission model is quite complex due to the complexity of the vector's (*I. scapularis*) life cycle, the broad host species and variable reservoir competence of different host species. Estimating the values of the input variables has a high degree of uncertainty. We now use the Latin Hypercube Sampling Method (LHS) and partial rank correlation coefficient (PRCC) [58] to identify the effect of the uncertainty in estimating the values of input parameters on the prediction imprecision of our outcome variable: the basic reproduction ratio of pathogen $\mathcal{R}_0^{d,p}$. All parameters in this study are changed by 20% from their start values and then

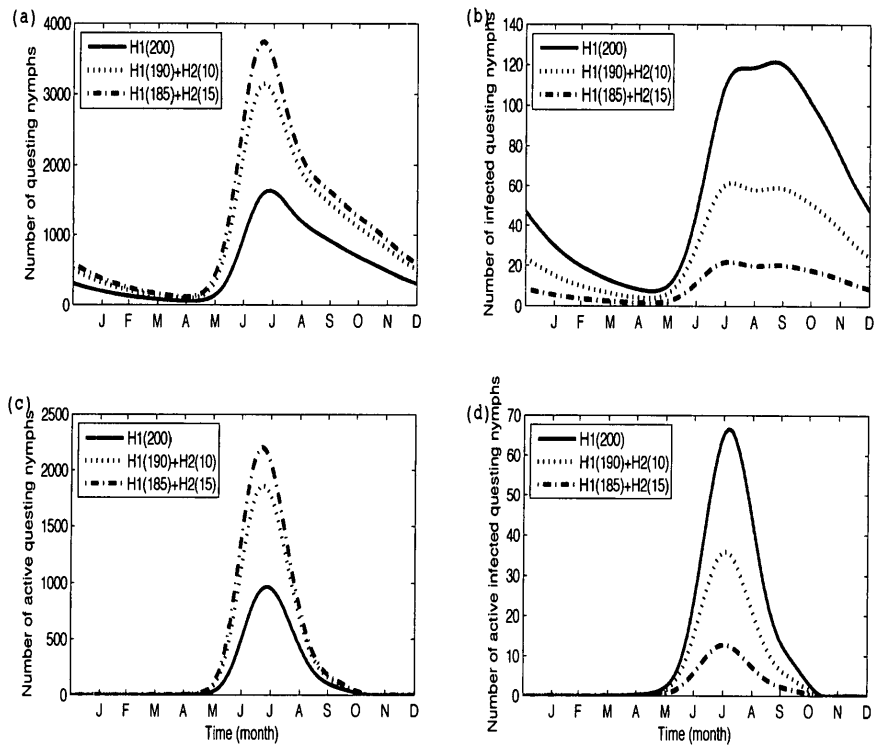

Figure 5.4: Variations of the abundance of (active) total questing nymphal ticks and (active) total infected questing nymphal ticks without/with an alternative host *Virginia opossum* when $p_1 = 7.2$, $p_2 = 36.9$. Blue solid lines represent the scenario without any alternative host; black dash lines represent the scenario when alternative host *Virginia opossum* is 10; red dot-dash lines represent the scenario when alternative host *Virginia opossum* is 15. Where $H_1 = 200$, $H_2 = 0$, $\mathcal{R}_0^{sv,p} = 2.1915$, $\mathcal{R}_0^{d,p} = 1.0867$; $H_1 = 190$, $H_2 = 10$, $\mathcal{R}_0^{sv,p} = 3.5788$, $\mathcal{R}_0^{d,p} = 1.0643$; $H_1 = 185$ and $H_2 = 15$, $\mathcal{R}_0^{sv,p} = 4.1041$, $\mathcal{R}_0^{d,p} = 1.0405$.

Table 5.3: Effects of adding alternative hosts with interspecific host competition.

Species	β_{H_2L}	β_{NH_2}	μ_{H_2}	p_1	p_2	Density	AIQN	INP	$\mathcal{R}_0^{sv,p}$	$\mathcal{R}_0^{d,p}$
Eastern chipmunk	0.569	0.971	0.00274	0.4	3.5	20	A	A	2.3221	1.2014
Raccoon	0.017	1.0	0.0005	8.5	5.3	10	A	A	2.7244	1.9461
				18.5	5.6	10	A	D	3.1340	2.6626
				1.3	11.1	10	A	D	2.5719	1.3454
Virginia opossum	0.004	0.261	0.0018	8.6	3.9	10	A	D	2.6668	1.0919
				7.6	8.0	10	A	D	2.7916	1.0894
				7.2	36.9	10	D	D	3.5788	1.0643
Striped skunk	0.191	0.530	0.00274	10.9	8.0	10	A	A	2.9407	1.8630
Short-tailed shrew	0.505	0.831	0.001	2*	1*	20	A	A	2.2843	1.5733
Sorex shrews	0.537	0.701	0.0018	2*	1*	20	A	A	2.2843	1.3164
Red and grey squirrel	0.061	0.831	0.0002	1.8	6.9	10	A	A	2.4587	1.9656
				1.3	4.4	10	A	A	2.3428	1.5527
Resources	[13]	[13]	[1]	[76]	[76]					

The table summarizes the results of dilution/amplification effect and two basic reproductive ratios. Here, A means amplification effect; D means dilution effect. The mean monthly temperatures are adapted from 2000-2009 period, and all other parameter values are the same as those in Table 5.1 in this study.

400 simulations are run. Figure 5.5 shows that $\mathcal{R}_0^{d,p}$ is particularly sensitive to the variation of warm temperatures (June/July/August); all parameters related to the main host (white-footed mice), including the density, mortality, transmission probabilities from hosts to ticks or from ticks to hosts, are moderately important to $\mathcal{R}_0^{d,p}$; alternative hosts are not negligible components in determining $\mathcal{R}_0^{d,p}$, thus the risk of Lyme disease. Table 5.4 lists parameters in a descending order of importance.

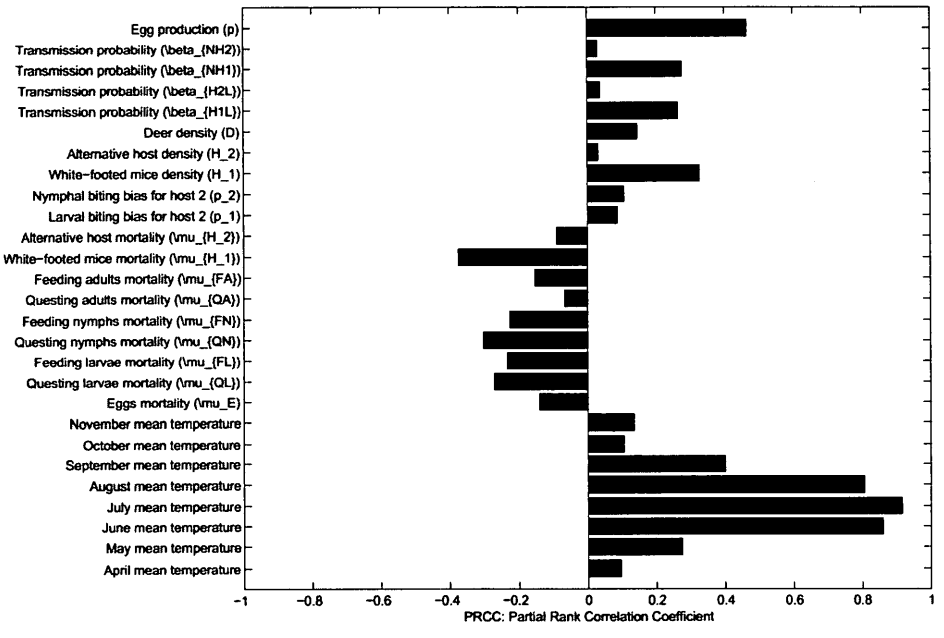

Figure 5.5: Global sensitivity of basic reproductive ratio of pathogen $\mathcal{R}_0^{d,p}$ to a 20% changes in the values of in the chosen different parameters. Here H_2 represents the species of *Eastern chipmunk*. The start mean monthly temperature values are taking from 2000-2009 period, $H_2 = 10$, $p_1 = 0.4$, $p_2 = 3.5$, $\beta_{H_2L} = 0.569$, $\beta_{NH_2} = 0.971$, $\mu_{H_2} = 0.00274$, and other parameter values are the same as listed in Table 5.1.

Table 5.4: PRCC results in the LHS/PRCC sensitivity analysis.

Parameter description	**PRCC**	**p-value**	**Significant** ($p < 0.01$)
July mean monthly temperature	0.9169	$1.8863e-150$	*
June mean monthly temperature	0.8597	$1.3856e-110$	*
August mean monthly temperature	0.8067	$5.5197e-087$	*
Eggs production (p)	0.4650	$1.8223e-021$	*
September mean monthly temperature	0.4001	$8.2466e-016$	*
White-footed mice mortality (μ_{H_1})	-0.3750	$6.2373e-014$	*
White-footed density (H_1)	0.3276	$8.386e-011$	*
Questing nymph mortality (μ_{QN})	-0.3027	$2.2952e-009$	*
Transmission probability (β_{NH_1})	0.2760	$5.7671e-008$	*
May mean monthly temperature	0.2737	$7.499e-008$	*
Questing larvae mortality (μ_{QL})	-0.2707	1.0553e-007	*
Transmission probability (β_{H_1L})	0.2659	$109784e-007$	*
Feeding larvae mortality (μ_{FL})	-0.2328	$5.3747e-006$	*
Feeding nymphs mortality (μ_{FN})	-0.2247	$1.1519e-005$	*
Feeding adults mortality (μ_{FA})	-0.1527	0.00307	*
White-tailed deer density (D)	0.1488	0.00503	*
Eggs mortality (μ_E)	-0.1398	0.0068	*

Continued on next page

Table 5.4 – continued from previous page

Parameter description	PRCC	p-value	Sig. ($p < 0.01$)
November mean monthly temperature	0.1344	0.0093	*
Nymphal biting bias for host H_2 (p_2)	0.1060	0.0405	
October mean monthly temperature	0.1045	0.0434	
April mean monthly temperature	0.0961	0.0633	
Alternative host H_2 mortality (μ_{H_2})	−0.0896	0.0836	
Larval biting bias for host H_2 (p_1)	0.0310	0.0903	
Questing adults mortality (μ_{QA})	−0.0660	0.2030	
Transmission probability (β_{H_2L})	0.0384	0.4588	
Alternative host density (H_2)	0.0310	0.5503	
Transmission probability (β_{NH_2})	0.0291	0.5748	

This table summarizes results in terms of PRCC and p-value when changing model parameter values by 20% from their start values. Here H_2 represents the species of *Eastern chipmunk*. $2000 - 2009$ period temperature data is considered, $H_2 = 10$, $p_1 = 0.4$, $p_2 = 3.5$, $\beta_{H_2L} = 0.569$, $\beta_{NH_2} = 0.971$, $\mu_{H_2} = 0.00274$, and all other parameters are the same as those in Table 5.1 in this study. The sign of PRCC represents the positive (+) or negative (-) response of $\mathcal{R}_0^{d,p}$ to the changed parameter values. The parameters are listed in descending order of the magnitude of the sensitivity of $\mathcal{R}_0^{d,p}$ to changes in their values. $*$: Significant at the $p < 0.01$.

5.4 Discussions

We now summarize our findings, based on a temperature-driven Lyme disease model, on how climate and host community composition jointly affect the tick distribution and pathogen invasion. Form this model, we derived two reproduction ratios simultaneously, the ecological reproduction ratio $\mathcal{R}_0^{sv,p}$ for the ticks (which predicts the tick persistence) and the epidemiological reproduction ratio $\mathcal{R}_0^{d,p}$ for the pathogen transmission. These ratios can predict successful pathogen invasion, and both ratios are affected by the abiotic factors (such as temperatures) and biotic factors (such as the host community composition). The model is calibrated by two temperature datasets corresponding to 1961-1990 and 2000-2009 periods from some tick endemic areas in Canada.

We calculated the reproduction ratios for two different periods, 1961-1990 and 2000-2009. The model predicted that the reproduction ratio for ticks $\mathcal{R}_0^{sv,p} = 1.6996$ and the reproduction ratio for the pathogen is $\mathcal{R}_0^{d,p} = 0.7585$ for the 1961-1990 period, while $\mathcal{R}_0^{sv,p} = 2.1915$ and $\mathcal{R}_0^{d,p} = 1.0867$ for the 2000-2009 period. Therefore, the reproduction ratios for 2000-2009 are larger than those for 1961-1990. In both periods, $\mathcal{R}_0^{sv,p}$ is larger than 1, and therefore, the tick can successfully survive in the habitat. Since $\mathcal{R}_0^{d,p}$ is smaller than 1 for the 1961-1990 period, the pathogen transmission cycle can not successfully establish. However, $\mathcal{R}_0^{d,p}$ is

brought to be larger than one for the 2000-2009 period, which ensures that the pathogen will remain endemic in the habitat. We can also see, from the numerical simulations (Figure 5.2), that the tick population size at the stabilized states for 2000-2009 is larger than that for the 1961-1990 period. The different predictions of the model come from the seeded temperatures, which affect the tick development rates and tick biting rates. Our findings demonstrate that the vector-transmitted pathogen is more likely to response to climate change, and climate warming may facilitate pathogen transmission and persistence. Because the dynamics of the pathogen is dominated by the dynamics of the vector population, many evidences [68, 104, 105] have shown that climate change, in particular temperature, is a decisive parameter to predict the distribution and establishment of tick populations. Sensitivity analysis (Figure 5.5) further proved that significant emphasis should be placed on the possible role of climate in determining the reproduction ratio of the pathogen.

We also conducted simulations to demonstrate that host community diversity may trigger the dilution or amplification effect [73]. The dilution or amplification effect has been observed in our model simulations with adding competent or incompetent hosts. Interestingly, both the dilution and amplification effects are observed by adding an incompetent reservoir. However we have noticed that the predicting results largely depend on the chosen parameters. Our prediction results

of adding an alternative host into the white-footed mouse/white-tailed deer community illustrate the importance of considering the detail of alternative host species and emphasize the importance of the underlying ecological mechanisms of the host diversity.

6 Basic reproductive ratio of a periodic system of delay differential equations with periodic delay

6.1 Introduction

The first model for Lyme disease dynamics in Canada developed by Ogden [68] formulated development times as time lags, and hence this first model becomes a system of delay differential equations. The simulations based on this model were performed season-by-season, and hence constant coefficients and delays were used. In reality, as pointed out in previous chapters, due to seasonality, these constant coefficients and delays should really be time-dependent, and periodicity may offer a reasonable approximation [52, 71, 68].

In the work of [86], Schuhmacher and Thieme developed a general model in terms of distributed delay to model temperature-driven development of insects. However, the maturation rate and development delay from previous stage to the next are still not clear. One of our goals in this chapter is to derive a stage-structured

tick population growth model in a seasonally varying environment. Following the standard argument for structured population dynamics [101], we derive a system of delay differential equations (DDEs) with temporally periodically varying delays and coefficients.

A natural and important problem associated with the system of DDEs with periodic delay is to define and compute the basic reproductive ratio, denoted by $\mathcal{R}_0^{v,pd}$. We will follow the work of Bacaër and Guernaoui [8] that suggested a definition of the basic reproductive ratio in a periodic environment, using the renewal equation satisfied by the birth rate $\beta(t)$ [96]:

$$\beta(t) = \int_0^\infty \mathcal{K}(t,x)\beta(t-x)\,dx, \tag{6.1.1}$$

where kernel $\mathcal{K}(t,x)$ is ω-periodic with respect to t. In this work, the basic reproductive ratio was defined as the spectral radius of the next generation integral operator

$$\mathcal{L} : u(t) \mapsto \int_0^\infty \mathcal{K}(t,x)u(t-x)\,dx \tag{6.1.2}$$

on the function space consisting of ω-periodic continuous functions. There have been a number of studies since then on the basic reproductive ratio in time-periodic environment: ordinary differential equations [5, 99, 7] (with specific applications [30, 78, 41]), delay differential equations with discrete constant delay [9, 6]. However, to the best of our knowledge, there is neither a formal definition nor algorithm for

the basic reproductive ratio of a system of delay differential equations with periodic delay. Our second goal in this chapter is to define and derive the basic reproductive ratio $\mathcal{R}_0^{v,pd}$, and to provide a numerical algorithm of computing $\mathcal{R}_0^{v,pd}$.

The remaining parts of this chapter are organized as follows. In the next section, we derive a stage-structured model of delay differential equations with periodic delay and verify the well-posedness of the model. Section 6.3 gives a detailed derivation of the basic reproductive ratio of the tick population and develops a numerical method of $\mathcal{R}_0^{v,pd}$. In section 6.4, we carry out some numerical simulations to illustrate the numerical method.

6.2 Model derivation

Here, we develop a dynamic population model of *I. scapularis* involving time-varying delay due to seasonality. The same notations are reused to embody the tick life cycle, namely egg-laying adult females (x_1), eggs (x_2), hardening larvae (x_3), questing larvae (x_4), feeding larvae (x_5), engorged larvae (x_6), questing nymphs (x_7), feeding nymphs (x_8), engorged nymphs (x_9), questing adults (x_{10}), feeding adult females (x_{11}) and engorged adult females (x_{12}). In our model formulation, we consider a transition process from one specific stage to the next as time-varying delay rather than development rate, namely we will replace $d_i/d_i(T)$ by $\tau_i(t)$ in Figure 2.1 of Chapter 2. Here $\tau_i(t)$ is the positive time-periodic delay so that the new developed

tick stage x_{i+1} at time t is evolved from the previous tick stage x_i at time $t - \tau_i(t)$.

In order to appropriately formulate the mathematical model, we make the following assumptions:

(H1). The seasonal temperature varies periodically with the periodicity ($\omega = 365$ days), each $\tau_i(t)$ $(i = 2, \cdots, 12)$ is a nonnegative periodic function of t (with period $\omega = 365$ days). We also assume $1 - \tau'(t) \geq 0$, which excludes the possibility of the i^{th} stage of the tick going back to the previous $(i-1)^{th}$ stage except by birth.

(H2). Each stage-wise tick has its typical density-dependent or density-independent death rate. In particular, following [68], we use the following death rates of the tick at time t and age a:

$$\mu(t, a, P(t, a)) = \begin{cases} \mu_1, & a \in [A_{12}(t), \infty), \\ \mu_i, & a \in [A_{i-1}(t), A_i(t)], \quad i \neq 1, 5, 8, 11, \\ \mu_i(x_i(t)), & a \in [A_{i-1}(t), A_i(t)], \quad i = 5, 8, 11, \end{cases} \tag{6.2.3}$$

where $A_{i-1}(t)$ and $A_i(t)$ are the minimum and maximum ages of ixodid ticks developing within the specific i^{th} stage.

(H3). The birth function of eggs is given by

$$b(x_1(t)) = p x_1(t) e^{-s_T x_1(t)}, \tag{6.2.4}$$

where p is the maximum number of eggs produced by per egg-laying adult female, s_T measures the strength of density-dependence. The assumption reflects the ecological consideration that the reproduction is linear in x_1 only for small densities,

decreases as a consequence of intraspecific competition, and then drops significantly at very large densities due to the available resources being utilized by the adults only for their own physiological maintenance.

We now introduce the tick age variable a and denote by $\rho(t,a)$ the density of the tick population at time t age a. Following the standard argument for population dynamics with age structure [101], we have

$$\begin{cases} (\frac{\partial}{\partial t}+\frac{\partial}{\partial a})\rho(t,a) = -\mu(t,a,P(t,a))\rho(t,a), \\ \rho(0,a) = \phi(a),\ a \geq 0, \\ \rho(t,0) = b(x_1(t)),\ t \geq 0, \end{cases} \tag{6.2.5}$$

where $P(t,a) = \int_{a_1}^{a_2} \rho(t,\theta)\,d\theta$ is the total number of tick population at time t between age $a_1 \geq 0$ and age $a_2 \geq 0$ (note that a_1 and a_2 can be time-dependent, namely, $a_1 = a_1(t)$ and $a_2 = a_2(t)$ can be functions of t). An integration of (6.2.5) along characteristics yields

$$\rho(t,a) = \begin{cases} \rho(0,a-t)e^{-\int_0^t \mu(r,a-t+r,P(r,a-t+r))\,dr},\ 0 \leq t \leq a, \\ \rho(t-a,0)e^{-\int_0^a \mu(t-a+r,r,P(t-a+r,r))\,dr},\ a < t. \end{cases} \tag{6.2.6}$$

In order to evaluate the rate of change of the specific tick state x_i at time t, we introduce a new variable $\rho_i(t,a_i)$, which represents the density of the tick in the i^{th} stage at time t and age a_i. In other words, a_i is the stage-specific age and a is tick age. For example, a_1 is the egg-laying adult age. Therefore, the total tick

population at the specific stage at time t is given by

$$\begin{cases} x_1(t) &= \int_0^{\infty} \rho_1(t,a_1)\,da_1 = \int_{A_{12}(t)}^{\infty} \frac{1}{2}\rho(t,a)\,da \\ x_i(t) &= \int_0^{\tau_i(t)} \rho_i(t,a_i)\,da_i = \int_{A_{i-1}(t)}^{A_i(t)} \rho(t,a)\,da,\ i=2,\cdots,10, \\ x_i(t) &= \int_0^{\tau_i(t)} \rho_i(t,a_i)\,da_i = \int_{A_{i-1}(t)}^{A_i(t)} \frac{1}{2}\rho(t,a)\,da,\ i=11,12. \end{cases} \tag{6.2.7}$$

Recall that $A_{i-1}(t)$ and $A_i(t)$ are the minimum and maximum ages of ticks who are developing in the specific i^{th} stage.

In order to proceed further, we need to know the relationship between tick age a and specific-stage age a_i at time t. Note that tick density $\rho(t,a)$ at time t and age a is developed from density of ticks $\rho(t-a,0)$ at time $t-a$ age 0. We depict this as,

$$\rho(t-a,0) \longrightarrow \rho(t,a).$$

It is obvious that $a = a_2$, $A_1(t) = 0$ and $A_2(t) = \tau_2(t)$. The hardening larvae $\rho_3(t,a_3)$ are developed from themselves at time $t-a_3$ and age 0, and then the hardening larvae $\rho_3(t-a_3,0)$ are developed from tick population at time $t-a_3-\tau_2(t-a_3)$ and the tick age 0. Namely, we have

$$\rho(t-a_3-\tau_2(t-a_3),0) \longrightarrow \rho_3(t-a_3,0) \longrightarrow \rho_3(t,a_3).$$

Therefore, the hardening larva age a_3 and the tick age a are related by

$$t-a_3-\tau_2(t-a_3) = t-a. \tag{6.2.8}$$

In particular,

$$a_3 = 0 \Leftrightarrow a = \tau_2(t);$$

$$a_3 = \tau_3(t) \Leftrightarrow a = \tau_3(t) + \tau_2(t - \tau_3(t)).$$

Then

$$A_3(t) = \tau_3(t) + \tau_2(t - \tau_3(t)).$$

Similarly, for each $i = 2, \cdots, 12$, we obtain

$$A_i(t) = \sum_{j=2}^{i} \tau_j \left(t - \sum_{k=j+1}^{i} \tau_k \left(t - \sum_{l=k+1}^{i} \tau_l \left(t - \cdots \tau_{i-1}(t - \tau_i(t)) \right) \right) \right). \quad (6.2.9)$$

Differentiating (6.2.7), we obtain

$$\begin{aligned} x_1'(t) &= \frac{1}{2} \left\{ \int_{A_{12}(t)}^{\infty} \frac{\partial}{\partial t} \rho(t,a)\, da - \rho(t, A_{12}(t)) A_{12}'(t) \right\} \\ &= \frac{1}{2} \left\{ \int_{A_{12}(t)}^{\infty} [-\frac{\partial}{\partial a} \rho(t,a) - \mu(t,a,P(t,a))\rho(t,a)]\, da - \rho(t, A_{12}(t)) A_{12}'(t) \right\} \\ &= \frac{1}{2} \{ -\rho(t,\infty) + \rho(t, A_{12}(t)) \\ &\quad - \int_{A_{12}(t)}^{\infty} \mu(t,a,P(t,a))\rho(t,a)\, da - \rho(t, A_{12}(t)) A_{12}'(t) \Big\} \\ &= \frac{1}{2}\rho(t, A_{12}(t))(1 - A_{12}'(t)) - \int_{A_{12}(t)}^{\infty} \mu(t,a,P(t,a)) \frac{1}{2} \rho(t,a)\, da, \quad (6.2.10) \end{aligned}$$

$$
\begin{aligned}
x_i'(t) &= \int_{A_{i-1}(t)}^{A_i(t)} \frac{\partial}{\partial t}\rho(t,a)\,da + \rho(t,A_i(t))A_i'(t) - \rho(t,A_{i-1}(t))A_{i-1}'(t) \\
&= \int_{A_{i-1}(t)}^{A_i(t)} \left[-\frac{\partial}{\partial a}\rho(t,a) - \mu(t,a,P(t,a))\rho(t,a)\right] da \\
&\quad +\rho(t,A_i(t))A_i'(t) - \rho(t,A_{i-1}(t))A_{i-1}'(t) \\
&= -\rho(t,A_i(t)) + \rho(t,A_{i-1}(t)) \\
&\quad - \int_{A_{i-1}(t)}^{A_i(t)} \mu(t,a,P(t,a))\rho(t,a)\,da + \rho(t,A_i(t))A_i'(t) - \rho(t,A_{i-1}(t))A_{i-1}'(t) \\
&= \rho(t,A_{i-1}(t))(1-A_{i-1}'(t)) - \rho(t,A_i(t))(1-A_i'(t)) \\
&\quad - \int_{A_{i-1}(t)}^{A_i(t)} \mu(t,a,P(t,a))\rho(t,a)\,da, \quad i=2,\cdots,10, \qquad (6.2.11)
\end{aligned}
$$

and

$$
\begin{aligned}
x_i'(t) &= \frac{1}{2}\left\{\int_{A_{i-1}(t)}^{A_i(t)} \frac{\partial}{\partial t}\rho(t,a)\,da + \rho(t,A_i(t))A_i'(t) - \rho(t,A_{i-1}(t))A_{i-1}'(t)\right\} \\
&= \frac{1}{2}\rho(t,A_{i-1}(t))(1-A_{i-1}'(t)) - \frac{1}{2}\rho(t,A_i(t))(1-A_i'(t)) \\
&\quad - \int_{A_{i-1}(t)}^{A_i(t)} \mu(t,a,P(t,a))\frac{1}{2}\rho(t,a)\,da, \quad i=11,12, \qquad (6.2.12)
\end{aligned}
$$

where we have made the biologically realistic assumption

$$\rho(t,\infty) = 0.$$

Along with the assumption (H2), equations (6.2.10-6.2.12) become

$$
\begin{aligned}
x_1'(t) &= \tfrac{1}{2}\rho(t, A_{12}(t))(1 - A_{12}'(t)) - \mu_1 x_1(t),\\
x_2'(t) &= \rho(t,0) - \rho(t, A_2(t))(1 - A_2'(t)) - \mu_2 x_2(t),\\
x_3'(t) &= \rho(t, A_2(t))(1 - A_2'(t)) - \rho(t, A_3(t))(1 - A_3'(t)) - \mu_3 x_3(t),\\
x_4'(t) &= \rho(t, A_3(t))(1 - A_3'(t)) - \rho(t, A_4(t))(1 - A_4'(t)) - \mu_4 x_4(t),\\
x_5'(t) &= \rho(t, A_4(t))(1 - A_4'(t)) - \rho(t, A_5(t))(1 - A_5'(t)) - \mu_5(x_5(t))x_5(t),\\
x_6'(t) &= \rho(t, A_5(t))(1 - A_5'(t)) - \rho(t, A_6(t))(1 - A_6'(t)) - \mu_6 x_6(t),\\
x_7'(t) &= \rho(t, A_6(t))(1 - A_6'(t)) - \rho(t, A_7(t))(1 - A_7'(t)) - \mu_7 x_7(t),\\
x_8'(t) &= \rho(t, A_7(t))(1 - A_7'(t)) - \rho(t, A_8(t))(1 - A_8'(t)) - \mu_8(x_8(t))x_8(t),\\
x_9'(t) &= \rho(t, A_8(t))(1 - A_8'(t)) - \rho(t, A_9(t))(1 - A_9'(t)) - \mu_9 x_9(t),\\
x_{10}'(t) &= \rho(t, A_9(t))(1 - A_9'(t)) - \rho(t, A_{10}(t))(1 - A_{10}'(t)) - \mu_{10} x_{10}(t),\\
x_{11}'(t) &= \tfrac{1}{2}\rho(t, A_{10}(t))(1 - A_{10}'(t)) - \tfrac{1}{2}\rho(t, A_{11}(t))(1 - A_{11}'(t)) - \mu_{11}(x_{11}(t))x_{11}(t),\\
x_{12}'(t) &= \tfrac{1}{2}\rho(t, A_{11}(t))(1 - A_{11}'(t)) - \tfrac{1}{2}\rho(t, A_{12}(t))(1 - A_{12}'(t)) - \mu_{12} x_{12}(t).
\end{aligned}
\tag{6.2.13}
$$

To obtain the equation of $x_i'(t)$, we then need to evaluate $\rho(t, A_i(t))$, this can be done by the method of integration along characteristic. Set $t = t_0 + s$, $a = a_0 + s$, and $V(s) = \rho(t_0 + s, a_0 + s)$. Then

$$
\begin{aligned}
\tfrac{dV(s)}{ds} &= \left(\tfrac{\partial}{\partial t}\rho(t,a) + \tfrac{\partial}{\partial a}\rho(t,a)\right)\Big|_{\substack{t=t_0+s;\\ a=a_0+s}}\\
&= -\mu(t_0+s, a_0+s, P(t_0+s, a_0+s))\rho(t,a)\Big|_{\substack{t=t_0+s;\\ a=a_0+s}}\\
&= -\mu(t_0+s, a_0+s, P(t_0+s, a_0+s))V(s).
\end{aligned}
\tag{6.2.14}
$$

Note that (6.2.14) is a linear first-order ordinary differential equation, we easily obtain

$$V(s_2) = V(s_1)e^{-\int_{s_1}^{s_2}\mu(t_0+r,a_0+r,P(t_0+r,a_0+r))dr}. \tag{6.2.15}$$

For $t > A_i(t)$, setting $s_2 = A_i(t)$, $s_1 = 0$, $t_0 = t - A_i(t)$, and $a_0 = 0$, we have

$$\begin{aligned} V(A_i(t)) &= \rho(t, A_i(t)) = \rho(t - A_i(t), 0)e^{-\int_0^{A_i(t)}\mu(t-A_i(t)+r,r,P(t-A_i(t)+r,r))\,dr} \\ &= \rho(t - A_i(t), 0)\alpha_i(t, \cdot), \end{aligned}$$

where $\alpha_i(t, \cdot) = e^{-\int_0^{A_i(t)}\mu(t-A_i(t)+r,r,P(r+t-A_i(t),r))\,dr}$ is the survival probability of eggs who were born at time $t - A_i(t)$ and can live until time t. Note that $\alpha(t, \cdot)$ can be density-dependent.

With some straightforward calculations, we obtain

$$\begin{aligned} \rho(t, A_2(t)) &= \rho(t - A_2(t), 0)e^{-\int_0^{A_2(t)}\mu(t-A_2(t)+r,r,P(t-A_2(t)+r,r))\,dr} \\ &= \rho(t - A_2(t), 0)e^{-\mu_2 A_2(t)} = \rho(t - A_2(t), 0)\alpha_2(t), \end{aligned}$$

$$\begin{aligned} \rho(t, A_3(t)) &= \rho(t - \tau_3(t), A_3(t) - \tau_3(t))e^{-\int_{A_3(t)-\tau_3(t)}^{A_3(t)}\mu(t-A_3(t)+r,r,P(t-A_3(t)+r,r))\,dr} \\ &= \rho(t - \tau_3(t), \tau_2(t - \tau_3(t))e^{-\mu_3\tau_3(t)} \\ &= \rho(t - A_3(t), 0)e^{-\int_0^{\tau_2(t-\tau_3(t))}\mu(t-A_3(t)+r,r,P(t-A_3(t)+r,r))\,dr}e^{-\mu_3\tau_3(t)} \\ &= \rho(t - A_3(t), 0)e^{-\mu_3\tau_3(t)}e^{-\mu_2\tau_2(t-\tau_3(t))} \\ &= \rho(t - A_3(t), 0)\alpha_3(t) = \rho(t - A_3(t), 0)e^{-\mu_3\tau_3(t)}\alpha_2(t - \tau_3(t)). \end{aligned}$$

Similarly, we have

$$\rho(t, A_4(t)) = \rho(t - A_4(t), 0)\alpha_4(t) = \rho(t - A_4(t), 0)e^{-\mu_4\tau_4(t)}\alpha_3(t - \tau_4(t)),$$

$$\rho(t, A_5(t)) = \rho(t - A_5(t), 0)\alpha_5(t, x_5) = \rho(t - A_5(t), 0)e^{-\int_{t-\tau_5(t)}^{t}\mu_5(x_5(\theta))\,d\theta}\alpha_4(t - \tau_5(t)),$$

and so on. Then we obtain the following relationship of $\alpha_i(t, \cdot)$:

$$\begin{aligned}
&\alpha_1(t) = 1;\\
&\alpha_2(t) = e^{-\mu_2\tau_2(t)};\\
&\alpha_3(t) = e^{-\mu_3\tau_3(t)}\alpha_2(t - \tau_3(t));\\
&\alpha_4(t) = e^{-\mu_4\tau_4(t)}\alpha_3(t - \tau_4(t));\\
&\alpha_5(t, x_5) = e^{-\int_{t-\tau_5(t)}^{t}\mu_5(x_5(r))dr}\alpha_4(t - \tau_5(t));\\
&\alpha_6(t, x_5) = e^{-\mu_6\tau_6(t)}\alpha_5(t - \tau_6(t), x_5);\\
&\alpha_7(t, x_5) = e^{-\mu_7\tau_7(t)}\alpha_6(t - \tau_7(t), x_5);\\
&\alpha_8(t, x_5, x_8) = e^{-\int_{t-\tau_8(t)}^{t}\mu_8(x_8(r))dr}\alpha_7(t - \tau_8(t), x_5);\\
&\alpha_9(t, x_5, x_8) = e^{-\mu_9\tau_9(t)}\alpha_8(t - \tau_9(t), x_5, x_8);\\
&\alpha_{10}(t, x_5, x_8) = e^{-\mu_{10}\tau_{10}(t)}\alpha_9(t - \tau_{10}(t), x_5, x_8);\\
&\alpha_{11}(t, x_5, x_8, x_{11}) = e^{-\int_{t-\tau_{11}(t)}^{t}\mu_{11}(x_{11}(r))dr}\alpha_{10}(t - \tau_{11}(t), x_5, x_8);\\
&\alpha_{12}(t, x_5, x_8, x_{11}) = e^{-\mu_{12}\tau_{12}(t)}\alpha_{11}(t - \tau_{12}(t), x_5, x_8, x_{11}).
\end{aligned} \tag{6.2.16}$$

Obviously, each $\alpha_i(t, \cdot)$ $(i = 2, \cdots, 12)$ represents the survival probability of tick population from eggs who are born at time $t - A_i(t)$ to one specific stage x_{i+1} at

time t age zero. Then when $t > A_{12}(t)$, the full model becomes

$$
\begin{aligned}
x_1'(t) &= \tfrac{1}{2}\alpha_{12}(t,x_5,x_8,x_{11})b(x_1(t-A_{12}(t)))(1-A_{12}'(t)) - \mu_1 x_1(t),\\
x_2'(t) &= b(x_1(t)) - \alpha_2(t)b(x_1(t-A_2(t)))(1-A_2'(t)) - \mu_2 x_2(t),\\
x_i'(t) &= \alpha_{i-1}(t)b(x_1(t-A_{i-1}(t)))(1-A_{i-1}'(t))\\
&\quad -\alpha_i(t)b(x_1(t-A_i(t)))(1-A_i'(t)) - \mu_i x_i(t),\ i=3,4,\\
x_5'(t) &= \alpha_4(t)b(x_1(t-A_4(t)))(1-A_4'(t))\\
&\quad -\alpha_5(t,x_5)b(x_1(t-A_5(t)))(1-A_5'(t)) - \mu_5(x_5(t))x_5(t),\\
x_i'(t) &= \alpha_{i-1}(t,x_5)b(x_1(t-A_{i-1}(t)))(1-A_{i-1}'(t))\\
&\quad -\alpha_i(t,x_5)b(x_1(t-A_i(t)))(1-A_i'(t)) - \mu_i x_i(t),\ i=6,7,\\
x_8'(t) &= \alpha_7(t,x_5)b(x_1(t-A_7(t)))(1-A_7'(t))\\
&\quad -\alpha_8(t,x_5,x_8)b(x_1(t-A_8(t)))(1-A_8'(t)) - \mu_8(x_8(t))x_8(t),\\
x_i'(t) &= \alpha_{i-1}(t,x_5,x_8)b(x_1(t-A_{i-1}(t)))(1-A_{i-1}'(t))\\
&\quad -\alpha_i(t,x_5,x_8)b(x_1(t-A_i(t)))(1-A_i'(t)) - \mu_i x_i(t),\ i=9,10,\\
x_{11}'(t) &= \tfrac{1}{2}\alpha_{10}(t,x_5,x_8)b(x_1(t-A_{10}(t)))(1-A_{10}'(t))\\
&\quad -\tfrac{1}{2}\alpha_{11}(t,x_5,x_8,x_{11})b(x_1(t-A_{11}(t)))(1-A_{11}'(t)) - \mu_{11}(x_{11}(t))x_{11}(t),\\
x_{12}'(t) &= \tfrac{1}{2}\alpha_{11}(t,x_5,x_8,x_{11})b(x_1(t-A_{11}(t))))(1-A_{11}'(t))\\
&\quad -\tfrac{1}{2}\alpha_{12}(t,x_5,x_8,x_{11})b(x_1(t-A_{12}(t))))(1-A_{12}'(t)) - \mu_{12}x_{12}(t).
\end{aligned}
\tag{6.2.17}
$$

The rest of this chapter will focus on (6.2.17). We will consider solutions to system (6.2.17) for all $t \geq 0$, our focus is on long-term dynamics for which we need only consider the system $t \geq A_{12}(t)$. The following lemma establishes the fact that the

i^{th} stage of the tick will not go back to the previous $(i-1)^{th}$ stage except by birth.

Lemma 6.2.1. *With the assumption (H1), we have*

(i) $A_i(t) \geq A_{i-1}(t)$ *and* $A_i(t) = \tau_i(t) + A_{i-1}(t - \tau_i(t))$, *for all* $t \geq 0$, $i = 2, \cdots, 12$;

(ii) $1 - A_i'(t) \geq 0$ *and* $1 - A_i'(t) = (1 - \tau_i'(t))(1 - A_{i-1}'(t - \tau_i(t)))$, *for all* $t \geq 0$, $i = 2, \cdots, 12$.

Proof. We prove $A_i(t) \geq A_{i-1}(t)$ by induction. Since $t - \tau_3(t) < t$, $t - \tau_2(t)$ is an increasing function, we have $t - \tau_3(t) - \tau_2(t - \tau_3(t)) \leq t - \tau_2(t)$. This is equivalent to $A_3(t) \geq A_2(t)$. Again $t - \tau_4(t) < t$, $t - \tau_3(t)$ is an increasing function, we have $t - \tau_4(t) - \tau_3(t - \tau_4(t)) \leq t - \tau_3(t)$. Since $t - \tau_2(t)$ is increasing, we have

$$t - \tau_4(t) - \tau_3(t - \tau_4(t)) - \tau_2(t - \tau_4(t) - \tau_3(t - \tau_4(t))) \leq t - \tau_3(t) - \tau_2(t - \tau_3(t)).$$

That is, $A_4(t) \geq A_3(t)$. By the same argument, we obtain $A_i(t) \geq A_{i-1}(t)$, $i = 2, \cdots, 12$. From equation (6.2.9), we can easily obtain $A_i(t) = \tau_i(t) + A_{i-1}(t - \tau_i(t))$ and $1 - A_i'(t) = (1 - \tau_i'(t))(1 - A_{i-1}'(t - \tau_i(t))) \geq 0$. □

6.2.1 Nonnegativity and boundedness

The initial data for the system (6.2.17) is not arbitrary. For biological reason the initial data must satisfy several constraints and we only consider solutions that satisfy these constraints. Define $\tau_m = \min_{t \in [0,\omega]} A_{12}(t)$, $\tau_M = \max_{t \in [0,\omega]} A_{12}(t)$. For the sake

of convenience, we denote $\hat{\alpha}_i(t) := \alpha_i(t,\cdot)$. It is easy to see that each exponential function $\hat{\alpha}_i(t)$ is always positive and $b(x_1(t))$ is nonnegative provided that $x_1(t)$ is nonnegative.

Theorem 6.2.2. *With the initial data $x_1(\theta) \geq 0$, $x_5(\theta) \geq 0$, $x_8(\theta) \geq 0$, $x_{11}(\theta) \geq 0$ for $-\tau_M \leq \theta < 0$, and*

$$\begin{cases} x_i(0) = \int_{-\tau_i(0)}^{0} e^{\mu_i s}\hat{\alpha}_{i-1}(s)b(x_1(s-A_{i-1}(s)))(1-A'_{i-1}(s))\,ds, \quad i \neq 1,5,8,11,12, \\ x_i(0) = \int_{-\tau_i(0)}^{0} e^{-\int_s^0 \mu_i(x_i(r))\,dr}\hat{\alpha}_{i-1}(s)b(x_1(s-A_{i-1}(s)))(1-A'_{i-1}(s))\,ds, \; i = 5,8, \\ x_{11}(0) = \frac{1}{2}\int_{-\tau_{11}(0)}^{0} e^{-\int_s^0 \mu_{11}(x_{11}(r))\,dr}\hat{\alpha}_{10}(s)b(x_1(s-A_{10}(s)))(1-A'_{10}(s))\,ds, \\ x_{12}(0) = \frac{1}{2}\int_{-\tau_{12}(0)}^{0} e^{\mu_{12}s}\hat{\alpha}_{11}(s)b(x_1(s-A_{11}(s)))(1-A'_{11}(s))\,ds, \end{cases} \tag{6.2.18}$$

each component $x_i(t)$ of the solution of the system (6.2.17) remains nonnegative for all $t \geq 0$, $i = 1, \cdots, 12$. Furthermore, each component of the solution is also bounded for all $t > 0$.

Proof. First we claim that $x_1(t) \geq 0$ for all $t \geq -\tau_M$ when $x_1(\theta) \geq 0$ for $-\tau_M \leq \theta \leq 0$. We prove the theorem (6.2.2) by showing that $x_i(t,\varepsilon)$ is the solution of the modified system obtained from system (6.2.17) by adding ε to each right hand side with ε being arbitrarily small. To show that $x_1(t,\varepsilon) \geq 0$ for all $t > 0$, we suppose that $x_1(t,\varepsilon) < 0$ for some $t > 0$. Let $t^* = \inf\{t : t > 0 \text{ and } x_1(t,\varepsilon) < 0\}$. Then $t^* \geq 0$, $x_1(t^*,\varepsilon) = 0$ and $x'_1(t^*,\varepsilon) \leq 0$. But, from the first equation of the modified

system

$$\begin{aligned} x_1'(t^*,\varepsilon) &= \frac{1}{2}\hat{\alpha}_{12}(t^*)b(x_1(t^*-A_{12}(t^*),\varepsilon))(1-A_{12}'(t^*))-\mu_1 x_1(t^*,\varepsilon)+\varepsilon, \\ &= \frac{1}{2}\hat{\alpha}_{12}(t^*)b(x_1(t^*-A_{12}(t^*),\varepsilon))(1-A_{12}'(t^*))+\varepsilon. \end{aligned}$$

Moreover, $A_{12}(t^*) > 0$ ensures $t^* - A_{12}(t^*) < t^*$, implying that $x_1(t^* - A_{12}(t^*), \varepsilon) \geq 0$ by the definition of t^*. This, in turn, implies that $x_1'(t^*, \varepsilon) \geq \varepsilon > 0$, giving rise to a contradiction. Therefore, $x_1(t, \varepsilon) \geq 0$ for each $t > 0$. This is true for arbitrary small $\varepsilon > 0$. Letting $\varepsilon \to 0$ gives

$$x_1(t) \geq 0$$

as a solution of system (6.2.17).

Then we claim the nonnegativity of $x_i(t)$ for all $t \geq 0$, $i = 2, \cdots, 12$. We start to prove nonnegativity of $x_2(t)$ for all $t \geq 0$. We move the term $\mu_2 x_2(t)$ to the left side of the second equation of system (6.2.17) and multiply $e^{\mu_2 t}$ at both sides to obtain

$$\begin{aligned} \left(e^{\mu_2 t}x_2(t)\right)' &= (x_2'(t)+\mu_2 x_2(t))e^{\mu_2 t} \\ &= e^{\mu_2 t}b(x_1(t)) - e^{\mu_2 t}e^{-\mu_2\tau_2(t)}b(x_1(t-\tau_2(t)))(1-\tau_2'(t)) \\ &= e^{\mu_2 t}b(x_1(t)) - e^{\mu_2(t-\tau_2(t))}b(x_1(t-\tau_2(t)))(1-\tau_2'(t)) \\ &= \left(\int_{t-\tau_2(t)}^{t} e^{\mu_2 s}b(x_1(s))\,ds\right)'. \end{aligned}$$

Then we have

$$x_2(t) = \int_{t-\tau_2(t)}^{t} e^{-\mu_2(t-s)} b(x_1(s))\, ds, \tag{6.2.19}$$

which is non-negative because of nonnegativity of $x_1(t)$ and the initial data (6.2.18) constraints. This expression is, ecologically reasonable, as it accounts for the total number of eggs at time t. Where $b(x_1(s))$ represents the number of eggs who were born at some time $s \in [t-\tau_2(t), t]$; $e^{-\mu_2(t-s)}$ is the survival probability of eggs who were born at time s and were able to survive until time t in egg stage. Here the variable $\tau_2(t)$ is the maturation time from eggs to the next stage at time t, the lower limit on the integral is $t-\tau_2(t)$ because any tick born before that time will have matured to next stage before time t.

Similarly, from the third equation of system (6.2.17) we have

$$\begin{aligned}
&\left(e^{\mu_3 t} x_3(t)\right)' \\
&= e^{\mu_3 t}(x_3'(t) + \mu_3 x_3(t)) \\
&= e^{\mu_3 t}\left[\hat{\alpha}_2(t) b(x_1(t-A_2(t)))(1-A_2'(t)) - \hat{\alpha}_3(t) b(x_1(t-A_3(t)))(1-A_3'(t))\right] \\
&= e^{\mu_3 t} e^{-\mu_2 \tau_2(t)} b(x_1(t-\tau_2(t)))(1-\tau_2'(t)) - e^{\mu_3(t-\tau_3(t))} e^{-\mu_2 \tau_2(t-\tau_3(t))} b(x_1(t-\tau_3(t) \\
&\quad -\tau_2(t-\tau_3(t))))(1-\tau_2'(t-\tau_3(t)))(1-\tau_3'(t)) \\
&= \left(\int_{t-\tau_3(t)}^{t} e^{\mu_3 s} e^{-\mu_2 A_2(s)} b(x_1(s-A_2(s)))(1-A_2'(s))\, ds\right)'.
\end{aligned}$$

Then we obtain

$$x_3(t) = \int_{t-\tau_3(t)}^{t} e^{-\mu_3(t-s)}\hat{\alpha}_2(s)b(x_1(s-A_2(s)))(1-A_2'(s))\,ds, \tag{6.2.20}$$

where $x_3(t)$ accounts for the total number of hardening larvae at time t. The quantity $\hat{\alpha}_2(s)b(x_1(s-A_2(s)))(1-A_2'(s))$ is the number of hardening larvae whose stage-specific age is zero at time s and evolved from eggs born at time $s-A_2(s)$.

Using similar calculations, we obtain the unfed tick stage as follows

$$x_i(t) = \int_{t-\tau_i(t)}^{t} e^{-\mu_i(t-s)}\hat{\alpha}_{i-1}(s)b(x_1(s-A_{i-1}(s)))(1-A_{i-1}'(s))\,ds,\ (i=2,3,4,6,7,9,10),$$

$$x_i(t) = \int_{t-\tau_i(t)}^{t} e^{-\int_s^t \mu_i(x_i(r))\,dr}\hat{\alpha}_{i-1}(s)b(x_1(s-A_{i-1}(s)))(1-A_{i-1}'(s))\,ds,\ i=5,8,$$

$$x_{11}(t) = \tfrac{1}{2}\int_{t-\tau_{11}(t)}^{t} e^{-\int_s^t \mu_{11}(x_{11}(r))\,dr}\hat{\alpha}_{10}(s)\hat{b}(s-A_{10}(s))(1-A_{10}'(s))\,ds,$$

$$x_{12}(t) = \tfrac{1}{2}\int_{t-\tau_{12}(t)}^{t} e^{-\mu_{12}(t-s)}\hat{\alpha}_{11}(s)b(x_1(s-A_{11}(s)))(1-A_{11}'(s))\,ds.$$

From the above equations, each component of the solution is nonnegative.

The boundedness of the solution of the system (6.2.17) can be easily obtained. Denote by $N(t)=\sum_{i=1}^{12}x_i(t)$ the total number of ticks. It is easy to see that the birth function is bounded when the size of egg-laying females is nonnegative since

$$b(x_1(t)) \le \frac{pe^{-1}}{s_T} := b_{\max}.$$

Adding all equations of system (6.2.17) yields

$$\begin{aligned} N'(t) &= b(x_1(t)) - \sum_{i\neq 5,8,11}\mu_i x_i(t) - \sum_{i=5,8,11}\mu_i(x_i(t))x_i(t) \\ &\le b_{\max} - \mu N(t), \end{aligned} \tag{6.2.21}$$

where

$$\mu = \min\left\{\mu_1, \mu_2, \mu_3, \mu_4, \mu_5(0), \mu_6, \mu_7, \mu_8(0), \mu_9, \mu_{10}, \mu_{11}(0), \mu_{12}\right\}.$$

From (6.2.21), it follows that

$$\limsup_{t\to\infty} N(t) \leq b_{\max}/\mu, \tag{6.2.22}$$

which implies the boundedness of all solutions of system (6.2.17) subject to the initial condition constraints. This completes the proof. □

6.3 Basic reproductive ratio ($\mathcal{R}_0^{v,pd}$)

System (6.2.17) has a tick-free equilibrium. Linearizing the system (6.2.17) at the tick-free equilibrium yields

$$\begin{aligned}
x_1'(t) &= \tfrac{1}{2}\alpha_{12}(t,0,0,0)px_1(t-A_{12}(t)))(1-A_{12}'(t)) - \mu_1 x_1(t),\\
x_2'(t) &= px_1(t) - \alpha_2(t)px_1(t-A_2(t))(1-A_2'(t)) - \mu_2 x_2(t),\\
x_i'(t) &= \alpha_{i-1}(t)px_1(t-A_{i-1}(t))(1-A_{i-1}'(t))\\
&\quad -\alpha_i(t)px_1(t-A_i(t))(1-A_i'(t)) - \mu_i x_i(t),\ i=3,4,\\
x_5'(t) &= \alpha_4(t)px_1(t-A_4(t))(1-A_4'(t))\\
&\quad -\alpha_5(t,0)px_1(t-A_5(t))(1-A_5'(t)) - \mu_5(0)x_5(t),\\
x_i'(t) &= \alpha_{i-1}(t,0)px_1(t-A_{i-1}(t))(1-A_{i-1}'(t))\\
&\quad -\alpha_i(t,0)px_1(t-A_i(t))(1-A_i'(t)) - \mu_i x_i(t),\ i=6,7\\
x_8'(t) &= \alpha_7(t,0)px_1(t-A_7(t))(1-A_7'(t))\\
&\quad -\alpha_8(t,0,0)px_1(t-A_8(t))(1-A_8'(t)) - \mu_8(0)x_8(t),\\
x_i'(t) &= \alpha_{i-1}(t,0,0)px_1(t-A_{i-1}(t))(1-A_{i-1}'(t))\\
&\quad -\alpha_i(t,0,0)px_1(t-A_i(t))(1-A_i'(t)) - \mu_i x_i(t),\ i=9,10,\\
x_{11}'(t) &= \tfrac{1}{2}\alpha_{10}(t,0,0)px_1(t-A_9(t))(1-A_{10}'(t))\\
&\quad -\tfrac{1}{2}\alpha_{11}(t,0,0,0)px_1(t-A_{11}(t))(1-A_{11}'(t)) - \mu_{11}(0)x_{11}(t),\\
x_{12}'(t) &= \tfrac{1}{2}\alpha_{11}(t,0,0,0)px_1(t-A_{11}(t)))(1-A_{11}'(t))\\
&\quad -\tfrac{1}{2}\alpha_{12}(t,0,0,0)px_1(t-A_{12}(t)))(1-A_{12}'(t)) - \mu_{12}x_{12}(t).
\end{aligned} \tag{6.3.23}$$

The system ha a 1-dimensional decoupled subsystem

$$\begin{aligned} x_1'(t) &= \tfrac{1}{2}p\alpha_{12}(t,0,0,0)(1-A_{12}'(t))x_1(t-A_{12}(t)) - \mu_1 x_1(t) \\ &:= a(t)x_1(t-A_{12}(t)) - \mu_1 x_1(t), \end{aligned} \tag{6.3.24}$$

where

$$a(t) = \tfrac{1}{2}p\alpha_{12}(t,0,0,0)(1-A_{12}'(t)). \tag{6.3.25}$$

The change rate of egg-laying adult females at time t depends on the number of egg-laying adults females at time $t - A_{12}(t)$. It is important to examine the number of newly generated egg-laying adult females per unit time at time t. We assume $h(t) := t - A_{12}(t)$ is a strictly increasing function of t. Then at time t, the egg-laying adult female population (with its size denoted by $x_1(t)$) will produce some new-borns who will eventually become egg-laying adult females at the future time $h^{-1}(t) := \tilde{t}$, where $h(\tilde{t}) = \tilde{t} - A_{12}(\tilde{t})$ is a strictly increasing function of $\tilde{t}$. We note that

$$\begin{aligned} \frac{d}{dt}x_1(\tilde{t}) &= \frac{d}{d\tilde{t}}x_1(\tilde{t})\frac{d\tilde{t}}{dt} = [a(\tilde{t})x_1(h(\tilde{t})) - \mu_1 x_1(\tilde{t})]\frac{1}{1-A_{12}'(\tilde{t})} \\ &= [a(h^{-1}(t))x_1(t) - \mu_1 x_1(h^{-1}(t))]\frac{1}{1-A_{12}'(h^{-1}(t))}. \end{aligned} \tag{6.3.26}$$

That is, the number of newly generated egg-laying adult females per unit time at time t is $y(t) = c(t)x_1(t)$ with $c(t) := a(h^{-1}(t))/(1 - A_{12}'(h^{-1}(t)))$.

Note that

$$\begin{aligned}(e^{\mu_1 t}x_1(t))' &= e^{\mu_1 t}(\mu_1 x_1(t) + x_1'(t)) \\ &= e^{\mu_1 t}(\mu_1 x_1(t) + a(t)x_1(t - A_{12}(t)) - \mu_1 x_1(t)) \\ &= e^{\mu_1 t}a(t)x_1(t - A_{12}(t)).\end{aligned}$$

Integrating from $-\infty$ to t which yields

$$x_1(t) = \int_{-\infty}^{t} e^{-\mu_1(t-s)}a(s)x_1(s - A_{12}(s))ds.$$

This gives (note $c(s - A_{12}(s)) = \frac{a(s)}{1-A_{12}'(s)}$)

$$\begin{aligned}y(t) &= c(t)\int_{-\infty}^{t} e^{-\mu_1(t-s)}\frac{a(s)}{c(s - A_{12}(s))}y(s - A_{12}(s))\,ds \\ &= \int_{-\infty}^{t} c(t)(1 - A_{12}'(s))e^{-\mu_1(t-s)}y(s - A_{12}(s))\,ds \\ &= \int_{A_{12}(t)}^{\infty} c(t)e^{-\mu_1(t-h^{-1}(t-r))}y(t - r)\,dr \\ &= \int_{0}^{\infty} \mathcal{K}(t, r)y(t - r)\,dr, \qquad (6.3.27)\end{aligned}$$

where

$$\mathcal{K}(t, r) = \begin{cases} \frac{1}{2}p\alpha_{12}(h^{-1}(t), 0, 0, 0)e^{-\mu_1(t-h^{-1}(t-r))} & , \quad r \geq A_{12}(t), \\ 0 & , \quad r < A_{12}(t). \end{cases} \qquad (6.3.28)$$

Note that $\mathcal{K}(t, r) = k(t + \omega, r)$.

In [96, 42], the solution $y(t)$ of (6.3.27) of the form $e^{\lambda t}u(t)$ is considered, where $u(t)$ is a periodic function with period ω and satisfies

$$u(t) = \int_{0}^{\infty} \mathcal{K}(t, r)e^{-\lambda r}u(t - r)\,dr. \qquad (6.3.29)$$

Let $\mathcal{C}_\omega := \{u : \mathcal{R} \to \mathcal{R}, u(t+\omega) = u(t)\}$ and $\mathcal{L} : \mathcal{C}_\omega \to \mathcal{C}_\omega$ such that

$$\mathcal{L}u(t) = \int_0^\infty \mathcal{K}(t,r)u(t-r)\,dr. \tag{6.3.30}$$

Following [8, 5, 99], we define the basic reproductive ratio as the spectral radius of the linear integral operator acting on the same space of ω-periodic continuous functions, i.e.,

$$\mathcal{R}_0^{v,pd} = \rho(\mathcal{L}). \tag{6.3.31}$$

In what follows, we derive a numerical algorithm to compute $\mathcal{R}_0^{v,pd}$ as defined in (6.3.28, 6.3.30, 6.3.31). Changing the variable $\theta = t - r$ of (6.3.30), we obtain

$$\begin{aligned}
\mathcal{L}u(t) &= \int_0^\infty \mathcal{K}(t,r)u(t-r)\,dr \\
&= \tfrac{1}{2}p\alpha_{12}(h^{-1}(t),0,0,0)e^{-\mu_1 t}\int_{A_{12}(t)}^\infty e^{\mu_1 h^{-1}(t-r)}u(t-r)\,dr \\
&= \bar{p}(t)\int_{-\infty}^{t-A_{12}(t)} e^{\mu_1 h^{-1}(\theta)}u(\theta)\,d\theta \\
&= \bar{p}(t)\left[\int_0^{t-A_{12}(t)} e^{\mu_1 h^{-1}(\theta)}u(\theta)d\theta + \int_{-\infty}^0 e^{\mu_1 h^{-1}(\theta)}u(\theta)\,d\theta\right],
\end{aligned} \tag{6.3.32}$$

where

$$\bar{p}(t) = \tfrac{1}{2}p\alpha_{12}(h^{-1}(t),0,0,0)e^{-\mu_1 t}.$$

Since $u(t)$ is ω-periodic, we have

$$\begin{aligned}
\int_{-\infty}^0 e^{\mu_1 h^{-1}(\theta)}u(\theta)\,d\theta &= \sum_{n=0}^\infty \int_{-(n+1)\omega}^{-n\omega} e^{\mu_1 h^{-1}(\theta)}u(\theta)\,d\theta \\
&= \int_0^\omega \sum_{n=0}^\infty e^{\mu_1 h^{-1}(\theta-(n+1)\omega)}u(\theta)\,d\theta.
\end{aligned}$$

So the eigenvalue problem (6.3.32) is equivalent to

$$\begin{aligned}
\mathcal{L}u(t) &= \bar{p}(t)\left[\int_0^{t-A_{12}(t)} e^{\mu_1 h^{-1}(\theta)}u(\theta)\,d\theta + \int_0^{\omega}\sum_{n=0}^{\infty} e^{\mu_1 h^{-1}(\theta-(n+1)\omega)}u(\theta)\,d\theta\right] \\
&= \bar{p}(t)\left[\int_0^{t-A_{12}(t)} e^{\mu_1 h^{-1}(\theta)}u(\theta)\,d\theta + \int_0^{t-A_{12}(t)}\sum_{n=0}^{\infty} e^{\mu_1 h^{-1}(\theta-(n+1)\omega)}u(\theta)\,d\theta\right. \\
&\quad \left. + \int_{t-A_{12}(t)}^{\omega}\sum_{n=0}^{\infty} e^{\mu_1 h^{-1}(\theta-(n+1)\omega)}u(\theta)\,d\theta\right] \\
&= \bar{p}(t)\left[\int_0^{t-A_{12}(t)}\sum_{n=0}^{\infty} e^{\mu_1 h^{-1}(\theta-n\omega)}u(\theta)\,d\theta\right. \\
&\quad \left. + \int_{t-A_{12}(t)}^{\omega}\sum_{n=0}^{\infty} e^{\mu_1 h^{-1}(\theta-\omega-n\omega)}u(\theta)\,d\theta\right] \\
&= \bar{p}(t)\left[\int_0^{t-A_{12}(t)} H(\theta)u(\theta)\,d\theta + \int_{t-A_{12}(t)}^{\omega} H(\theta-\omega)u(\theta)\,d\theta\right], \qquad (6.3.33)
\end{aligned}$$

with

$$H(\theta) = \sum_{n=0}^{\infty} e^{\mu_1 h^{-1}(\theta-n\omega)}.$$

In the previous equation, $u(t)$ is a ω-periodic function. To compute the $\mathcal{R}_0^{v,pd}$ numerically, we partition the interval $[0,\omega]$ into N (enough large integer) subinterval of equal length. Set $t_i = (i-1)\omega/N$ for $i = 1, 2, \cdots, N$. Then at the point t_i, Equation (6.3.33) becomes

$$\mathcal{L}u(t_i) = \bar{p}(t_i)\left[\int_0^{t_i-A_{12}(t_i)} H(\theta)u(\theta)\,d\theta + \int_{t_i-A_{12}(t_i)}^{\omega} H(\theta-\omega)u(\theta)\,d\theta\right]. \qquad (6.3.34)$$

For each $t_i \in [0,\omega)$, there is a unique integer k_i such that $t_i + k_i\omega - A_{12}(t_i) \in [0,\omega)$. Denote $l_i := [\frac{t_i+k_i\omega-A_{12}(t_i)}{\frac{\omega}{N}} + 1] \in \{1, 2, \cdots, N\}$, i.e., the nearest integer less than or

equal to $\frac{t_i+k_i\omega-A_{12}(t_i)}{\frac{\omega}{N}}+1$. Replacing $t_i+k_i\omega$ by t_i in Equation (6.3.34), we obtain

$$\begin{aligned}
\mathcal{L}u(t_i) &= \bar{p}(t_i+k_i\omega)\left[\int_0^{t_i+k_i\omega-A_{12}(t_i)} H(\theta)u(\theta)\,d\theta+\int_{t_i+k_i\omega-A_{12}(t_i)}^{\omega} H(\theta-\omega)u(\theta)\,d\theta\right] \\
&= \bar{p}(t_i+k_i\omega)\left[\int_0^{t_{l_i}} H(\theta)u(\theta)\,d\theta+\int_{t_{l_i}}^{t_i+k_i\omega-A_{12}(t_i)} H(\theta)u(\theta)\,d\theta\right. \\
&\quad \left.+\int_{t_i+k_i\omega-A_{12}(t_i)}^{t_{l_i+1}} H(\theta-\omega)u(\theta)\,d\theta+\int_{t_{l_i+1}}^{\omega} H(\theta-\omega)u(\theta)\,d\theta\right]. \qquad (6.3.35)
\end{aligned}$$

In the case where $t_{l_i}=t_i+k_i\omega-A_{12}(t_i)$, equation (6.3.35) becomes

$$\begin{aligned}
\mathcal{L}u(t_i) &= \bar{p}(t_i+k_i\omega)\left[\sum_{j=2}^{l_i} H(t_j)u(t_j)\frac{\omega}{N}+\sum_{j=l_i+1}^{N+1} H(t_j-\omega)u(t_j)\frac{\omega}{N}\right] \\
&= \bar{p}(t_i+k_i\omega)\left[\sum_{j=2}^{l_i} H(t_j)u(t_j)\frac{\omega}{N}+\sum_{j=l_i+1}^{N} H(t_j-\omega)u(t_j)\frac{\omega}{N}\right. \\
&\quad \left.+H(t_{N+1}-\omega)u(t_{N+1})\frac{\omega}{N}\right] \\
&= \bar{p}(t_i+k_i\omega)\left[\sum_{j=2}^{l_i} H(t_j)u(t_j)\frac{\omega}{N}+\sum_{j=l_i+1}^{N} H(t_j-\omega)u(t_j)\frac{\omega}{N}+H(t_1)u(t_1\frac{\omega}{N})\right] \\
&= \bar{p}(t_i+k_i\omega)\left[\sum_{j=1}^{l_i} H(t_j)u(t_j)\frac{\omega}{N}+\sum_{j=l_i+1}^{N} H(t_j-\omega)u(t_j)\frac{\omega}{N}\right].
\end{aligned}$$

In the case where $t_{l_i}<t_i+k_i\omega-A_{12}(t_i)$, equation (6.3.35) becomes

$$\begin{aligned}
\mathcal{L}u(t_i) &= \bar{p}(t_i+k_i\omega)\left[\sum_{j=1}^{l_i-1} H(t_j)u(t_j)\frac{\omega}{N}+\int_{t_{l_i}}^{t_i+k_i\omega-A_{12}(t_i)} H(\theta)u(\theta)\,d\theta\right. \\
&\quad \left.+\int_{t_i+k_i\omega-A_{12}(t_i)}^{t_{l_i+1}} H(\theta-\omega)u(\theta)\,d\theta+\sum_{j=l_i+1}^{N} H(t_j-\omega)u(t_j)\frac{\omega}{N}\right] \\
&= \bar{p}(t_i+k_i\omega)\left[\sum_{j=1}^{l_i-1} H(t_j)u(t_j)\frac{\omega}{N}+H(t_{l_i})u(t_{l_i})\frac{\omega}{N}+\sum_{j=l_i+1}^{N} H(t_j-\omega)u(t_j)\frac{\omega}{N}\right] \\
&= \bar{p}(t_i+k_i\omega)\left[\sum_{j=1}^{l_i} H(t_j)u(t_j)\frac{\omega}{N}+\sum_{j=l_i+1}^{N} H(t_j-\omega)u(t_j)\frac{\omega}{N}\right].
\end{aligned}$$

Let $W_i = u(t_i)$. Then the problem of estimating of $\mathcal{R}_0^{v,pd}$ of (6.3.31) reduces to the calculation of the spectral radius of a given matrix. Namely we have the matrix eigenvalue problem of the form $\tilde{\mathcal{R}}_0^{v,pd}\mathbf{W} = \mathbf{X}\mathbf{W}$, where $\mathbf{W} = (W_1, W_2, \cdots, W_N)^T$, and $\tilde{\mathcal{R}}_0^{v,pd}$ is the spectral radius of a $N \times N$ positive matrix $\mathbf{X}$. In this matrix, the (i,j) element is given by

$$x_{ij} = \begin{cases} \frac{1}{2}p\alpha_{12}(h^{-1}(t_i),0,0,0)\frac{\omega}{N}\sum\limits_{n=0}^{\infty} e^{-\mu_1(t_i - h^{-1}(t_j - k_i\omega - n\omega))}, & 1 \le j \le l_i, \\ \frac{1}{2}p\alpha_{12}(h^{-1}(t_i),0,0,0)\frac{\omega}{N}\sum\limits_{n=0}^{\infty} e^{-\mu_1(t_i - h^{-1}(t_j - k_i\omega - (n+1)\omega))}, & l_i + 1 \le j \le N. \end{cases} \tag{6.3.36}$$

Remark 6.3.1. Since $h(t) = t - A_{12}(t)$ is a strictly increasing function with respect to t, we have the existence of h^{-1}, and it can be easily verified that $h^{-1}(t + n\omega) = h^{-1}(t) + n\omega$, $n \in \mathcal{Z}$.

It is useful to rewrite $\mathbf{X}$ in the following form:

$$\mathbf{X} = \begin{pmatrix} r_1 s_{1,1} & r_1 s_{1,2} & \cdots & r_1 s_{1,l_1} & r_1 s_{1,l_1+1} & \cdots & r_1 s_{1,N} \\ r_2 s_{2,1} & r_2 s_{2,2} & \cdots & r_2 s_{2,l_2} & r_2 s_{2,l_2+1} & \cdots & r_2 s_{1,N} \\ \vdots & \vdots & & \vdots & \vdots & & \vdots \\ r_N s_{N,1} & r_N s_{N,2} & \cdots & r_N s_{N,l_N} & r_N s_{N,l_N+1} & \cdots & r_N s_{N,N} \end{pmatrix} \frac{\omega}{N} \cdot \frac{1}{1 - e^{-\mu_1 \omega}},$$

where $r_i = \frac{1}{2}p\alpha_{12}(h^{-1}(t_i),0,0,0)$ $(i = 1, \cdots, N)$ is the number of newly generated egg-laying adults females per unit time produced by the per egg-laying adult female at time t_i. $l_i = [\frac{t_i + k_i\omega - A_{12}(t_i)}{\frac{\omega}{N}} + 1] \in \{1, 2, \cdots, N\}$ $(i = 1, \cdots, N)$, the nearest integer less than or equal to $\frac{t_i + k_i\omega - A_{12}(t_i)}{\frac{\omega}{N}} + 1$, where k_i is a unique integer k_i such that

$t_i + k_i\omega - A_{12}(t_i) \in [0, \omega)$. $s_{i,j}$ given below

$$s_{i,j} = \begin{cases} e^{-\mu_1(t_i - h^{-1}(t_j - k_i\omega))}, & 1 \le j \le l_i, \\ e^{-\mu_1(t_i - h^{-1}(t_j - k_i\omega - \omega))}, & l_i + 1 \le j \le N, \end{cases} \tag{6.3.37}$$

is the survival probability of egg-laying adult females at time t_i who developed from eggs at time $t_j - k_i\omega$ or $t_j - k_i\omega - \omega$, will become egg-laying adult females at the future time $h^{-1}(t_j - k_i\omega)$ or $h^{-1}(t_j - k_i\omega - \omega)$, and have survived until the time t_i. This can be observed easily since $t_{l_i} \le t_i + k_i\omega - A_{12}(t_i)$ and $t_{l_i} = t_j + (l_i - j)\omega/N$ implies

$$\begin{aligned} t_j - k_i\omega &= t_{l_i} - (l_i - j)\frac{\omega}{N} - k_i\omega \le t_i + k_i\omega - A_{12}(t_i) - k_i\omega - (l_i - j)\frac{\omega}{N} \\ &= t_i - A_{12}(t_i) - (l_i - j)\frac{\omega}{N} \le t_i - A_{12}(t_i), \quad j = 1, \cdots, l_i; \end{aligned}$$

and

$$\begin{aligned} t_j - k_i\omega - \omega &= t_{l_i} - (l_i - j)\frac{\omega}{N} - k_i\omega - \omega \le t_i + k_i\omega - A_{12}(t_i) - k_i\omega - (l_i - j)\frac{\omega}{N} - \omega \\ &= t_i - A_{12}(t_i) - (l_i - j + N)\frac{\omega}{N} < t_i - A_{12}(t_i), \quad j = l_i + 1, \cdots, N. \end{aligned}$$

x_{ij} is the total number of newly generated egg-laying adult females per $\frac{\omega}{N}$-unit time at time t_i caused by the eggs at time $t_j - k_i\omega - n\omega$ ($j = 1, 2, \cdots, l_i$; $n = 0, 1, 2, \cdots$) or $t_j - (k_i + 1)\omega - n\omega$ ($j = l_i + 1, \cdots, N$; $n = 0, 1, 2, \cdots$).

Leslie Matrix was invented by Patrick Holt Leslie in 1945 to model the growth of the number of female rats population over a period of time [10]. He divided the female rats population into n groups based on age, and each (i, j)th cell of the

matrix represents how many individuals of female rats will be in the age group i at the next time step for each individuals from group j. Compared to the classical Leslie matrix, we divide the population of egg-laying adult females into n groups based on time in a period $[0, \omega]$, then each (i, j)th cell of our matrix $\mathbf{X}$ indicates how many egg-laying adult females will be in the class i at the next time period for each individual in group j from all previous time period. Therefore in the classical demographic models, this $\mathbf{X}$ is nothing but the Leslie matrix. Note that the initial and end age of a specific stage is time-dependent.

6.4 Simulation tests

In this section, we conduct some numerical simulations using our proposed numerical algorithm for $\mathcal{R}_0^{v,pd}$. We will conduct our simulations using the following 1-periodic function:

$$\tau(t) = a + b\cos(\frac{2\pi}{365}(t+\phi)),$$

where $a > b > 0$ and $0 < b < \frac{365}{2\pi}$. For this parameter set, $1 - \tau'(t) > 0$ is satisfied. We choose $\tau_i(t)$ $(i = 2, 4, 6, 7, 9, 10, 12)$ as 1-periodic functions given by

$$\tau_i(t) = \tau_{i0}(1 + \varepsilon_i \cos(\frac{2\pi}{365}(t+\phi_i))).$$

All other time delays are considered as constants.

In what follows, we fix some parameter values as listed below:

$\tau_{20} = 100$, $\tau_{40} = 120$, $\tau_{60} = 90$, $\tau_{70} = 120$, $\tau_{90} = 90$, $\tau_{100} = 20$, $\tau_{120} = 60$, $\tau_3 = 21$, $\tau_5 = 3$, $\tau_8 = 5$, $\tau_{11} = 10$, $p = 3000$, $\mu_2 = 0.002$, $\mu_3 = 0.006$, $\mu_4 = 0.006$, $\mu_5 = 0.4$, $\mu_6 = 0.003$, $\mu_7 = 0.006$, $\mu_8 = 0.3$, $\mu_9 = 0.002$, $\mu_{10} = 0.006$, $\mu_{11} = 0.35$, $\mu_{12} = 0.0001$. Other parameters will be varied in our simulations. In what follows, we let $[\mathcal{R}_0^{v,pd}]$ be the basic reproductive ratio of the corresponding time-averaged autonomous delay differential system of (6.3.24). Such a system is obtained by replacing the periodic delay $\tau_i(t)$ with its corresponding time-averaged delay $\bar{\tau}_i = \frac{1}{\omega}\int_0^\omega \tau_i(t)\,dt = \tau_{i0}$ for the original system of (6.3.24). This allows us to compare the basic reproductive ratio $\mathcal{R}_0^{v,pd}$ in the periodic environment with $[\mathcal{R}_0^{v,pd}]$ in the time-averaged constant environment.

We first discuss the convergence of the proposed numerical method. We set $\varepsilon_i = 0.4$ and $\phi_i = 270$ for all $i = 2, 4, 6, 7, 9, 10, 12$. We show in Table 6.1 the approximation of $\mathcal{R}_0^{v,pd}$ and $[\mathcal{R}_0^{v,pd}]$ (in fact, the dominant eigenvalue of matrix X) when we increase the number N of partitions 365 to 365×13 with $\mu_1 = 1, 0.5, 0.1$, respectively. The simulations are summarized in Table 6.1 and illustrated in Figure 6.1.

We now conduct some numerical simulations to gain insights about the relationship between our basic reproductive ratio and the amplitudes and phases of the periodic delays. In what follows, we fix the number of equal partition $N = 3650$. We firstly assume only one periodic delay $\tau_2(t) = \tau_{20}(1 + \varepsilon_2 \cos(\frac{2\pi}{365}(t + \phi_2)))$ is

Table 6.1: Convergence of the proposed numerical algorithm with increasing number N of points equally discretizing the interval $[0, \omega)$, which represents 365 days.

N	365	365× 3	365× 5	365× 7	365× 9	365× 11	365× 13
$(\mu_1 = 1)\, \mathcal{R}_0^{v,pd}$	0.3361	0.3278	0.3266	0.3239	0.3242	0.3233	0.3233
$(\mu_1 = 1)\, [\mathcal{R}_0^{v,pd}]$	0.4630	0.3178	0.3022	0.3003	0.3000	0.2958	0.2943
$(\mu_1 = 0.5)\, \mathcal{R}_0^{v,pd}$	0.6513	0.6519	0.6505	0.6496	0.6494	0.6494	0.6494
$(\mu_1 = 0.5)\, [\mathcal{R}_0^{v,pd}]$	0.7438	0.6087	0.5930	0.5925	0.5923	0.5882	0.5867
$(\mu_1 = 0.1)\, \mathcal{R}_0^{v,pd}$	3.2107	3.2164	3.2174	3.2169	3.2170	3.2172	3.2172
$(\mu_1 = 0.1)\, [\mathcal{R}_0^{v,pd}]$	3.0753	2.9487	2.9327	2.9333	2.9333	2.9292	2.9277

involved in the system (6.3.24) and all other six periodic (delay) functions are constants, i.e., $\varepsilon_i = \phi_i = 0$ for $i = 4, 6, 7, 9, 10, 12$. We test how $\mathcal{R}_0^{v,pd}$ changes when ε_2 and ϕ_2 change separately.

We first fix $\varepsilon_i = 0$ $(i = 4, 6, 7, 9, 10, 12)$ and $\mu_1 = 0.1$, and we vary $\phi_2 \in [0, \omega]$. The dependence of $\mathcal{R}_0^{v,pd}$ on ϕ_2 is given in Figure 6.2, which shows that the basic reproductive ratio $\mathcal{R}_0^{v,pd}$ remains at a constant value with varying ϕ_2, means that $\mathcal{R}_0^{v,pd}$ is independent of the phase difference.

Next we choose $\phi_2 = 270$ and vary ε_2 in the interval $[0, 0.4]$. We obtain the relations of the basic reproductive ratio $\mathcal{R}_0^{v,pd}$ and $[\mathcal{R}_0^{v,pd}]$ with time-averaged to

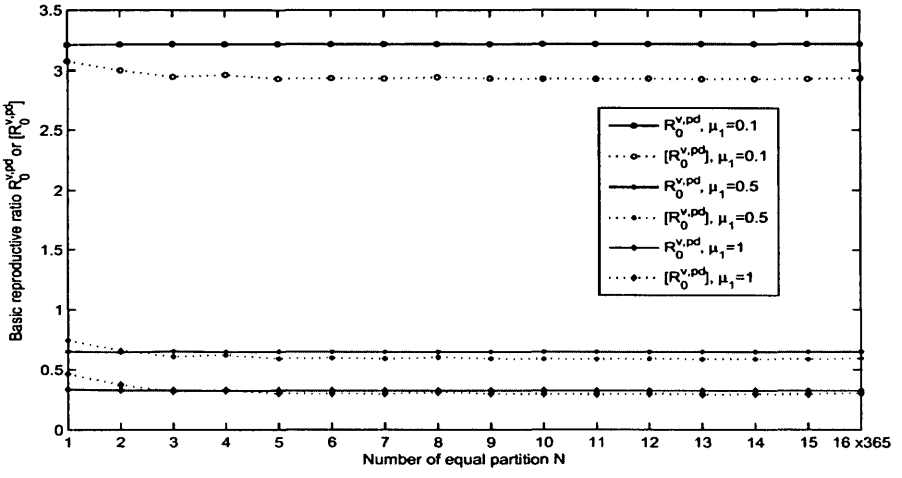

Figure 6.1: The convergence of the numerical simulation of the basic reproductive ratio $\mathcal{R}_0^{v,pd}$ or the average basic reproductive ratio $[\mathcal{R}_0^{v,pd}]$ as N is increased.

ε_2 (Figure 6.3). This figure shows increasing the amplitude of the periodic delay reduces the basic reproductive ratio $\mathcal{R}_0^{v,pd}$, and that using the corresponding time-averaged delay differential system tends to overestimate the ratio ($[\mathcal{R}_0^{v,pd}] > \mathcal{R}_0^{v,pd}$).

Figures 6.4 and 6.5 report the simulations involving two periodic delays. We assume that $\tau_2(t)$ and $\tau_4(t)$ are periodic delays, all other delays are constants. i.e., $\varepsilon_i = 0$ for $i = 6, 7, 9, 10, 12$. Figure 6.4 shows that the increase of the amplitude (ε_4) of $\tau_4(t)$ while keeping $\tau_2(t)$ and ϕ_4 unchanged can change the basic reproductive ratio $\mathcal{R}_0^{v,pd}$ of system (6.3.24) from below the time-averaged basic reproductive ratio $[\mathcal{R}_0^{v,pd}]$ to above. Hence, using the time-averaged delay differential system can underestimate and overestimate the basic reproductive ratio of the corresponding

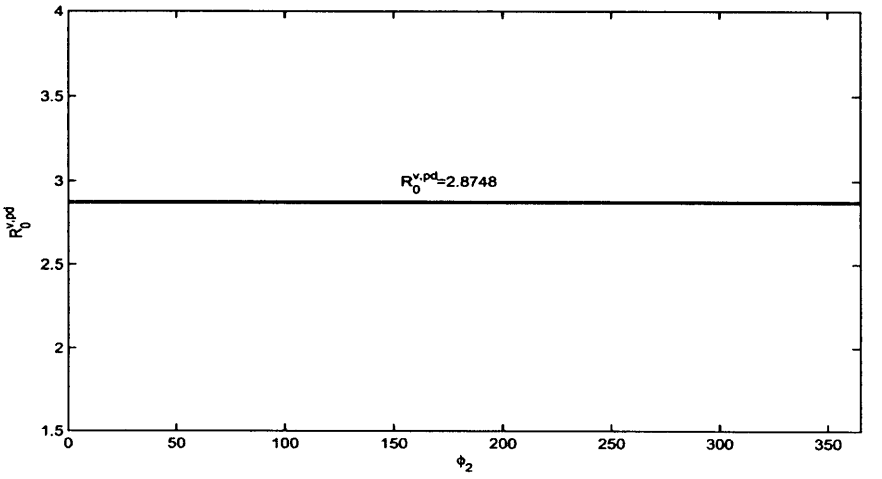

Figure 6.2: The basic reproductive ratio $\mathcal{R}_0^{v,pd}$ versus ϕ_2. Where $\tau_2(t) = \tau_{20}(1 + \varepsilon_2 \cos(\frac{2\pi}{365}(t + \phi_2)))$, $\tau_i(t) = \tau_{i0}$ $(i = 4, 6, 7, 9, 10, 12)$, $\varepsilon_2 = 0.4$, $\mu_1 = 0.1$, ϕ_2 varies in the interval [0, 365].

period system of DDEs.

In Figure 6.5, we change phase ϕ_4 over the interval $[0, 365 \times 2]$ while keeping $\tau_2(t)$ and ε_4 unchanged. We noticed the 1-year periodicity of $\mathcal{R}_0^{v,pd}$ as a function of ϕ_4. Moreover, an increase of phase of ϕ_2 yields the shift of $\mathcal{R}_0^{v,pd}$ to the right. For instance, the blue curve of $\mathcal{R}_0^{v,pd}$ corresponds to $\phi_2 = 0$ while the red one corresponds to $\phi_2 = 100$. Therefore, difference in peak timings of the two periodic delays can change the value of the basic reproductive ratio $\mathcal{R}_0^{v,pd}$.

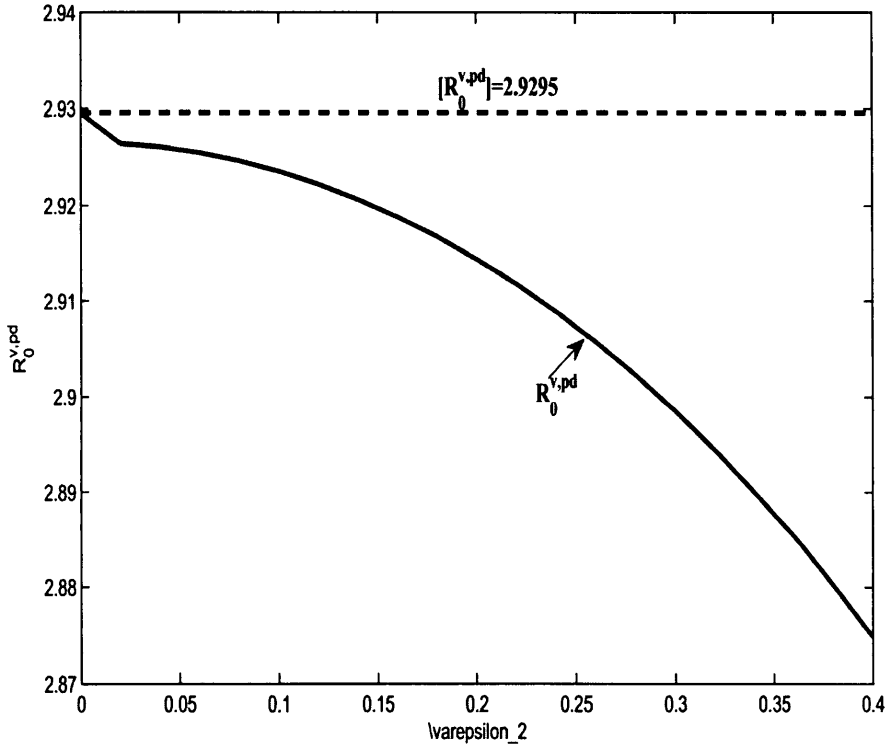

Figure 6.3: The graph of the basic reproductive ratio $\mathcal{R}_0^{v,pd}$ and the time-averaged basic reproductive ratio $[\mathcal{R}_0^{v,pd}]$ versus ε_2. Here $\tau_2(t) = \tau_{20}(1 + \varepsilon_2 \cos(\frac{2\pi}{365}(t + \phi_2)))$, $\tau_i(t) = \tau_{i0}$ $(i = 4, 6, 7, 9, 10, 12)$, $\phi_2 = 270$, $\mu_1 = 0.1$, ε_2 varies to [0, 0.4].

6.5 Discussion

In summary, we have derived a stage-structured population model with both periodic coefficients and delays, and we have derived the basic reproductive ratio $\mathcal{R}_0^{v,pd}$ for the scalar linearized periodic system (linearized at the trivial solution). We have

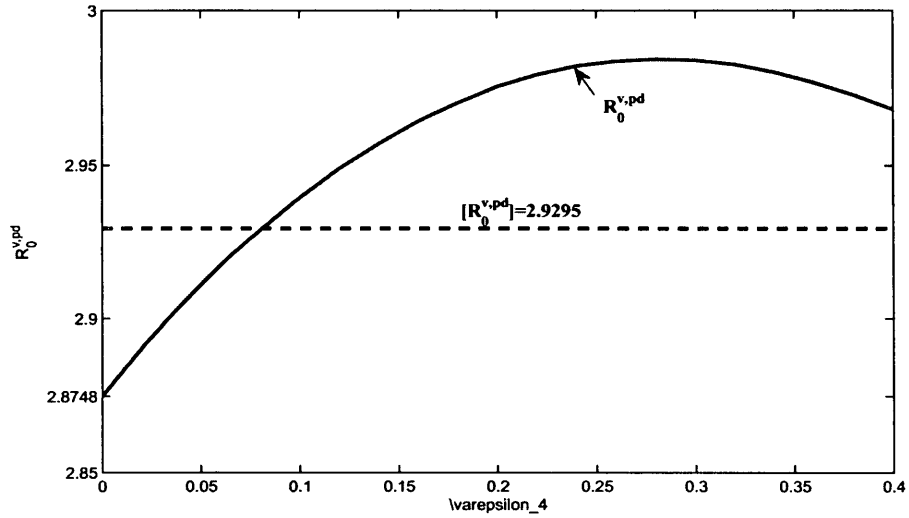

Figure 6.4: The graph of the basic reproductive ratio $\mathcal{R}_0^{v,pd}$ and the time-averaged basic reproductive ratio $[\mathcal{R}_0^{v,pd}]$ versus ϕ_4. Here, $\tau_i(t) = \tau_{i0}(1 + \varepsilon_i \cos(\frac{2\pi}{365}(t + \phi_i)))$ (i=2,4), and $\tau_i(t) = \tau_{i0}$ (i=6,7,9,10,12); $\varepsilon_2 = 0.4$, $\phi_2 = \phi_4 = 270$, $\mu_1 = 0.1$, ε_4 varies in the interval $[0, 0.4]$.

proposed a discretization-based method, where the periodic coefficients and the delays are both approximated by constants over a short time interval. This method then reduces the problem of calculating the spectral radius of a linear integral operator (defined as the basic reproductive ratio $\mathcal{R}_0^{v,pd}$) to that of the spectral radius of a matrix (the dominant eigenvalue of $\mathbf{X}$). Our numerical simulations indicate that this method is quite effective.

We then performed some simulations to gain insights how the basic reproductive

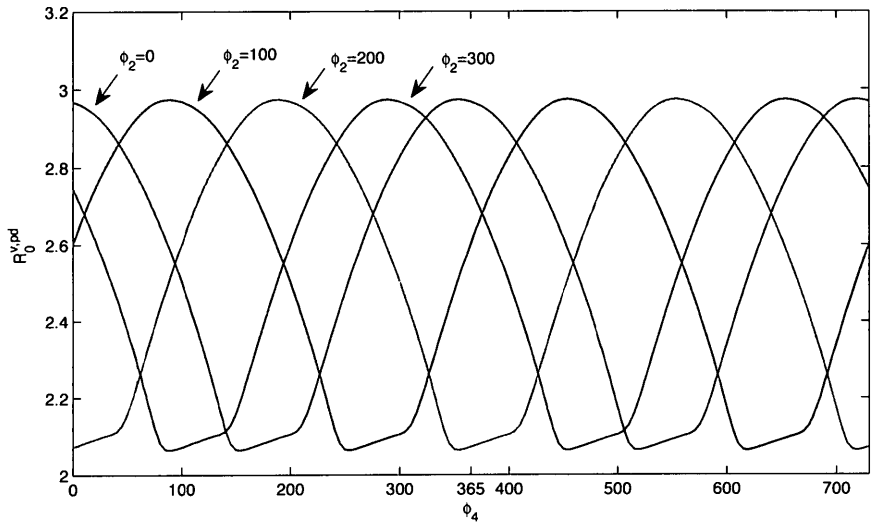

Figure 6.5: The graph of the basic reproductive ratio $\mathcal{R}_0^{v,pd}$ versus ϕ_4 when $\phi_2 = 0, 100, 200, 300$. Here $\tau_i(t) = \tau_{i0}(1 + \varepsilon_i \cos(\frac{2\pi}{365}(t + \phi_i)))$ $(i = 2, 4)$, and $\tau_i(t) = \tau_{i0}$ for $i = 6, 7, 9, 10, 12$. $\varepsilon_2 = \varepsilon_4 = 0.4$, $\mu_1 = 0.1$, ϕ_4 varies in $[0, 730]$. Blue line represents the basic reproductive ratio $\mathcal{R}_0^{v,pd}$ versus ϕ_4 with $\phi_2 = 0$; Red line represents the basic reproductive ratio $\mathcal{R}_0^{v,pd}$ versus ϕ_4 with $\phi_2 = 100$; Magenta line represents the basic reproductive ratio $\mathcal{R}_0^{v,pd}$ versus ϕ_4 with $\phi_2 = 200$; Dark green line represents the basic reproductive ratio $\mathcal{R}_0^{v,pd}$ versus ϕ_4 with $\phi_2 = 300$.

ratio $\mathcal{R}_0^{v,pd}$ depends on the parameters. With a single periodic delay (while all other fixed to constants), we noticed that the basic reproductive ratio $\mathcal{R}_0^{v,pd}$ may increase or decrease as the amplitude of the periodic delay is increased (see Figure 6.3, Figure 6.4). However, we observed that the value of $\mathcal{R}_0^{v,pd}$ is independent of the

phase change of the periodic delay (see Figure 6.2). We then have focused on the issue how phase differences can influence the basic reproductive ratio $\mathcal{R}_0^{v,pd}$ if two time-periodic delays are involved in a periodic system. In particular, Figure 6.5 shows that change of peak timings of two periodic delays can change the value of the basic reproductive ratio. The study in Ogden et al (2006) [74] showed that seasonal activities of different tick instars changed due to the projected increased temperatures, from the current pattern "nymphal activities are ahead of larvae in a year" to the one "larvae become active earlier than nymphs in a year" in the future. Therefore, the result in [68] and our simulations combined indicate that switch of peak timings of larvae and nymphs may alter the basic reproductive ratio for the tick population, hence influence the risk of Lyme disease.

7 Conclusion and Discussions

In this thesis, we focus on modelling the impact of climate change on the spread of one of the important infectious vector-borne diseases in Canada–Lyme disease. We have gone through a few iterative cycles of modeling and analysis: mathematical formulation, parameterization and analysis, comparison, validation and tests. From different angles of complexity and relevance to public health, we study the spatial-temporal interaction, climate change and host diversity integrating individual tick physiological activity and evolution on the tick population dynamics and the Lyme disease spread. This is a part of the NCE center GEOIDE project "CODIGEOSIM–Geosimulation Tools for Simulating Spatial-Temporal Spread Patterns and Evaluating Health Outcomes of Communicable Diseases", and this thesis work has involved close collaboration with the Center for Food-borne, Environmental and Zoonotic Infectious Diseases, Zoonoses Division of the Public Health Agency of Canada.

In order to identify the threshold conditions to inform the risk analysis of the

tick population establishment and Lyme disease spread, we employ the techniques of dynamical systems with aid of population-based models of ordinary different equations, partial differential equations and delay differential equations with seasonal forcing. By utilizing some recently developed results about the qualitative theory of epidemic models with periodic coefficients and the qualitative theory of monotone dynamic systems, we successfully calculated key thresholds (including basic reproductive ratios) for the establishment of tick population and persistence of disease spread, and we are able to obtain some important information (such as the minimal wave speed) for tick population range expansion. Some statistical methods are also used to identify environmental threshold conditions (such as cumulative annual degree-days) of establishment of tick population in Canada. We believe these results are useful to the public health policy makers for their consideration of the prevention and control of Lyme disease spread in Canadian landscape under varying environmental conditions.

We develop complex models for a systematic study of parasite/pathogen population while maintaining a certain degree balance between the mathematical feasibility and ecological/epidemiological reality. In Chapter 2, a model of ordinary differential equations with temperature-dependent (time-independent) development rates is used to study tick population dynamics in a spatially homogeneous habitat. We show that the basic reproductive ratio determines the survival or extinction of

the tick population depends on temperature and host densities. We identify that lower or higher temperatures can limit the northward expansion of ticks by directly killing the ticks as studied in [71, 68], prohibiting or shortening time available of host-seeking activities, and potentially causing the increase of their mortality rate. We dedicate Chapter 3 to the qualitative assessment of the tick population establishment risk in the Canadian landscape using a deterministic model with seasonality. The predictor, basic reproductive ratio $\mathcal{R}_0^{v,p}$ of the tick population, is derived in the presence of seasonal variation in temperature. The value is obtained by parameterizing the model and utilizing mathematical techniques such as spectral analysis, and then we validate model using some existing surveillance data, including cumulative annual degree-days in comparison with our calculated basic reproductive ratios by running model simulations in 30 locations of Canada. Our finding suggests climate warming would increase the basic reproductive ratio, and thereby accelerate the range expansion of tick population northward. The reason maybe that climate warming would give rise to accelerate the accumulation of degree-days for tick development, which underlying leads to come earlier of egg deposition and larval hatch, and more nymphs molted in the same year and more time available for host-seeking activities. This work can be extended to predict future tick population range expansion of *Ixodes scapularis* in Canada or other countries. In Chapter 4, we explore the relative importance of local connectivity

in driving the patterns of tick range expansion by a reaction-diffusion model with seasonality. Using the qualitative theory of strongly order-preserving periodic process, we obtain the existence of minimal wave speed due to tick seasonal on-or-off activities. In order to assess the real risk of Lyme disease, in Chapter 5, we use a periodic system of ordinary differential equations to study the disease transmission involving stage-structured tick population, seasonal forcing and host diversity. Our findings indicate that climate warming will promote the spread of the disease and increasing the level of host diversity may dilute or amplify the Lyme disease risk to public health, depending on the model parameters and reservoir competence of the alternative host. Sensitivity analysis is conducted to identify key climate and environmental conditions which have great impact on disease spread. In Chapter 6, motivated by the tick ecological activity, we derive a periodic system of delay differential equations with multiple time-periodic delays following the standard age-structured argument. We define the basic reproductive ratio for this type of DDEs with time-periodic terms and introduce a numerical algorithm to calculate the basic reproductive ratio. One of the particular observations is that switch of peak timings of different time-periodic delays may have significant impact on the basic reproductive ratio.

This thesis seems to be the first systematic study of Lyme disease and its vector in a periodically varying environment. The developed approach and techniques

could and should be expended to other vector-borne disease. To better understand the range expansion and accurately predict the distribution of the tick population, we need to examine the future trends of *Ixodes scapularis* population with different scenarios of climate changes. Furthermore, more realistic models accounting for the effects of landscape heterogeneity on the movement of mammals and resident birds needs to be studied since species are affected differently by landscape fragmentation because of their specific range size, dispersal ability, habitat and food requirements, and behaviors. In order to better understand the spread of Lyme disease, we will need to model spirochete dispersal as a complex function of tick dispersal, host competency to incubate bacterium, bacterial virulence, duration of infection and potential effect of infection on migratory behavior.

The calculation of the basic reproduction ratio, and hence the potential persistence/extinction of tick populations is affected by the sex ratio of ticks, which we have assumed as 1:1 in our thesis. However there have been studies which indicate that this ratio may be different, for example, female-to-male sex ratio of 1.6:1 was determined in the work of [18]. Therefore it is more reasonable to consider sex ratio as a parameter rather than a fixed constant. It is possible to extend our sensitivity analysis to express how the basic reproduction ratio changed on this ratio and deserves future study. In our thesis, we have assumed the deer and rodents populations be fixed constants. How the basic reproduction ratio depends on these

numbers should be further studied to inform the effectiveness of any intervention involving the control and dynamics of deer and rodents populations.

8 Appendix A

Fourier series analysis

In our model, there are seven periodic coefficients to be determined for the given meteorological stations for the 1971-2000 period: $d_{12}(t)$, $d_2(t)$, $d_6(t)$, $d_9(t)$ (development rates of POP, PEP, larva-to-nymph and nymph-to-adult, respectively) and $d_4(t)$, $d_7(t)$ and $d_{10}(t)$ (host attaching rates of larvae, nymphs and adults, respectively). The host attaching rates are given by the following relationship

$$d_4(t) = \lambda_{ql} \times \theta^i(t), \quad d_7(t) = \lambda_{qn} \times \theta^i(t), \quad d_{10}(t) = \lambda_{qa} \times \theta^a(t), \tag{8.0.1}$$

with $\theta^i(t)$, $\theta^a(t)$ being the respective activity proportions of immature and adult ticks which depend on temperature.

The following "7th order Fourier series" was employed to estimate the seven periodic coefficients of the tick stage and seasonally specific development and activity,

$$f(t) = c_0 + \sum_{i=1}^{7}(a_i \sin\frac{2\pi it}{365} + b_i \cos\frac{2\pi it}{365}). \tag{8.0.2}$$

MATLAB (R2010a) was used for the Fourier series analysis by fitting the tick data into the equation (8.0.2). For instance, Figure 8.1 presents the fitted devel-

opment rates of POP, PEP, larva-to-nymph and nymph-to-adult at Delhi CDA meteorological station for the 1971-2000 periods, the detailed periodic functions are presented in the following subsection.

Figure 8.1: Fourier series projected development rates of POP ($d_{12}(t)$), PEP ($d_2(t)$), larva-to-nymph ($d_6(t)$) and nymph-to-adult ($d_9(t)$) from the 1971-2000 mean monthly normal temperature at Delhi CDA meteorological station.

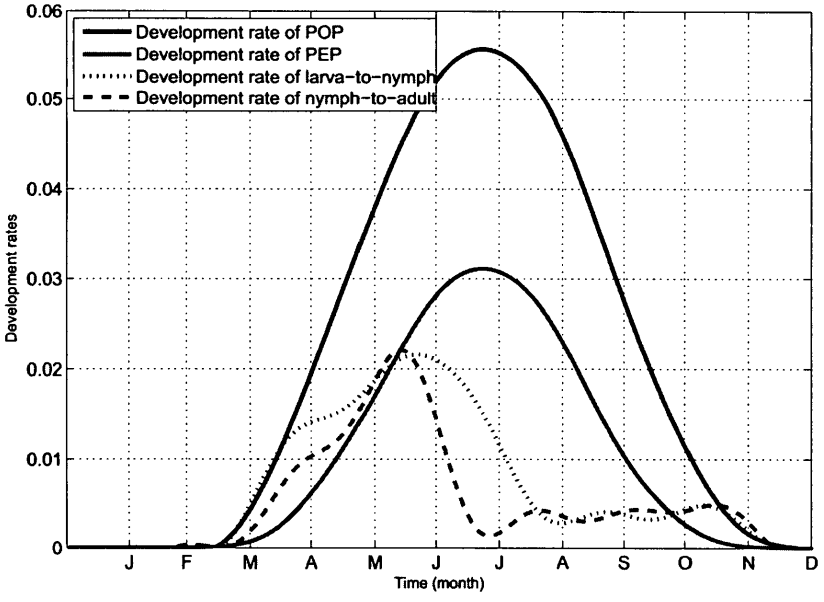

Periodic functions at Delhi CDA meteorological station for the 1971-2000 periods

In what follows, we used $t(m365)$ to denote the modular after division $(t/365)$.

The periodic developmental rate of POP is given by:

$$d_{12}(t) = \frac{sign[(t(m365) - 47.8683)(358.9047 - t(m365))] + 1}{2} \times f_1(t),$$

where

$$f_1(t) = c_0 + \sum_{i=1}^{7}(a_i \sin\frac{2i\pi t}{365} + b_i \cos\frac{2i\pi t}{365}),$$

$c_0 = 0.02139$, $a_1 = -0.01048$, $b_1 = -0.02676$, $a_2 = 0.004188$,

$b_2 = 0.005002$, $a_3 = 0.000749$, $b_3 = 0.00054$, $a_4 = 0.000213$,

$b_4 = -0.000291$, $a_5 = -0.000038$, $b_5 = -0.000159$, $a_6 = -0.000188$,

$b_6 = 0.000140$, $a_7 = -0.000088$, $b_7 = 0.0000139$;

the periodic developmental rate of PEP is given by:

$$d_2(t) = \frac{sign[(t(m365) - 35.8068)(355.5969 - t(m365))] + 1}{2} \times f_2(t),$$

where

$$f_2(t) = c_0 + \sum_{i=1}^{7}(a_i \sin\frac{2i\pi t}{365} + b_i \cos\frac{2i\pi t}{365}),$$

$c_0 = 0.009975$, $a_1 = -0.005363$, $b_1 = -0.01394$, $a_2 = 0.003866$,

$b_2 = 0.004296$, $a_3 = -0.000659$, $b_3 = -0.000245$, $a_4 = -0.000099$,

$b_4 = -0.000123$, $a_5 = 0.000031$, $b_5 = 0.000007$, $a_6 = -0.000023$,

$b_6 = 0.000091$, $a_7 = -0.000004$, $b_7 = -0.000079$;

the periodic developmental rate of larva-to-nymph is given by:

$$d_6(t) = \frac{sign[(t(m365) - 53.3081)(351.8854 - t(m365))] + 1}{2} \times f_3(t),$$

where

$$f_3(t) = c_0 + \sum_{i=1}^{5}(a_i \sin\frac{2i\pi t}{365} + b_i \cos\frac{2i\pi t}{365}),$$

$c_0 = 0.006907$, $a_1 = 0.001712$, $b_1 = -0.008659$, $a_2 = -0.003768$,

$b_2 = 0.002882$, $a_3 = 0.000717$, $b_3 = -0.00127$, $a_4 = 0.000972$,

$b_4 = 0.00057$, $a_5 = -0.000064$, $b_5 = -0.00115$, $a_6 = -0.000041$,

$b_6 = 0.000036$, $a_7 = 0.000079$, $b_7 = 0.000655$;

the periodic developmental rate of nymph-to-adult is given by:

$$d_9(t) = \frac{sign[(t(m365) - 51.2829)(347.2452 - t(m365))] + 1}{2} \times f_4(t),$$

where

$$f_4(t) = c_0 + \sum_{i=1}^{5}(a_i \sin\frac{2i\pi t}{365} + b_i \cos\frac{2i\pi t}{365}),$$

$c_0 = 0.005122$, $a_1 = 0.001326$, $b_1 = -0.00574$, $a_2 = -0.004511$,

$b_2 = 0.001516$, $a_3 = 0.002741$, $b_3 = -0.0006858$, $a_4 = -0.001363$,

$b_4 = -0.0003076$, $a_5 = 0.00155$, $b_5 = -0.0004824$, $a_6 = -0.0009726$,

$b_6 = 0.0001277$, $a_7 = 0.001129$, $b_7 = 8.877e-005$;

the periodic host attaching rate of immature (larva, nymph)$d_4(t)$ (or $d_7(t)$) is given by:

$$d_4(t) = \frac{sign[(t(m365) - 106.9692)(315.0422 - t(m365))] + 1}{2} \times f_5(t),$$

where

$$f_5(t) = c_0 + \sum_{i=1}^{7}(a_i \sin\frac{2i\pi t}{365} + b_i \cos\frac{2i\pi t}{365}),$$

$$c_0 = 0.002924, \quad a_1 = -0.001779, \quad b_1 = -0.004538, \quad a_2 = 0.001854,$$

$$b_2 = 0.002125, \quad a_3 = -0.001022, \quad b_3 = -0.000588, \quad a_4 = 0.000431,$$

$$b_4 = -0.000036, \quad a_5 = -0.000065, \quad b_5 = 0.000173, \quad a_6 = -0.000079,$$

$$b_6 = 0.000043, \quad a_7 = -0.000063, \quad b_7 = -0.0001740;$$

and the periodic host finding rate of adults is given by:

$$d_{10}(t) = \{sign[(t(m365) - 74.2957)(t(m365) - 175.3725)\cdot$$

$$(t(m365) - 254.2905)(356.5154 - t(m365))] + 1\}/2 \times f_6(t),$$

where

$$f_6(t) = c_0 + \sum_{i=1}^{7}(a_i \sin\frac{2i\pi t}{365} + b_i \cos\frac{2i\pi t}{365}),$$

$$c_0 = 0.1077, \quad a_1 = -0.008856, \quad b_1 = 0.007085, \quad a_2 = -0.1382,$$

$$b_2 = -0.1115, \quad a_3 = -0.006589, \quad b_3 = -0.005471, \quad a_4 = 0.09107,$$

$$b_4 = -0.01059, \quad a_5 = 0.006597, \quad b_5 = -0.007067, \quad a_6 = -0.02838,$$

$$b_6 = -0.002206, \quad a_7 = 0.001399, \quad b_7 = 0.005272.$$

9 Appendix B

Proof: the continuity of $Q_t(\varphi)$ in $(t,\varphi) \in [0,\infty) \times \mathcal{C}_{u^*(0)}$ with respect to the compact open topology and the compactness of $Q_t[\mathcal{C}_{u^*(0)}]$ in $\mathcal{C}_{u^*(0)}$ (Lemma 4.4.2)

Firstly, we have to show that $T(t) = \{T_i(t)\}_{i=1}^7$ is compact for each $t > 0$. Let $\mathcal{D}_M := \{\phi \in \mathcal{D} : 0 \le \phi(x) \le M, x \in \mathbb{R}\}$. It is easy to check $T_i(t)\mathcal{D}_M \subset \mathcal{D}_M$ for every $t > 0$. Since for any $\phi \in \mathcal{D}_M$, $x \in \mathbb{R}$

$$\begin{aligned} |T_i(t)\phi(x)| &= \tfrac{1}{\sqrt{4\pi\bar{D}_i t}} \int_{\mathbb{R}} e^{-\frac{(x-y)^2}{4D_i t}} |\phi(y)| dy \le M \tfrac{1}{\sqrt{4\pi\bar{D}_i t}} \int_{\mathbb{R}} e^{-\frac{(x-y)^2}{4D_i t}} d\tfrac{y-x}{\sqrt{4\bar{D}_i t}} \sqrt{4\bar{D}_i t} \\ &= M \tfrac{1}{\sqrt{\pi}} \int_{\mathbb{R}} e^{-x^2} dx = M \cdot \tfrac{1}{\sqrt{\pi}} \cdot \sqrt{\pi} = M. \end{aligned}$$

Moreover, for any $\phi \in \mathcal{D}_M$, $x_1, x_2 \in \mathbb{R}$, we have

$$\begin{aligned} |T_i(t)\phi(x_1) - T_i(t)\phi(x_2)| &= |\tfrac{1}{\sqrt{4\pi\bar{D}_i t}} (\int_{\mathbb{R}} e^{-\frac{(x_1-y)^2}{4D_i t}} \phi(y) dy - \int_{\mathbb{R}} e^{-\frac{(x_2-y)^2}{4D_i t}} \phi(y) dy)| \\ &\le \tfrac{1}{\sqrt{4\pi\bar{D}_i t}} \int_{\mathbb{R}} |e^{-\frac{(x_1-y)^2}{4D_i t}} - e^{-\frac{(x_2-y)^2}{4D_i t}}| \cdot |\phi(y)| dy \\ &\le \tfrac{M}{\sqrt{4\pi\bar{D}_i t}} \int_{\mathbb{R}} |e^{-\frac{(x_1-x_2+y)^2}{4D_i t}} - e^{-\frac{y^2}{4D_i t}}| dy \\ &= g(x_1 - x_2) < \varepsilon \end{aligned}$$

where $g(\xi) = \frac{M}{\sqrt{4\pi\bar{D}_i t}} \int_{\mathbb{R}} |e^{-\frac{(\xi+y)^2}{4D_i t}} - e^{-\frac{y^2}{4D_i t}}| dy$. Clearly, $\lim_{\xi \to 0} g(\xi) = 0$. Therefore,

$\{T_i(t)\mathcal{D}_M\}_{i=1}^7$ is an equicontinuous family of functions for every $t > 0$. It then follows from the Arzelá-Ascoli Theorem and a standard diagonal argument, $\{T_i(t)\mathcal{D}_M\}_{i=1}^7$ is precompact with respect to the compact topology for every $t > 0$. Thus, $\{T_i(t)\}_{i=1}^7$ is compact for every $t > 0$. So, we have $\{T(t)\}_{t\geq 0}$ is compact.

We suppose that each $0 < \nu < \infty$ and $\{\varphi_n\}_1^\infty$ is a sequence in $\mathcal{C}_{u^*(0)}$ with $\varphi_n \to \varphi$ as $n \to \infty$. Set $u_n(t) = Q_t(\varphi_n)$ for all $t \in [0, \nu]$. Since for any $\varphi_n \in \mathcal{C}_{u^*(0)}$, i.e., $0 \leq \varphi_n(x) \leq u^*(0)$, by monotonicity, we have $0 = Q_t(0) \leq Q_t(\varphi_n) = u_n(t) \leq Q_t(u^*(0)) = u^*(0)$, this means $u_n(t) \in \mathcal{C}_{u^*(0)}$. Then there exist M_1, $M_2 > 0$ such that $\|T(s)\| \leq M_1$, $|G(s, u_n(s))| \leq M_2$ for all $s \in [0, \nu]$ and $n \geq 1$. Now let $t \in (0, \nu]$ and $\epsilon > 0$. Choose $\delta, \rho > 0$ such that $\rho < t$, $\delta < t - \rho$, $(t + \delta - \rho)M_1M_2 \leq \epsilon/4$ and $|T(t)\varphi_n - T(s)\varphi_n| \leq \epsilon/4$ whenever $n \geq 1$ and $|t - s| \leq \delta$. In particular, $s \leq t + \delta$.

Then if $n \geq 1$ and $|t-s| \leq \delta$, it follows that

$$
\begin{aligned}
& |u_n(t) - u_n(s)| \\
= \; & |T(t)\varphi_n + \int_0^t T(t-r)G(r,u_n(r))dr - T(s)\varphi_n - \int_0^s T(s-r)G(r,u_n(r))dr| \\
= \; & |T(t)\varphi_n - T(s)\varphi_n + \int_0^\rho T(t-r)G(r,u_n(r))dr - \int_0^\rho T(s-r)G(r,u_n(r))dr \\
& + \int_\rho^t T(t-r)G(r,u_n(r))dr - \int_\rho^s T(s-r)G(r,u_n(r))dr| \\
\leq \; & |T(t)\varphi_n - T(s)\varphi_n| + \int_0^\rho \|T(t-r) - T(s-r)\|M_2 dr \\
& + \int_\rho^t \|T(t-r)\||G(r,u_n(r))|dr + \int_\rho^s \|T(s-r)\||G(r,u_n(r))|dr \\
\leq \; & |T(t)\varphi_n - T(s)\varphi_n| + \zeta + M_1M_2[(t-\rho) + (s-\rho)] \\
\leq \; & |T(t)\varphi_n - T(s)\varphi_n| + \zeta + M_1M_2[(t+\delta-\rho) + (t+\delta-\rho)] \\
\leq \; & \epsilon/4 + \zeta + \epsilon/4 + \epsilon/4 \\
= \; & 3\epsilon/4 + \zeta,
\end{aligned}
$$

where $\zeta = \int_0^\rho \|T(t-r) - T(s-r)\|M_2 dr$. Since $T(t)$ is compact for every $t > 0$, from [59, Proposition 7.5.1], the map $t \to T(t)$ is continuous in the uniform operator topology on $(0,\infty)$. Then we can also assume that δ is sufficiently small so that $\|T(t-r) - T(s-r)\| \leq \epsilon/(4\rho M_2)$ for all $r \in [0,\rho]$, and hence $\zeta \leq \frac{\epsilon}{4\rho M_2}\rho M_2 = \epsilon/4$. Therefore $|u_n(t) - u_n(s)| \leq \epsilon$ holds whenever $|t-s| \leq \delta$ and $n \geq 1$. Then $Q_t(\varphi)$ is continuous on $[0,\infty)$ for each $\varphi \in \mathcal{C}_{u^*(0)}$. Moreover, $\{u_n\}_1^\infty$ is equicontinuous on $[0,\nu]$ and we have from Ascoli-Arzela Theorem that $\{u_n : n \geq 1\}$ is relatively compact in $C([0,\nu],\mathcal{C}_{u^*(0)})$. If u is any limit point of $\{u_n\}_1^\infty$, then $u(t)$ satisfies the

integral equation (4.4.16). This means that u is a solution to (4.4.16) on $[0,\nu]$, and hence $u(t) = Q_t(\varphi)$ for all $t \in [0,\nu]$ by uniqueness of solutions. Since each limit point of $\{u_n\}_1^\infty$ is the map $t \to Q_t(\varphi)$ of $[0,\nu]$ into $\mathcal{C}_{u^*(0)}$, one concludes that $\lim_{n\to\infty} Q_t(\varphi_n) = Q_t(\varphi)$ uniformly in $[0,\nu]$. Therefore, $\|Q_t(\varphi_n) - Q_t(\varphi)\|_{\mathcal{C}} \to 0$ as $n \to \infty$ for any $t \in [0,\nu]$ and $\varphi_n \in \mathcal{C}_{u^*(0)}$. Since $\nu > 0$ is arbitrary, we conclude that $Q_t(\varphi)$ in $(t,\varphi) \in [0,\infty) \times \mathcal{C}_{u^*(0)}$ is continuous with respect to the compact open topology and $Q_t[\mathcal{C}_{u^*(0)}]$ is precompact in $\mathcal{C}_{u^*(0)}$.

Bibliography

[1] http://animaldiversity.umm2.umich.edu/site/index.html.

[2] R. M. Anderson and R. M. May. *Infectious Diseases of Humans: Dynamics and Control.* Oxford University Press, Oxford, 1991.

[3] T. E. Awerbuch and S. Sandberg. Trends and oscillations in tick population dynamics. *J. Theor. Biol.*, 175:511–516, 1995.

[4] T. Awerbuch-Friedlander, R. Levins, and M. Predescu. The role of seasonality in the dynamics of deer tick populations. *Bull. Math. Biol.*, 67:467–486, 2005.

[5] N. Bacaër. Approximation of the basic reproduction number R_0 for vector-borne diseases with a periodic vector population. *Bull. Math. Biol.*, 69:1067–1091, 2007.

[6] N. Bacaër and X. Abdurahman. Resonance of the epidemic threshold in a periodic environment. *J. Math. Biol.*, 57:649–673, 2008.

[7] N. Bacaër and M. G. M. Gomes. On the final size of epidemics with seasonality. *Bull. Math. Biol.*, 71:1954–1966, 2009.

[8] N. Bacaër and S. Guernaoui. The epidemic threshold of vector-borne diseases with seasonality. *J. Math. Biol.*, 53:421–436, 2006.

[9] N. Bacaër and R. Ouifki. Growth rate and basic reproduction number for populationmodels with a simple periodic factor. *Math. Biosci.*, 210:647–658, 2007.

[10] Nicolas Bacaër. *A short histroy of mathematical population dynamics.* Springer-Verlag London Ltd, London, 2011.

[11] M. Begon. *Infectious Disease Ecology: Effects of Ecosystems on Disease and of Disease on Ecosystems*, chapter Effects of host diversity on disease dynamics. Princeton University Press, Princeton, 2008.

[12] C. Bowman, A. B. Gumel, P. van den Driessche, J. Wu, and H. Zhu. A mathematical model for assessing control strategies against West Nile virus. *Bull. Math. Biol.*, 67:1107–1133, 2005.

[13] J. L. Brunner, K. LoGiudice, and R. Ostfeld. Estimating reservior competence of *Borrelia burgdorferi* hosts: prevalence and infectivity, sensitivity and specificity. *J. Med. Entomol.*, 45:139–147, 2008.

[14] J. Van Buskirk and R. S. Ostfeld. Controlling Lyme disease by modifying the density and species composition of tick hosts. *Ecol. Appl.*, 5(4):1133–1140, 1995.

[15] J. Van Buskirk and R. S. Ostfeld. Habitat heterogeneity, dispersal, and local risk of exposure to Lyme disease. *Ecol. Appl.*, 8:365–378, 1998.

[16] T. Caraco, S. Glavanakov, G. Chen, J. E. Flaherty, T. K. Ohsumi, and B. K. Szymanski. Stage-structured infection transmission and a spatial epidemic: a model for Lyme disease. *Am. Nat.*, 160:348–359, 2002.

[17] CDC. Summary of notifiable diseases–United States, 2010. *Morbidity and Mortality Weekly Report*, 59:1–111, 2012.

[18] M. R. Cortinas and U. Kitron. County-level surveillance of white-tailed deer infestation by *Ixodes scapularis* and *Dermacentor albipictus* (Acari: Ixodidae) along the Illinois river. *J. Med. Entomol.*, 43(5):810–819, 2006.

[19] T. J. Daniels, R. C. Falco, K. L. Curran, and D. Fish. Timing of *Ixodes scapularis* (Acari: Ixodidae) oviposition and larval activity in southern New York. *J. Med. Entomol.*, 33:140–147, 1996.

[20] T. J. Daniels, D. Fish, and R. C. Falco. Seasonal activity and survival of adult *Ixodes dammini* (Acari: Ixodidae) in southern New York State. *J. Med. Entomol.*, 26:610–614, 1989.

[21] O. Diekmann and J. A. P. Heesterbeek. *Mathematical epidemiology of infectious disease: model building, analysis and interpretation.* Wiley, New York, 2000.

[22] O. Diekmann, J. A. P. Heesterbeek, and J. A. J. Metz. On the definition and the computation of the basic reproduction ratio R_0 in models for infectious diseases. *J. Math. Biol.*, 35:503–522, 1990.

[23] A. Dobson. Population dynamics of pathogens with multiple host species. *Am. Nat.*, 164:s64–78, 2004.

[24] A. D. M. Dobson, T. J. R. Finnie, and S. E. Randolph. A modified matrix model to describe the seasonal population ecology of the European tick *Ixodes ricinus*. *J. Appl. Ecol.*, 48:1017–1028, 2011.

[25] M. C. Dolan, G. O. Maupin, B. S. Schneider, C. Denatale, N. Hamon, C. Cole, N. S. Zeidner, and K. C. Stafford. Control of immature *Ixodes scapularis* (Acari: Ixodidae) on rodent reservoirs of *Borrelia burgdorferi* in a residential community of southeastern Connecticut. *J. Med. Entomol.*, 41:1043–1054, 2004.

[26] C. Fraser *et al.* Pandemic potential of a strain of influenza A (H1N1): early findings. *Science*, 324:1557–1561, 2009.

[27] R. C. Falco and D. Fish. Horizontal movement of adult *Ixodes dammini* (Acari: Ixodidae) attracted to carbon dioxide-baited traps. *J. Med. Entomol.*, 28:726–729, 1991.

[28] N. M. Ferguson, D. A. Cummings, S. Cauchemez, C. Fraser, S. Riley, A. Meeyai, S. Iamsirithaworn, and D. S. Burke. Strategies for containing an emerging influenza pandemic in southeast Asia. *Nature*, 437:209–214, 2005.

[29] I. M. Foppa. The basic reproductive number of tick-borne encephalitis virus. An empirical approach. *J. Math. Biol.*, 51:616–628, 2005.

[30] T. Gedeon, C. Bodelón, and A. Kuenzi. Hantavirus transmission in sylvan and peridomestic environments. *Bull. Math. Biol.*, 72:541–564, 2010.

[31] M. Ghosh and A. Pugliese. Seasonal population dynamics of ticks, and its inuence on infection transmission: a semi-discrete approach. *Bull. Math. Biol.*, 66:1659–1684, 2004.

[32] A. Gumel, S. Ruan, T. Day, J. Watmough, P. van den Driessche, D. Gabrielson, C. Bowman, M. E. Alexander, S. Ardal, J. Wu, and B. M. Sahai. Modeling strategies for controlling SARS outbreaks based on Toronto, Hong Kong, Singapore and Beijing experience. *Proc. Roy. Soc. London*, 271:2223–2232, 2004.

[33] J. K. Hale. *Ordinary differential equations.* Krieger, 2nd edition, 1980.

[34] N. Hartemink, S. O. Vanwambeke, H. Heesterbeek, D. Rogers, D. Morley, B. Pesson, C. Davies, S. Mahamdallie, and P. Ready. Integrated mapping of establishment risk for emerging vector-borne infections: a case study of canine leishmaniasis in southwest France. *PLoS One*, 6:e20817, 2011.

[35] N. A. Hartemink, B. V. Purse, R. Meiswinkel, H. E. Brown, A. de Koeijer, A. R. Elbers, G. J. Boender, D. J. Rogers, and J. A. P. Heesterbeek. Mapping the basic reproduction number (R_0) for vector-borne diseases: a case study on bluetongue virus. *Epidemics*, 1:153–161, 2009.

[36] N. A. Hartemink, S. E. Randolph, S. A. Davis, and J. A. P. Heesterbeek. The basic reproduction number for complex disease systems: defining $R(0)$ for tick-borne infections. *Am. Nat.*, 171:743–754, 2008.

[37] M. W. Hirsch. System of differential equations that are competitive or cooperative II: convergence almost everywhere. *SIAM J. Math. Anal.*, 16(3):423–439, 1985.

[38] M. W. Hirsch, H. L. Smith, and X.-Q. Zhao. Chain transitivity, attractivity, and strong repellors for semidynamical systems. *J. Dynam. Differential Equations*, 13:107–131, 2001.

[39] D. Holly and J. Louis. Modeling tick-borne disease: a metapopulation model. *Bull. Math. Biol.*, 69:265–288, 2007.

[40] G. R. Hosack, P. A. Rossignol, and P. van den Driessche. The control of vector-borne disease epidemics. *J. Theor. Biol.*, 255:16–25, 2008.

[41] X. Hu. Threshold dynamics for a Tuberculosis model with seasonality. *Math. Biosci. Eng.*, 9:111–122, 1012.

[42] P. Jagers and O. Nerman. Branching processes in periodically varying environment. *Ann. Prob.*, 13:254–268, 1985.

[43] J. G. Kingsolver. Mosquito host choice and the epidemiology of malaria. *Am. Nat.*, 130:811–827, 1987.

[44] M. Klich, M. Lankester, and K. W. Wu. Spring migratory birds (Aves) extend the northern occurrence of blacklegged tick (Acari: Ixodidae). *J. Med. Entomol.*, 33:581–585, 1996.

[45] K. Kurtenbach, K. Hanincova, J. Tsao, G. Margos, D. Fish, and N. H. Ogden. Fundamental processes in the evolutionary ecology of Lyme borreliosis. *Nat. Rev. Microbiol.*, 4:660–669, 2006.

[46] P. A. Leighton, J. K. Koffi, Y. Pelcat, L. R. Lindsay, and N. H. Ogden. Predicting the speed of tick invasion: an empirical model of range expansion for the Lyme disease vector *Ixodes scapularis* in Canada. *J. Appl. Ecol.*, 49:457–464, 2012.

[47] M. L. Levin and D. Fish. Density-dependent factors regulating feeding success of *Ixodes scapularis* larvae (Acari: Ixodidae). *J. Parasitol.*, 84:36–43, 1998.

[48] X. Liang, Y. Yi, and X.-Q. Zhao. Spreading speeds and traveling waves for periodic evolution systems. *J. Diff. Eqns.*, 231:57–77, 2006.

[49] X. Liang and X.-Q. Zhao. Asymptotic speeds of spread and traveling waves for monotone semiflow with applications. *Pure Appl. Math.*, 60:1–40, 2007.

[50] X. Liang and X.-Q. Zhao. Spreading speeds and traveling waves for the abstract monostable evolution systems. *J. Functional Analysis*, 259:857–903, 2010.

[51] L. R. Lindsay, I. K. Barker, G. A. Surgeoner, S. A. McEwen, T. J. Gillespie, and E. M. Addison. Survival and development of the different life stages of *Ixodes scapularis* (Acari: Ixodidae) held within four habitats on Long Point, Ontario, Canada. *J. Med. Entomol.*, 35:189–199, 1989.

[52] L. R. Lindsay, I. K. Barker, G. A. Surgeoner, S. A. McEwen, T. J. Gillespie, and J. T. Robinson. Survival and development of *Ixodes scapularis* (Acari: Ixodidae) under various climatic conditions in Ontario. *J. Med. Entomol.*, 32:143–152, 1995.

[53] K. LoGiudice, R. S. Ostfeld, K. A. Schmidt, and F. Keesing. The ecology of infectious disease: effects of host diversity and community composition on Lyme disease risk. *Proc. Natl. Acad. Sci.*, 100:567–571, 2003.

[54] C. C. Lord. Mortality of unfed nymphal *Ixodes dammini* (Acari: Ixodidae) in field enclosures. *Envir. Ent.*, 22:82–87, 1993.

[55] Y. Lou and X.-Q. Zhao. The periodic Ross-Macdonald model with diffusion and advection. *Appl. Anal.*, 89:1067–1089, 2010.

[56] K. Madhav, S. Broenstein, I. Tsao, and D. Fish. A dispersal model for the range expansion of blacklegged tick (Acari: Ixodidae). *J. Med. Entomol.*, 41(5):842–852, 2004.

[57] The malERA Consultative Group on Modeling. A research agenda for malaria eradication: modeling. *PLoS Med.*, 8:e1000403, 2011.

[58] S. Marino, I. B. Hogue, C. J. Ray, and D. E. Kirschner. A methodology for performing global uncertainty and sensitivity analysis in systems biology. *J. Theor. Biol.*, 254:178–196, 2008.

[59] R. H. Martin. *Nonlinear operators and differential equations in Banach space.* Wiley-interscience, New York, 1976.

[60] R. H. Martin and H. L. Smith. Abstract functional differential equations and reaction-diffusion systems. *Trans. Amer. Math. Soc.*, 321:1–44, 1990.

[61] M. D. Mckay, R. J. Beckman, and W. J. Conover. Comparison of 3 methods for selecting values of input variables in the analysis of output from a computer code. *Technometrics*, 21:239–245, 1979.

[62] M. G. Morshed, J. D. Scott, S. N. Banerjee, M. Banerjee, T. Fitzgerald, K. Fernando, R. Mann, and J. Isaac-Renton. First isolation of Lyme disease spirochete, *Borrelia burgdorferi*, from blacklegged tick, *Ixodes scapularis*, removed from a bird in Nova Scotia, Canada. *CCDR*, 25:153–155, 1999.

[63] G. A. Mount and D. G. Haile. Computer simulation of population dynamics of the American dog tick (Acari: Ixodidae). *J. Med. Entomol.*, 26:60–76, 1989.

[64] G. A. Mount, D. G. Haile, and E. Daniels. Simulation of blacklegged tick (Acari: Ixodidae) population dynamics and transmission of *Borrelia burgdorfei*. *J. Med. Entomol.*, 34:461–484, 1997.

[65] H. G. Mwambi, J. Baumgärtner, and K. P. Hadeler. Ticks and tick-borne diseases: a vector-host interaction model for the brown ear tick (Rhipicephalus appendiculatus). *Stat. Methods. Med. Res.*, 9:279–301, 2000.

[66] R. Norman, R. G. Bowers, M. Begon, and P. J. Hudson. Persistence of tick-borne virus in the presence of multiple host species: tick reservoirs and parasite mediated competitio. *J. Theor. Biol.*, 200:111–118, 1999.

[67] N. H. Ogden, I. K. Barker, G. Beauchamp, S. Brazeau, D. F. Charron, A. Maarouf, M. G. Morshed, C. J. O'Callaghan, R. A. Thompson, D. Waltner-Toews, M. Waltner-Toews, and L. R. Lindsay. Investigation of ground level and remote-sensed data for habitat classification and prediction of survival of *Ixodes scapularis* in habitats of southeastern Canada. *J. Med. Entomol.*, 43:403–414, 2006.

[68] N. H. Ogden, M. Bigras-Poulin, C. O'Callaghan, I. Barker, L. Lindsay, A. Maarouf, K. Smoyer-Tomic, D. Waltner-Toews, and D. Charron. A dynamic population model to investigate effects of climate on geographic range and seasonality of the tick *Ixodes scapularis*. *Int. J. Parasitol.*, 35:375–389, 2005.

[69] N. H. Ogden, M. Bigras-Poulin, C. J. O'callaghan, I. K. Barker, K. Kurtenbach, L. R. Lindsay, and D. F. Charron. Vector seasonality, host infection dynamics and fitness of pathogens transmitted by the tick *Ixodes scapularis*. *Parasitology*, 134:209–227, 2007.

[70] N. H. Ogden, C. Bouchard, K. Kurtenbach, G. Margos, L. R. Lindsay, L. Trudel, S. Nguon, and F. Milord. Active and passive surveillance and phylogenetic analysis of *Borrelia burgdorferi* elucidate the process of Lyme disease risk emergence in Canada. *Environ. Health Persp.*, 118:909–914, 2010.

[71] N. H. Ogden, L. R. Lindsay, G. Beauchamp, D. Charron, A. Maarouf, C. J. O'Callaghan, D. Waltner-Toews, and I. K. Barker. Investigation of relationships between temperature and developmental rates of tick *Ixodes scapularis* (Acari: Ixodidae) in the laboratory and field. *J. Med. Entomol.*, 41:622–633, 2004.

[72] N. H. Ogden, L. R. Lindsay, K. Hanincová, I. K. Barker, M. Bigras-Poulin, D. F. Charron, A. Heagy, C. M. Francis, C. J. O'Callaghan, I. Schwartz, and R. A. Thompson. Role of migratory birds in introduction and range expansion of *Ixodes scapularis* ticks and of *Borrelia burgdorferi* and *Anaplasma phagocytophilum* in Canada. *Appl. Environ. Microbiol.*, 74:1780–1790, 2008.

[73] N. H. Ogden, L. R. Lindsay, M. Morshed, and et al. The emergence of Lyme disease in Canada. *CMAJ*, 180:1221–1224, 2009.

[74] N. H. Ogden, A. Maarouf, I. K. Barker, M. Bigras-Poulin, L. R. Lindsay, M. G. Morshed, C. J. O'Callaghan, F. Ramay, D. Waltner-Toews, and F. F. Charron. Climate change and the potential for range expansion of the Lyme disease vector *Ixodes scapularis* in Canada. *Int. J. Parasitol.*, 36:63–70, 2006.

[75] N. H. Ogden, L. St-Onge, I. K. Barker, S. Brazeau, M. Bigras-Poulin, D. F. Charron, C. M. Francis, A. Heagy, L. R. Lindsay, A. Maarouf, P. Michel, F. Milord, C. J. O'Callaghan, L. Trudel, and R. A. Thompson. Risk maps for range expansion of the Lyme disease vector, *Ixodes scapularis*, in Canada now and with climate change. *International Journal of Health Geographics*, 22:7–24, 2008.

[76] N. H. Ogden and J. I. Tsao. Biodiversity and Lyme disease: dilution or amplification? *Epidemics*, 1:196–206, 2009.

[77] R. S. Ostfeld. *Lyme Disease: The Ecology of a Complex System.* Oxford University Press, New York, 2011.

[78] P. E. Parham and E. Michael. Modelling the effects of weather and climate change on malaria transmission. *Environ. Health Persp.*, 118:620–626, 2010.

[79] T. C. Porco. A mathematical model of the ecology of Lyme disease. *IMA Journal of Mathematics Applied in Medicine and Biology*, 16:261–296, 1999.

[80] S. E. Randolph, D. Miklisova, J. Lysy, D. J. Rogers, and M. Labuda. Incidence from coincidence: patterns of tick infestations on rodents facilitate transmission of tick-borne encephalitis virus. *Parasitology*, 118:177–186, 1999.

[81] S. E. Randolph and D. J. Rogers. A generic population model for the African tick *Rhipicephalus appendiculatus*. *Parasitology*, 115:265–279, 1997.

[82] R. Rosá and A. Pugliese. Effects of tick population dynamics and host densities on the persistence of tick-borne infections. *Math. Biosci.*, 208:216–240, 2007.

[83] R. Rosá, R. Pugliese, R. Norman, and P. J. Hudson. Thresholds for disease persistence in models for tick-borne infections including non-viraemic transmission, extended feeding and tick aggregation. *J. Theor. Biol.*, 224:359–376, 2003.

[84] S. Sandberg, T. E. Awerbuch, and A. Spielman. A comprehensive multiple matrix model representing the life cycle of the tick that transmits the agent of Lyme disease. *J. Theor. Biol.*, 157:203–220, 1992.

[85] K. A. Schmidt and R. S. Ostfeld. Biodiversity and the dilution effect in disease ecology. *Ecology*, 82:609–619, 2001.

[86] K. Schuhmacher and H. Thieme. Some theoretical and numerical aspects of modelling dispersion in the development of ectotherms. *Comut. Math. Applic.*, 15:565–594, 1988.

[87] J. D. Scott, K. Fernando, S. N. Banerjee, L. A. Durden, S. K. Byrne, M. Banerjee, R. B. Mann, and M. G. Morshed. Birds disperse Ixodid (Acari: Ixodidae) and Borrelia burgdorferi-infected ticks in Canada. *J. Med. Entomol.*, 38:493–500, 2001.

[88] T. J. Slowik and R. S. Lane. Feeding preferences of the immature stages of three western north American ixodid ticks (Acari) for avian, reptilian, or rodent hosts. *J. Med. Entomol.*, 46:115–122, 2009.

[89] D. L. Smith, F. E. McKenzie, R. W. Snow, and S. I. Hay. Revisiting the basic reproductive number for malaria and its implications for malaria control. *PLoS Biol.*, 5:e42, 2007.

[90] H. L. Smith. Monotone semiflows generated by functional differential equations. *J. Diff. Eqns.*, 66(3):420–442, 1987.

[91] H. L. Smith. Systems of ordinary differential equations which generate an order preserving flow. A survey of results. *SIAM Rev.*, 30(1):87–113, 1988.

[92] H. L. Smith. *Monotone Dynamical Systems: An Introduction to the Theory of Competitive and Cooperative Systems*, volume 41 of *Math. Surveys Monogr.* AMS, Providence, RI, 1995.

[93] R. P. J. R. Smith, P. W. Rand, E. H. Lacombe, S. R. Morris, D. W. Holmes, and D. A. Caporale. Role of bird migration in the long-distance dispersal of *Ixodes dammini*, the vector of Lyme disease. *J. Infect. Dis.*, 174:221–224, 1996.

[94] D. E. Sonenshine. *Biology of ticks.* Oxford University Press, New York, 1991.

[95] A. C. Steere, S. E. Malawista, D. R. Snydman, and et al. Lyme arthritis: an epidemic of oligoarticular arthritis in children and adults in three Connecticut communities. *Arthritis Rheum.*, 20:7–17, 1977.

[96] H. R. Thieme. Renewal theorems for linear periodic Volterra integral equations. *J. Integr. Equ.*, 7:253–277, 1984.

[97] H. R. Thieme. *Mathematics in Population Biology.* Princeton University Press, Princeton, 2003.

[98] P. van den Driessche and J. Watmough. Reproduction numbers and subthreshold endemic equilibria for compartmental models of disease transmission. *Math. Biosci.*, 180:29–48, 2002.

[99] W. Wang and X.-Q. Zhao. Threshold dynamics for compartmental epidemic models in periodic environments. *J. Dyn. Differ. Equ.*, 20:699–717, 2008.

[100] G. Webb, M. Blaser, H. Zhu, S. Ardal, and J. Wu. Critical role of nosocomial transmission in the Toronto SARS outbreak. *Math. Biosci. Eng.*, 1:1–13, 2004.

[101] G. F. Webb. *Theory of nonlinear age-dependent population dynamics.* M. Dekker, New York, 1985.

[102] P. Weng and X.-Q. Zhao. Spatial dynamics of a nonlocal and delayed population model in a periodic habitat. *Discrete Cont. Dyn. S. (Ser. A)*, 29:343–366, 2011.

[103] J. Wu. *Theory and Applications of Partial Functional Differential Equations*, volume 119 of *Applied Mathematical Science*. Springer, Berlin, 1996.

[104] X. Wu, V. R. Duvvuri, Y. Lou, N. H. Ogden, Y. Pelcat, and J. Wu. Developing a temperature-driven map of the basic reproductive numbers of the emerging tick vector of Lyme disease *Ixodes scapularis* in Canada. *J. Theor. Biol.*, 319:50–61, 2013.

[105] X. Wu, V. R. S. K Duvvuri, and J. Wu. Modeling dynamical temperature influence on the *Ixodes scapularis* population. *2010 International Congress on Environmental Modelling and Software*, 2010.

[106] B. Yuval and A. Spielman. Duration and regulation of the developmental cycle of *Ixodes dammini* (Acari: Ixodidae). *J. Med. Entomol.*, 27:196–201, 1996.

[107] F. Zhang and X.-Q. Zhao. A periodic epidemic model in a patchy environment. *J. Math. Anal. Appl.*, 325:496–516, 2007.

[108] X.-Q. Zhao. *Dynamical Systems in Population Biology*. Springer-Verlag, New York, 2003.

[109] X.-Q. Zhao and Z. Jing. Global asymptotic behavior in some cooperative systems of functional-differential equations. *Canad. Appl. Math. Quart.*, 4:421–444, 1996.